


2016

# Optimizing the Safety Margins Governing a Deterministic Design Process while Considering the Effects of a Future Test and Redesign on Epistemic Model Uncertainty

Nathaniel B. Price

University of Florida, nprice3@unl.edu

Follow this and additional works at: <https://digitalcommons.unl.edu/natresdiss>

 Part of the [Hydrology Commons](#), [Natural Resources and Conservation Commons](#), [Natural Resources Management and Policy Commons](#), [Other Environmental Sciences Commons](#), and the [Water Resource Management Commons](#)

---

Price, Nathaniel B., "Optimizing the Safety Margins Governing a Deterministic Design Process while Considering the Effects of a Future Test and Redesign on Epistemic Model Uncertainty" (2016). *Dissertations & Theses in Natural Resources*. 286.  
<https://digitalcommons.unl.edu/natresdiss/286>

This Article is brought to you for free and open access by the Natural Resources, School of at DigitalCommons@University of Nebraska - Lincoln. It has been accepted for inclusion in Dissertations & Theses in Natural Resources by an authorized administrator of DigitalCommons@University of Nebraska - Lincoln.

OPTIMIZING THE SAFETY MARGINS GOVERNING A DETERMINISTIC DESIGN  
PROCESS WHILE CONSIDERING THE EFFECTS OF A FUTURE TEST AND  
REDESIGN ON EPISTEMIC MODEL UNCERTAINTY

By

NATHANIEL B. PRICE

A DISSERTATION PRESENTED TO THE GRADUATE SCHOOL  
OF THE UNIVERSITY OF FLORIDA IN PARTIAL FULFILLMENT  
OF THE REQUIREMENTS FOR THE DEGREE OF  
DOCTOR OF PHILOSOPHY

UNIVERSITY OF FLORIDA

2016

© 2016 Nathaniel B. Price

## ACKNOWLEDGMENTS

First and foremost, I would like to thank my advisers Dr. Nam-Ho Kim and Dr. Raphael Haftka from the University of Florida, Dr. Mathieu Balesdent and Sébastien Defoort from ONERA - The French Aerospace Lab, and Dr. Rodolphe Le Riche from École des Mines de Saint-Étienne. I am grateful for the opportunity to have studied under your supervision and deeply appreciate your insight, guidance, patience, and support.

I wish to thank my committee members Dr. Ashok Kumar and Dr. Stanislav Uryasev for their advice and thoughtful questions. Special thanks to Dr. Ashok Kumar and Dr. Jérôme Morio for taking the time to serve as reviewers of this dissertation.

Thank you to the past and present members of the Structural and Multidisciplinary Optimization Group and all the student researchers at ONERA for your friendship, collaborations, and enlightening discussions.

I am grateful for the encouragement and support of my friends and family that made this dissertation possible.

This research was supported by Air Force Office of Scientific Research (Contract 84796) and ONERA - The French Aerospace Lab. This support is gratefully acknowledged.

## TABLE OF CONTENTS

	<u>page</u>
ACKNOWLEDGMENTS . . . . .	3
LIST OF TABLES . . . . .	7
LIST OF FIGURES . . . . .	8
ABSTRACT . . . . .	11
CHAPTER	
1 INTRODUCTION . . . . .	13
1.1 Motivation . . . . .	13
1.2 Objectives . . . . .	17
1.3 Outline . . . . .	18
2 BACKGROUND AND LITERATURE REVIEW . . . . .	19
2.1 Uncertainty Classification . . . . .	19
2.2 Multi-fidelity Modeling . . . . .	21
2.2.1 Sensitivity-Based Scaling Methods . . . . .	21
2.2.2 Gaussian Process (GP) Model Based Methods . . . . .	23
2.3 Design Under Uncertainty . . . . .	26
2.3.1 Deterministic Safety-Factor Based Design . . . . .	26
2.3.2 Reliability-Based Design Optimization (RBDO) . . . . .	29
2.3.2.1 Reliability index approach (RIA) . . . . .	30
2.3.2.2 Performance measure approach (PMA) . . . . .	30
2.3.2.3 Sequential optimization and reliability assessment (SORA) . . . . .	31
2.3.3 RBDO with Epistemic Model Uncertainty . . . . .	32
2.3.4 Uncertainty Reduction Measures . . . . .	34
2.4 Global Optimization . . . . .	34
3 DECIDING DEGREE OF CONSERVATIVENESS IN INITIAL DESIGN CONSIDERING A FUTURE TEST AND POSSIBLE REDESIGN . . . . .	37
3.1 Introduction . . . . .	38
3.2 Methods . . . . .	41
3.2.1 Optimization of Safety Margins . . . . .	41
3.2.2 Monte-Carlo Simulation of Epistemic Model Error . . . . .	43
3.2.3 Deterministic Design / Redesign Process . . . . .	44
3.2.3.1 Initial design . . . . .	44
3.2.3.2 Testing initial design and redesign decision . . . . .	45
3.2.3.3 Model calibration . . . . .	46
3.2.3.4 Redesign . . . . .	46
3.2.4 Probabilistic Evaluation . . . . .	47

3.3	Test Cases	49
3.3.1	Uniaxial Tension Test	49
3.3.1.1	Problem description	49
3.3.1.2	Expected performance versus probability of redesign	50
3.3.1.3	Expected performance versus level of high-fidelity model error	52
3.3.2	Supersonic Business Jet Engine Design	53
3.3.2.1	Problem description	53
3.3.2.2	Expected performance versus probability of redesign	60
3.3.2.3	Expected performance versus level of high-fidelity model error	60
3.4	Discussion and Conclusion	61
3.5	Limitations and Future work	66
4	CONSIDERING SPATIAL CORRELATIONS IN THE EPISTEMIC MODEL ERROR WHEN SIMULATING A FUTURE TEST AND REDESIGN	68
4.1	Research Context in Relation to Scope of Dissertation	69
4.2	Introduction	69
4.3	Methods	72
4.3.1	Optimization of Safety Margins	73
4.3.2	Monte-Carlo Simulation of Epistemic Model Error	75
4.3.3	Deterministic Design Process	77
4.3.3.1	Initial design	78
4.3.3.2	Testing initial design and redesign decision	78
4.3.3.3	Calibration and redesign	79
4.3.4	Probabilistic Evaluation	80
4.4	Demonstration Example	82
4.4.1	Overview	82
4.4.2	Error Model	83
4.4.3	Results	84
4.5	Discussion and Conclusions	87
5	SOUNDING ROCKET DESIGN UNDER MIXED EPISTEMIC MODEL UNCERTAINTY AND ALEATORY PARAMETER UNCERTAINTY	93
5.1	Research Context in Relation to Scope of Dissertation	93
5.2	Introduction	94
5.3	Methods	97
5.3.1	Preliminary Reliability-Based Design Optimization (RBDO)	97
5.3.2	Optimization of Standard Deviation Offsets	98
5.3.3	Monte-Carlo Simulation of Epistemic Model Error	100
5.3.4	Deterministic Design Process	101
5.3.4.1	Initial design	102
5.3.4.2	Testing initial design and redesign decision	102
5.3.4.3	Calibration and redesign	103

5.3.5	Probabilistic Evaluation	103
5.4	Test Cases	106
5.4.1	Cantilever Beam Bending Example	106
5.4.1.1	Problem description	106
5.4.1.2	Application of the proposed method	107
5.4.2	Multidisciplinary Sounding Rocket Design Example	112
5.4.2.1	Problem description	112
5.4.2.2	Standard atmosphere models	114
5.4.2.3	Discipline models	117
5.4.2.4	Low-fidelity model	124
5.4.2.5	Application of the proposed method	125
5.5	Discussion Conclusions	129
6	CONCLUSIONS	133
	REFERENCES	137
	BIOGRAPHICAL SKETCH	147

## LIST OF TABLES

<u>Table</u>	<u>page</u>
3-1 Problem definition for uniaxial tension test example . . . . .	50
3-2 Uncertain parameters for uniaxial tension test example . . . . .	50
3-3 Results for uniaxial tension example for 20% probability of redesign . . . . .	52
3-4 Problem definition for SSBJ Example . . . . .	57
3-5 Uncertain Parameters for SSBJ Example . . . . .	58
3-6 Coefficients for calculating throttle upper bound (Equation 3–20) . . . . .	59
3-7 Results for SSBJ example for 20% probability of redesign . . . . .	62
4-1 95% confidence interval for relative error of surrogate models based on LOOCV	75
4-2 Parameters for cantilever beam example . . . . .	83
5-1 Parameters for cantilever beam example . . . . .	107
5-2 Coefficients for calculating speed of sound as a function of altitude (5–25) . . .	116
5-3 Inputs and outputs of propulsion discipline . . . . .	118
5-4 Inputs and outputs of structures discipline . . . . .	119
5-5 Notation used in weights estimation . . . . .	119
5-6 Coefficients for tank mass WER's . . . . .	120
5-7 Inputs and outputs of aerodynamics discipline . . . . .	122
5-8 Inputs and outputs of trajectory discipline . . . . .	124
5-9 Data read from design curve . . . . .	125



## LIST OF FIGURES

<u>Figure</u>	<u>page</u>
3-1 The safety margins are optimized based on a MCS of the deterministic design / redesign process . . . . .	42
3-2 Flowchart showing steps in two-stage deterministic design / redesign process. Safety margins $\mathbf{n} = \{n_{ini}, n_{lb}, n_{ub}, n_{re}\}$ are shown as inputs at relevant steps. . .	45
3-3 Uniaxial tension test - Comparison of expected cross sectional area after possible redesign as a function of probability of redesign for redesign for performance (conservative initial design) versus redesign for safety (ambitious initial design). . .	53
3-4 Uniaxial tension test - Epistemic uncertainty in cross sectional area for 20% probability of redesign. . . . .	54
3-5 Uniaxial tension test - Epistemic uncertainty in safety margin with respect to high-fidelity model for 20% probability of redesign. Plots show overlapping transparent histograms. . . . .	54
3-6 Uniaxial tension test - Epistemic uncertainty in safety margin with respect to true model for 20% probability of redesign. Plots show overlapping transparent histograms. . . . .	55
3-7 Uniaxial tension test - Epistemic uncertainty in reliability index for 20% probability of redesign. Plots show overlapping transparent histograms. . . . .	55
3-8 Uniaxial tension test - Epistemic uncertainty in failure for 20% probability of redesign. The figures are plotted with different scales to show the change in the tail of the distribution. Plots show overlapping transparent histograms. . . .	56
3-9 Uniaxial tension test - Redesign for safety is preferred when high-fidelity model error is low, but redesign for performance is preferred when high-fidelity model error is high. Plot is for fixed probability of redesign of 20%. . . . .	57
3-10 A response surface of the engine performance map calculates maximum available thrust at a given Mach number, $M$ , and altitude, $h$ . The throttle setting is normalized to one at an altitude of approximately 32000 ft and Mach 1.9. . . . .	59
3-11 SSBJ Engine - Comparison of expected engine weight after possible redesign as a function of probability of redesign for redesign for performance (conservative initial design) versus redesign for safety (ambitious initial design). . . . .	61
3-12 SSBJ Engine - Epistemic uncertainty in throttle setting for 20% probability of redesign. . . . .	62
3-13 SSBJ Engine - Epistemic uncertainty in safety margin with respect to high-fidelity model for 20% probability of redesign. Plots show overlapping transparent histograms. . . . .	63

3-14	SSBJ Engine - Epistemic uncertainty in engine weight for 20% probability of redesign. . . . .	63
3-15	SSBJ Engine - Epistemic uncertainty in probability of failure for 20% probability of redesign. The figures are plotted with different scales to show the change in the tail of the distribution. Plots show overlapping transparent histograms. . . . .	64
3-16	SSBJ Engine - Redesign for safety is preferred when high-fidelity model error is low, but redesign for performance is preferred when high-fidelity model error is high. Plot is for fixed probability of redesign of 20%. . . . .	65
4-1	The optimization of the safety margins is based on a MCS of the deterministic design process . . . . .	74
4-2	The figure on the left shows the design optimization when using a safety margin $n_{ini} = 0$ and fixed conservative values $\mathbf{u}_{det}$ in place of aleatory variables $\mathbf{U}$ . The figure on the right shows the reliability of the optimum design found on the left by plotting the limit-state function in standard normal space. . . . .	85
4-3	On the left, the mean and variance of the error are plotted in a normalized design space with fixed conservative values $\mathbf{u}_{det}$ in place of aleatory variables $\mathbf{U}$ . On the right, the mean and variance of the error are plotted in standard normal aleatory space for optimum design found using $n_{ini} = 0$ . The error is in inches. . . . .	86
4-4	Tradeoff curves for expected cost (cross sectional area in square inches) as a function of probability of redesign. The curve labeled “mixed” corresponds to simultaneous optimization of $\mathbf{n} = \{n_{ini}, n_{lb}, n_{ub}, n_{re}\}$ . The curve labeled “safety” corresponds to optimizing $\{n_{ini}, n_{lb}, n_{re}\}$ with $n_{ub} = +\infty$ . The curve labeled “performance” corresponds to optimizing $\{n_{ini}, n_{ub}, n_{re}\}$ with $n_{lb} = -\infty$ . Error bars are based on surrogate models used during optimization. . . . .	88
4-5	Histograms of possible safety margin distributions for 20% probability of redesign. Plots show overlapping transparent histograms. . . . .	89
4-6	Joint distribution of design variables for possible final designs for 20% probability of redesign. Peak is located at initial design. . . . .	89
4-7	Histograms of cross-sectional area distributions for 20% probability of redesign. . . . .	90
4-8	Histograms of reliability index distributions for 20% probability of redesign. Plots show overlapping transparent histograms. . . . .	90
4-9	Joint distribution of possible most probable points (MPP’s) for 20% probability of redesign. . . . .	91
5-1	The beam is subject to horizontal and vertical tip loads . . . . .	108

5-2	The figure on the left shows the design optimization with standard deviation offset $k = 0$ and fixed conservative values $\mathbf{u}_{det}$ in place of aleatory variables. The figure on the right shows the limit-state function in standard normal space for the optimum design found on the left. The reliability index is the distance in standard normal space from the origin to the limit-state. . . . .	109
5-3	Tradeoff curve for expected cross sectional area versus probability of redesign . . . . .	110
5-4	Distribution of safety margin and reliability index for 20% probability of redesign. Plots show overlapping transparent histograms. . . . .	112
5-5	Distribution of most probable point (MPP) for 20% probability of redesign. . . . .	113
5-6	Distribution of optimum design variables and design performance for 20% probability of redesign. Peak is located at initial design. . . . .	114
5-7	Design structure matrix for sounding rocket design example. There are couplings between propulsion/structures, aerodynamics/structures, and trajectory/aerodynamics. . . . .	115
5-8	Speed of sound as a function of altitude (5–25) . . . . .	116
5-9	Drag coefficient as a function of Mach number based on Missile DATCOM. PCHIP interpolation is used between data points. . . . .	123
5-10	A second order polynomial was fit to the inert mass fraction as a function of the log of the propellant mass. The model is extrapolated to the region of interest for sounding rocket design. . . . .	125
5-11	A cloud of 10,000 designs in 6-dimensions is projected onto a one dimensional plane and compared to the low-fidelity model prediction . . . . .	126
5-12	Tradeoff curve for expected GLOW versus probability of redesign . . . . .	127
5-13	Distributions of safety margin and probability of failure for 20% probability of redesign. Plots show overlapping transparent histograms. . . . .	130
5-14	Distribution of optimum design variables for 20% probability of redesign. Plots show marginal distributions of 5-dimensional joint distribution. . . . .	131
5-15	Distributions of GLOW and dry mass for 20% probability of redesign. Plots show overlapping transparent histograms. . . . .	132

Abstract of Dissertation Presented to the Graduate School  
of the University of Florida in Partial Fulfillment of the  
Requirements for the Degree of Doctor of Philosophy

OPTIMIZING THE SAFETY MARGINS GOVERNING A DETERMINISTIC DESIGN  
PROCESS WHILE CONSIDERING THE EFFECTS OF A FUTURE TEST AND  
REDESIGN ON EPISTEMIC MODEL UNCERTAINTY

By

Nathaniel B. Price

August 2016

Chair: Nam-Ho Kim

Major: Mechanical Engineering

At the initial design stage, engineers often rely on low-fidelity models that have high uncertainty. Model uncertainty is reducible and is classified as epistemic uncertainty; uncertainty due to variability is irreducible and classified as aleatory uncertainty. In a deterministic safety-margin-based design approach, uncertainty is implicitly compensated for by using fixed conservative values in place of aleatory variables and ensuring the design satisfies a safety-margin with respect to design constraints. After an initial design is selected, testing (e.g. physical experiment or high-fidelity simulation) is performed to reduce epistemic uncertainty and ensure the design achieves the targeted levels of safety. Testing is used to calibrate low-fidelity models and prescribe redesign when tests are not passed. After calibration, reduced epistemic model uncertainty can be leveraged through redesign to restore safety or improve design performance; however, redesign may be associated with substantial costs or delays. In this work, the possible effects of a future test and redesign are considered while the initial design is optimized using only a low-fidelity model. The goal is to develop a general method for the integrated optimization of the design, testing, and redesign process that allows for the tradeoff between the risk of future redesign and the associated performance and reliability benefits. This is accomplished by formulating the design, testing, and redesign

process in terms of safety-margins and optimizing these margins based on expected performance, expected probability of failure, and probability of redesign.

The first objective of this study is to determine how the degree of conservativeness in the initial design relates to the expected design performance after a test and possible redesign. The second objective is to develop a general method for modeling epistemic model uncertainty and calibration when simulating a possible future test and redesign. The third objective is to apply the method of simulating a future test and redesign to a sounding rocket design example.

## CHAPTER 1 INTRODUCTION

### 1.1 Motivation

According to Box and Draper [1], "Essentially, all models are wrong, but some are useful." At the initial design stage, engineers often rely on low-fidelity models that have high uncertainty. Model uncertainty is reducible and is classified as epistemic uncertainty; uncertainty due to variability is irreducible and classified as aleatory uncertainty. In a deterministic safety-margin-based design approach, uncertainty is implicitly compensated for by using fixed conservative values in place of aleatory variables and ensuring the design satisfies a safety-margin with respect to design constraints. After an initial design is selected, testing (e.g. physical experiment or high-fidelity simulation) is performed to reduce epistemic uncertainty and ensure the design achieves the targeted levels of safety. Testing is used to calibrate low-fidelity models and prescribe redesign when tests are not passed. After calibration, reduced epistemic model uncertainty can be leveraged through redesign to restore safety or improve design performance; however, redesign may be associated with substantial costs or delays. In this work, the possible effects of a future test and redesign are considered while the initial design is optimized using only a low-fidelity model. The goal is to develop a general method for the integrated optimization of the design, testing, and redesign process that allows for the tradeoff between the risk of future redesign and the associated performance and reliability benefits. This is accomplished by formulating the design, testing, and redesign process in terms of safety-margins and optimizing these margins based on expected performance, expected probability of failure, and probability of redesign.

In this research, a safety-margin-based design approach is applied while considering epistemic model uncertainty and aleatory parameter uncertainty. In order for the method to be applicable under current safety-margin-based design regulations [2], the optimum

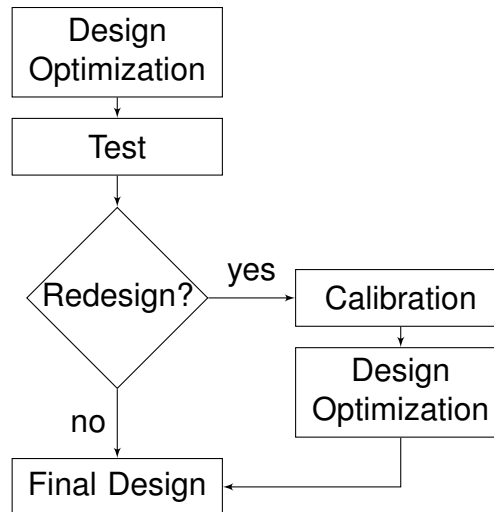


Figure 1-1. An initial design is tested. If the test is not passed, a calibration and redesign process is triggered.

design is found using a deterministic safety-margin-based approach. The safety factors are optimized based on probabilistic criteria. Traditionally, safety factors have been selected based on combination of regulations and previous experience, however, simple probabilistic guidelines for selecting safety factors have been proposed [3]. Safety-margin-based design, testing, and redesign processes are entrenched in the aircraft industry where these practices have evolved over more than 50 years, often by trial and error [4]. More recently, studies have shown the parallels between safety-margin-based design and reliability-based design optimization (RBDO) approaches while developing methods to reduce the computational cost of RBDO [5–7]. However, these studies have not considered epistemic model uncertainty. On the other hand, when there is only epistemic model uncertainty a safety margin balances the need for the final design to be feasible while at the same time not being so conservative that design performance suffers [8]. Few studies have considered the effects of both aleatory parameter uncertainty and epistemic model uncertainty. Mahadevan and Rebba have shown that failing to account for epistemic model uncertainty may lead to an overestimation of reliability and unsafe designs or underestimation of the reliability and designs that are heavier than needed [9]. Studies that use surrogate models in RBDO

also encounter a situation of mixed uncertainty. However, unlike this study where we are interested in epistemic model uncertainty as an inherent part of the low-fidelity model, these studies are usually motivated by a desire to reduce computational cost. Kim and Choi have shown that when using response surfaces in RBDO the epistemic model uncertainty results in uncertainty in the reliability index and additional sampling can be used to avoid being overly conservative [10].

One of the important aspects of this research is the integration of the design and testing process. In this research, the effects of a future test and possible redesign are considered while optimizing the initial design. Since the test will be performed in the future, the test result is an epistemic random variable. Predicting possible test results requires a probabilistic formulation of the relationship between the low-fidelity model prediction, the true value, and the test result. In the context of calibrating computer models, Kennedy and O'Hagan proposed that the true process can be related to a computer model by multiplying by an uncertain constant scale parameter and adding an uncertain discrepancy function [11]. Similar formulations have subsequently been applied in many other studies [12–17]. These formulations are similar in that they all relate the true process to the low-fidelity model by adding an uncertain discrepancy function. The formulations differ in the representation of the scale parameter. Methods range from omitting the scale parameter [13, 14] to considering an uncertain scaling function [16]. A simpler alternative method is to use only uncertain scaling parameters to formulate the relationship between the true process, the low-fidelity model, and the measurement. Zio and Apostolakis referred to this approach as the adjustment factor approach where the uncertain adjustment factor may either be additive or multiplicative [18]. However, this simple modeling method is only applicable when there is a constant model scaling or bias.

In addition to the integration of design and testing, this study also seeks to integrate a redesign process. Redesign refers to changing the design variables conditional on



the test result. Calibration is performed conditional on the test result prior to redesign. Since the future test result is modeled as an epistemic random variable the design variable after redesign is also considered a random variable. It is important to note that the design after redesign is random because it is uncertain at the initial design stage, not because there is any inherent variability. Villanueva et al. developed a method for simulating the effects of future tests and redesign when there is a constant but unknown model bias in the calculation and measurement [19]. Matsumura et al. compared RBDO considering future redesign to traditional RBDO [20]. Villanueva et al., 2014, showed that a minimum mass integrated thermal protection system is achieved by starting with a conservative (heavier) initial design and primarily using redesign to reduce mass if the test reveals the design is overly conservative [21].

In general, engineering design is an iterative process that requires gathering new knowledge and refining the initial design. Testing followed by possible redesign is an essential part of the aircraft design industry [22]. The safety-margin-based deterministic design process has a rich history that is well integrated into the design, testing, calibration, and redesign process. Currently, there is a push to transition from deterministic design methods to probabilistic approaches [4]. However, most proposed probabilistic design methods neglect the iterative nature of design and fail to consider epistemic model uncertainty. Unlike aleatory uncertainty, epistemic uncertainty is reducible by gaining new knowledge. Accounting for the possible changes in epistemic model uncertainty that occur during the design process is an important part of a probabilistic design approach. Considering epistemic model uncertainty is particularly important at the initial design stage when the the epistemic model uncertainty is very high. When there is high epistemic model uncertainty, it is important to consider the effects of future uncertainty reduction measures such as testing and redesign while selecting the initial design.

## 1.2 Objectives

The first objective of this study is to determine how the degree of conservativeness in the initial design relates to the expected design performance after a test and possible redesign. Failing a critical safety test (e.g. measured safety margin too low) typically triggers a redesign process to restore safety. It is also worthwhile to implement a redesign trigger associated with being too conservative (e.g. measured safety margin is too high) in order to redesign when it is possible to significantly improve design performance. A high probability of redesign for performance or redesign for safety should be avoided due to the associated costs and program delays related to performing redesign. To avoid redesign for safety, designers may add more conservativeness to the initial design by using a higher safety margin which typically results in worse initial design performance. Conversely, to avoid redesign for performance, a lower safety margin can be used to achieve better initial design performance. This leads to a dilemma in whether to start with a more conservative initial design and possibly redesign for performance or to start with a less conservative initial design and risk redesigning to restore safety.

The second objective is to develop a general method for modeling epistemic model uncertainty and calibration when simulating a possible future test and redesign. Previous work on simulating a future test and redesign has shown important benefits in terms of selecting the initial design when using only a low-fidelity model [21]. However, this method required the assumption of a constant but unknown error in the low-fidelity model and test result. This is a strong assumption that may be difficult to satisfy in the majority of engineering design problems. In order for the method to be applicable to most engineering problems a more sophisticated method is needed for modeling, updating, and propagating the epistemic model uncertainty. In particular, it is important to consider epistemic model uncertainties that are correlated with respect to design variables when predicting the reliability for a design that is considerably different from

the design that was tested. In addition, correlations with respect to aleatory variables become important when predicting the safety of a design at conditions that are different from the test conditions.

The third objective is to apply the method of simulating a future test and possible redesign to the design of a sounding rocket under mixed epistemic model uncertainty and aleatory parameter uncertainty.

### **1.3 Outline**

This dissertation is organized into six chapters. The motivation, objectives, and outline are discussed in Chapter 1. Chapter 2 provides a literature review of uncertainty classification, multi-fidelity modeling, and design under uncertainty. Chapter 3 discusses the research to determine how the degree of conservativeness in the initial design relates to the expected design performance after a test and possible redesign [23, 24]. In particular, this chapter analyzes the dilemma of whether to start with a more conservative initial design and possibly redesign for performance or to start with a less conservative initial design and risk redesigning to restore safety. Chapter 4 builds on the work in the first chapter to develop a generalized method for simulating a future test and possible redesign that accounts for spatial correlations in the epistemic model error [25]. Chapter 5 discusses the application of the method of simulating a future test and possible redesign to the design of a sounding rocket under mixed epistemic model uncertainty and aleatory parameter uncertainty [26]. Chapter 6 summarizes conclusions and provides perspectives for future work. The chapters are written so they can be read separately, but there is a natural progression in the method and increasing complexity of the examples from chapters 3 to 5.

## CHAPTER 2 BACKGROUND AND LITERATURE REVIEW

### 2.1 Uncertainty Classification

Uncertainty is often broadly classified into two categories. Aleatory uncertainty is due to natural variability and is irreducible. Epistemic uncertainty is due to lack of knowledge and is reducible. However, sometimes it can be challenging to classify uncertainty as epistemic, aleatory, or a mixture of both. Faber argues that the classification of uncertainty has a dependence on modeling scale as well as time [27]. The question of how modeling scale affects uncertainty classification has also been raised by O'Hagan and Oakley and leads to the question of whether there is any true randomness or if all uncertainty might be considered epistemic [28]. O'Hagan and Oakley use the term residual variability to describe the variation of a real process when repeated under the same conditions. The fundamental question is whether this residual variability is due to natural variability (aleatory uncertainty) or if by specifying additional conditions the variability could be eliminated or reduced (epistemic uncertainty). In addition to modeling scale, Faber also identified time dependence of knowledge as an important factor affecting uncertainty classification. According to Faber, the uncertainty in a model concerning the future transforms from a mixture of aleatory and epistemic uncertainty to purely epistemic when the modeled event is observed. Kiureghian and Ditlevsen describe this time dependence in the context of assessing the reliability of an existing versus a future building [29]. Kiureghian and Ditlevsen argue that there is a degree of subjectivity in the categorization of uncertainties, but it is nonetheless useful to do so in engineering design. Interestingly, the questions regarding the fundamental differences between aleatory and epistemic uncertainty may contribute to the proliferation of new methods for modeling and propagating epistemic uncertainty.

There is considerable diversity in the methods for modeling different types of uncertainty [30]. While probability theory is widely accepted as the appropriate choice

for modeling aleatory uncertainty, several alternative methods have been proposed for modeling epistemic uncertainty. These alternative methods are partially motivated by perceived difficulties associated with trying to represent lack of knowledge using classical probability theory in engineering design. Ferson and Ginzburg describe the inadequacies of probability theory when trying to represent a constant but unknown value that lies within a given interval [31]. Ferson and Ginzburg conclude that interval theory or probability bounds analysis is better suited for modeling epistemic uncertainty. Other alternative methods for representing epistemic uncertainty include Dempster-Shafer structures and possibility theory [32, 33]. However, according to O'Hagan and Oakley, "...to claim that the only information available about a parameter is that it lies in some interval is to deny the possibility of eliciting expert information effectively" [28]. The proper elicitation of expert opinion is an important topic when trying to represent expert opinion using probability theory. Kadane and Wolfson offer an overview of general and applications specific elicitation methods for constructing prior distributions based on expert opinion [34]. Moreover, as pointed out by O'Hagan and Oakley, some alternative methods that may work well for parameter uncertainty might not be easily applicable to represent other sources of uncertainty such as model inadequacy.

In addition to classifying uncertainty as aleatory or epistemic, it is useful to identify different uncertainty sources. One classification of uncertainty in computer codes, provided by Kennedy and O'Hagan [11] and simplified by O'Hagan and Oakley [28], is to classify uncertainty as parameter uncertainty, model inadequacy, residual variability, and code uncertainty. Parameter uncertainty is uncertainty about model inputs. Model inadequacy refers to the discrepancy between the model and the true process. Residual variability is the variation of the real process under the same conditions. Code uncertainty may refer to evaluating the code at previously untried inputs. Model inadequacy is of particular interest in this study, however, Nilsen and Aven have argued that focus on model uncertainty leads to muddling of risk analysis

[35]. An alternative classification by Oberkampf et al. is simply to classify uncertainties as aleatory uncertainty, epistemic uncertainty, and error [36, 37]. Error is defined as "a recognizable inaccuracy in any phase or activity of modeling and simulation that is not due to lack of knowledge" and may further be subdivided into acknowledged or unacknowledged errors. Identifying different sources and types of uncertainty is important because different methods of modeling and propagating uncertainty may be better suited for different types of uncertainty.

## 2.2 Multi-fidelity Modeling

### 2.2.1 Sensitivity-Based Scaling Methods

Model approximations can be divided into two classes [38]. There are local derivative-based approximations (e.g. Taylor-series expansions) and global approximations. Consider a low-fidelity model of a single variable  $g_L(x)$  that is a global approximation of a high-fidelity model  $g_H(x)$ . One method of relating the high-fidelity model  $g_H(x)$  to the low-fidelity model  $g_L(x)$  is to consider a scaling factor  $\rho(\cdot)$  at a design point  $x_0$

$$\rho(x_0) = \frac{g_H(x_0)}{g_L(x_0)} \quad (2-1)$$

An approximation of the high-fidelity model  $\hat{g}_H(x)$  can be obtained using a constant scaling as

$$\hat{g}_H(x) = \rho(x_0)g_L(x) \quad (2-2)$$

where a hat accent is used to denote a prediction  $\hat{g}_H(\cdot)$  that may be different than the true high fidelity model  $g_H(\cdot)$ . Obviously, the accuracy of the approximation will deteriorate at points that are far away from  $x_0$ . An improved approximation is to use a linearly varying scaling function

$$\hat{\rho}(x) = \rho(x_0) + (x - x_0)\rho'(x_0) \quad (2-3)$$

where prime denotes the derivative with respect to  $x$ . Note that the linear approximation of the scaling function  $\hat{\rho}(\cdot)$  may be considerably different from the true scaling  $\rho(\cdot)$ . The

linear scaling factor can be formulated as

$$\hat{\rho}(x) = \rho(x_0) \left[ 1 + (x - x_0) \left( \frac{g'_H(x_0)}{g_H(x_0)} - \frac{g'_L(x_0)}{g_L(x_0)} \right) \right] \quad (2-4)$$

Haftka refers to this method as the global-local approximation (GLA) method because it combines the global approximation  $g_L(x)$  with the local information contained in the scaling factor  $\hat{\rho}(x_0)$  [38]. The method is easily applicable to any number of variables by using a first-order Taylor series expansion. Chang et al. compared the GLA method to a constant scaling method when modeling a wing-box structure [39]. In addition to multiplicative scaling, it is also possible to use an additive scaling

$$\delta(x) = g_H(x_0) - g_L(x_0) \quad (2-5)$$

and to consider a second-order approximation [40]. Gano et al. proposed an adaptive hybrid scaling where the approximation is based on a weighted average of a multiplicative and additive scaling model [40]. Gano et al. applied this type of sensitivity-based scaling to develop a variable fidelity reliability-based design optimization (VF-RBDO) method [41]. One of the drawbacks to sensitivity-based scaling methods is that noise in the high-fidelity model can result in inaccurate derivative calculations and poor approximations [42].

Similar additive and multiplicative scaling methods have also been proposed for representing model uncertainty. Zio and Apostolakis describe an adjustment factor approach

$$\hat{G}_H(x) = g_L(x) \hat{E} \quad (2-6)$$

where  $\hat{G}_H(\cdot)$  is a random variable representing the possible high fidelity model and  $\hat{E}$  is a random variable representing possible model bias [18]. Zio and Apostolakis also discuss using an adjustment factor that is additive instead of multiplicative. This method of representing the model error has been applied in several studies [19–21, 23, 43, 44]. Let the superscript  $(i)$  denote a realization of the model  $\hat{G}_H(\cdot) = \hat{g}_H^{(i)}(\cdot)$  corresponding

to the error realization  $\hat{E} = \hat{e}^{(i)}$ . The main assumption of the method is that there exists an error realization,  $\exists \hat{e}^{(i)} \in \hat{E}$ , such that the scaled model corresponds to the true model,  $\hat{g}_H^{(i)}(x) = g_H(x)$ . Obviously, this is only true if the relationship between the high and low-fidelity models can be represented by some constant scaling. Therefore, the adjustment factor method of representing model uncertainty from Zio and Apostolakis corresponds to a constant approximation of the model scaling. Due to the assumption of constant model bias, only a single evaluation of the high-fidelity model is needed to remove all the model uncertainty. An improved method is to consider an uncertain scaling function (multiplicative or additive) that depends on the location  $x$ .

## 2.2.2 Gaussian Process (GP) Model Based Methods

Keane proposed a multi-fidelity optimization formulation based on creating a Kriging surrogate for the difference between a high and a low-fidelity model [45]. This method was shown to work better than simply building a surrogate for the high fidelity model alone when applied to the optimization of a wing design. Gano et al. also used a Kriging-based scaling function and applied the method to the design optimization of a supercritical high-lift airfoil [40]. Gano et al. noted that the scaling can be either additive or multiplicative. An approximation of a high-fidelity model using a multiplicative scaling is

$$\hat{g}_H(\mathbf{x}) = \hat{\rho}(\mathbf{x})g_L(\mathbf{x}) \quad (2-7)$$

where  $\hat{\rho}(\mathbf{x}) \sim \mathcal{GP}(m(\mathbf{x}), k(\mathbf{x}, \mathbf{x}'))$  is a Gaussian process (GP) model with mean function  $m(\mathbf{x})$  and covariance function  $k(\mathbf{x}, \mathbf{x}')$ . Note that the GP model is constructed for the scaling function  $\rho(\mathbf{x})$  and not the high-fidelity model  $g_H(\mathbf{x})$ . Using the Kriging approximation for the scaling, rather than the high-fidelity model, may provide a better approximation when the low-fidelity model includes physics of the modeled process [40, 45]. However, when it is not very cheap to evaluate the low-fidelity model it may be better to build the approximation using only limited evaluations of the low and high-fidelity models. In this case, co-kriging can be used as demonstrated by Forrester



et al. on a multi-fidelity wing optimization problem [12]. Co-kriging allows for the direct approximation of  $g_H(\mathbf{x})$  while accounting for the higher uncertainty in the observations from  $g_L(\mathbf{x})$ . Scaling methods may have advantages over multi-fidelity surrogates such as co-kriging because they incorporate more of the physics from the low-fidelity model, but they may be more expensive when the computational cost of the low-fidelity model is not insignificant. A compromise between the two methods is to first build a surrogate for the low-fidelity model and then build another surrogate for the scaling on top of this model. Qian et al. demonstrated this approach on an electronics cooling application involving cellular materials [15].

A variation of the multiplicative or additive Kriging method is to consider separate terms for “scale” and “location” change. For example, the relationship between the high and low-fidelity models can be formulated as

$$g_H(\mathbf{x}) = \rho(\mathbf{x})g_L(\mathbf{x}) + \delta(\mathbf{x}) \quad (2-8)$$

where  $\rho(\cdot)$  is a function for scale change and  $\delta(\cdot)$  is a function for location change. This formulation is somewhat similar to the proposed hybrid sensitivity-based scaling method of Gano et al. [40] in that it includes both additive and multiplicative terms. Gano et al. found either additive scaling or multiplicative scaling may work better depending on the problem, but by including both types of scaling in a single model it alleviated the need to make this decision a priori. Including both scale and location functions in the GP model may have a similar effect. Kennedy and O’Hagan considered a constant (but uncertain) scaling term  $\rho$  and a GP model of the location function  $\delta(\cdot)$  in a Bayesian framework for the calibration of computer codes [11]. Kennedy and O’Hagan also used a constant scaling and GP location function in the formulation for predicting a top level code when one or more lower level codes are available [46]. Bayarri et al. omitted the scale function from the proposed Bayesian framework for the validation of computer models [47]. In other studies the scale function has been based on linear regression [15, 17]. Qian and

Wu used GP models for both the scale function and the location function [16]. In some sense, including both a scale function  $\rho(\cdot)$  and a location function  $\delta(\cdot)$  is similar to adding additional terms in a regression model and may allow for a better fit of the true relationship. However, even with a constant scale term there may be issues with indentifiability because many different model parameters could result in the same observations [48].

Using a GP model to relate a high and low-fidelity model not only allows for the modeling of complex relationships between models, but also provides an estimate of the model uncertainty. The uncertainty in the GP model agrees with our intuition in that the variance of the model uncertainty reaches a minimum at observations and increases to a maximum value  $\sigma^2$  as the distance from the observations increases. The GP model framework can also be extended to include some noise in the high-fidelity model (e.g. measurement error)

$$g_T(\mathbf{x}_i) = g_H(\mathbf{x}_i) + \epsilon_i = \rho(\mathbf{x}_i)g_L(\mathbf{x}_i) + \delta(\mathbf{x}_i) + \epsilon_i \quad (2-9)$$

where the subscript  $i$  is used because the measurement error  $\epsilon_i$  at any location  $\mathbf{x}_i$  is independent identically distributed (i.i.d) Gaussian noise. Huang et al. used the uncertainty estimate from the GP model to develop a sequential sampling algorithm for multi-fidelity optimization based on an augmented expected improvement function that accounted for the difference in computational cost between model evaluation [14]. Xiong, Chen, and Tsoi used the uncertainty estimate from the GP model to develop an objective oriented sequential sampling algorithm for multi-fidelity optimization [17]. Chen et al. developed a design confidence metric based on the probability that an alternative design is better than the current optimum design [13].

## 2.3 Design Under Uncertainty

### 2.3.1 Deterministic Safety-Factor Based Design

A basic formulation of a deterministic safety-factor based design optimization problem with a single constraint is

$$\begin{aligned} \min_{\mathbf{x}} \quad & f(\mathbf{x}) \\ \text{s.t.} \quad & g(\mathbf{x}, \mathbf{u}_{det}) > 0 \end{aligned} \tag{2-10}$$

where  $\mathbf{x} \in \mathbb{R}^d$  is a vector of deterministic design variables,  $\mathbf{u}_{det} \in \mathbb{R}^p$  is a vector of conservative deterministic values used in place of aleatory random variables,  $f(\cdot)$  is a known objective function, and  $g(\cdot, \cdot)$  is a known constraint function. A safety factor may be incorporated into the specification of the conservative deterministic values  $\mathbf{u}_{det}$ . For example, Federal Aviation Regulations (FAR) for aircraft design require a safety factor of 1.5 applied to the prescribed limit loads (the maximum loads to be expected in service) [2, 49]. For a random load  $P$  we can define a conservative deterministic value

$$p_{det} = n \times \max(P) \tag{2-11}$$

where  $n = 1.5$  is a safety factor. Similarly, Federal Aviation Regulations 25.613 require allowable failure stresses for critical members that are below 99% (or 90% for redundant members) of the test failure stress with 95% confidence [50]. Neglecting the uncertainty in the distribution of  $S$  due to the limited testing sample size (i.e. 100% confidence), we can specify a conservative deterministic value

$$s_{det} = F_S^{-1}(1 - \alpha) \tag{2-12}$$

where  $F_S^{-1}(\cdot)$  is the inverse cumulative distribution function (inverse cdf) of  $S$  and  $\alpha = 0.99$  is the probability that the actual failure stress is less than the conservative value.

Engineers often compensate for uncertainty by using conservativeness such as conservative material properties, conservative limit loads, safety margins, and safety factors. Variation in material properties is addressed by Federal Aviation Regulations 25.613 which requires allowable failure stresses for critical members that are below 99% (or 90% for redundant members) of the test failure stress with 95% confidence [50]. Federal Aviation Regulations (FAR) for aircraft design require a safety factor of 1.5 applied to the prescribed limit loads (the maximum loads to be expected in service) [49][2]. The use of a factor of safety of 1.5 is widely accepted in the aircraft industry and the value can be traced back to the 1920's and 1930's when it was considered representative of the ratios of design to operating maneuver load factors [51]. A factor of safety of 1.4 is often used in spacecraft design [52]. The ultimate factor of safety is intended to cover [52]:

1. "Inadvertent in-service loads greater than the design limit load."
2. "Structural deflections above limit load that could compromise vehicle structural integrity."
3. "As-built part thickness within tolerance, but less than that assumed in the stress analysis."

According to Zipay, Modlin, and Larsen, the ultimate factor of safety is *not* intended to cover [52]:

1. "...errors in the structural analysis or structural math modeling"
2. "...poor design practice"
3. "...statistical material property variations"
4. "...process escapes"

Furthermore, Zipay et al. state "it is clear that no portion of the factor of safety can be used to correct for the necessary idealizations and potential errors that can occur in using these tools [sophisticated computation modeling] to analyze a complex structure."

Designers and engineers may add additional conservativeness, outside of that specified by regulations, to account for additional uncertainties. Ullman describes the following classical rule-of-thumb method for estimating the factor of safety

$$FS = FS_{\text{material}} \times FS_{\text{stress}} \times FS_{\text{geometry}} \times FS_{\text{failure analysis}} \times FS_{\text{reliability}} \quad (2-13)$$

where there are contributions from uncertainty in material properties, uncertainty in load, uncertainty in manufacturing tolerances, uncertainty in failure theory, and a factor related to the desired level of reliability [3, 53]. Ullman also proposes some simple steps for estimating a factor of safety based on coefficients of variation.

The selection of a safety factor has important implications in terms of structural weight. It has been estimated that reducing the factor of safety from 1.5 to 1.4 may reduce aircraft structural weight by 4% and that reducing the factor of safety from 1.5 to 1.25 may reduce weight 10.5% [52]. This is a significant reduction considering, for example, that weight scrub activities for Apollo were budgeted approximately \$10,000 per pound and for Shuttle \$50,000 per pound [52]. In order to achieve high levels of reliability without sacrificing performance, safety-factor based deterministic design is coupled with a variety of uncertainty reduction measures. One of the most important ways of reducing uncertainty in aircraft design is through building-block testing where tests of increasing complexity are performed starting with coupon tests on materials to determine properties and culminating in component and full-scale validation testing [22]. Safety factor based design, testing, and redesign processes are entrenched in the aircraft industry where these practices have evolved over more than 50 years, often by trial and error [4]. More modern probabilistic design approaches offer the promise of reducing cost and improving performance, however, it is likely the transition will be difficult due to the rich history of deterministic based design approaches.

### 2.3.2 Reliability-Based Design Optimization (RBDO)

A basic formulation of a reliability-based design optimization (RBDO) problem with a single constraint is

$$\begin{aligned} \min_{\mathbf{x}} \quad & f(\mathbf{x}) \\ \text{s.t.} \quad & P_U [g(\mathbf{x}, \mathbf{U}) < 0] \leq \bar{p}_f \end{aligned} \quad (2-14)$$

where  $\mathbf{x} \in \mathbb{R}^d$  is a vector of deterministic design variables,  $\mathbf{U} \in \mathbb{R}^p$  is a vector of aleatory random variables,  $f(\cdot)$  is a known objective function,  $g(\cdot, \cdot)$  is a known constraint function,  $\bar{p}_f$  is the target probability of failure, and  $P_U[\cdot]$  is a probability operator with respect to aleatory uncertainty  $\mathbf{U}$ . The reliability constraint from 2-14 can be written as

$$F_G(0) \leq \Phi(-\bar{\beta}) \quad (2-15)$$

where  $F_G(\cdot)$  is the cumulative distribution function (cdf) for  $g(\mathbf{x}, \mathbf{U})$ ,  $\Phi(\cdot)$  is the cdf for the standard normal distribution, and  $\bar{\beta} = -\Phi^{-1}(\bar{p}_f)$  is the target reliability index [54]. The cdf  $F_G(\cdot)$  is defined as

$$F_G(z) = P_U [g(\mathbf{x}, \mathbf{U}) < z] = \int_{g(\mathbf{x}, \mathbf{u}) < z} \dots \int f_U(\mathbf{u}) du_1 \dots du_n \quad (2-16)$$

Tu, Choi, and Park describe two alternative formulations of 2-15 through the use of inverse transformations

$$-\Phi^{-1}(F_G(0)) \geq \bar{\beta} \quad (2-17a)$$

$$F_G^{-1}(\Phi(-\bar{\beta})) \geq 0 \quad (2-17b)$$

where 2-17a is referred to as the reliability index approach (RIA) and 2-17b is referred to as the performance measure approach (PMA) [54]. In the reliability index approach reliability analysis is required and in the performance measure approach *inverse* reliability analysis is required.

### 2.3.2.1 Reliability index approach (RIA)

Using the reliability index approach, the RBDO formulation is

$$\begin{aligned} \min_{\mathbf{x}} \quad & f(\mathbf{x}) \\ \text{s.t.} \quad & \Phi(-\beta(\mathbf{x})) \leq \bar{p}_f \end{aligned} \quad (2-18)$$

where  $\Phi(\cdot)$  is the cumulative distribution function (cdf) for the standard normal distribution and  $\beta(\cdot)$  is the reliability index. The reliability index can be calculated through first-order reliability method (FORM) by solving an optimization problem for the most probable point (MPP)

$$\begin{aligned} \min_{\check{\mathbf{u}}} \quad & (\check{\mathbf{u}}^T \check{\mathbf{u}})^{1/2} \\ \text{s.t.} \quad & g(\mathbf{x}, \check{\mathbf{u}}) = 0 \end{aligned} \quad (2-19)$$

where  $\check{\mathbf{u}}$  is the vector  $\mathbf{U}$  transformed to standard normal space. The solution to 2-19 is the MPP  $\check{\mathbf{u}}_{MPP}$  and the reliability index is defined as

$$\beta(\mathbf{x}) = (\check{\mathbf{u}}_{MPP}^T \check{\mathbf{u}}_{MPP})^{1/2} \quad (2-20)$$

The reliability index approach with FORM is considered a double loop RBDO strategy because the design variables are manipulated in the outer loop and the reliability analysis is performed in the inner loop. This formulation is a nested optimization problem because the FORM optimization problem is solved for every constraint evaluation.

### 2.3.2.2 Performance measure approach (PMA)

In the performance measure approach, the RBDO formulation is [7, 54]

$$\begin{aligned} \min_{\mathbf{x}} \quad & f(\mathbf{x}) \\ \text{s.t.} \quad & g(\mathbf{x}, \mathbf{u}_{MPP}^{inv}) \leq 0 \end{aligned} \quad (2-21)$$

The *inverse* MPP  $\mathbf{u}_{MPP}^{inv}$  is found through inverse FORM [54] by solving an optimization problem

$$\begin{aligned} \min_{\check{\mathbf{u}}} \quad & g(\mathbf{x}, \check{\mathbf{u}}) \\ \text{s.t.} \quad & (\check{\mathbf{u}}^T \check{\mathbf{u}})^{1/2} = -\Phi^{-1}(\bar{p}_f) \end{aligned} \quad (2-22)$$

The solution to 2–22 is the inverse MPP  $\mathbf{u}_{MPP}^{inv}$ . Note that the inverse MPP  $\mathbf{u}_{MPP}^{inv}$  is equal to the MPP  $\mathbf{u}_{MPP}$  only if the target reliability index  $\bar{\beta}$  is equal to the reliability index of the design  $\beta(\mathbf{x})$ . This formulation is also referred to as the percentile formulation [7] because  $g(\mathbf{x}, \mathbf{u}_{MPP}^{inv})$  is the percentile of  $g(\mathbf{x}, \mathbf{U})$  such that

$$P_U [g(\mathbf{x}, \mathbf{U}) < g(\mathbf{x}, \mathbf{u}_{MPP}^{inv})] = \bar{p}_f \quad (2-23)$$

The performance measure approach with inverse FORM is also considered a double loop RBDO strategy because the design variables are manipulated in the outer loop and the reliability analysis is performed in the inner loop. This formulation is a nested optimization problem because the inverse FORM optimization problem is solved for every constraint evaluation.

### 2.3.2.3 Sequential optimization and reliability assessment (SORA)

The RIA and PMA formulations of RBDO are considered double-loop methods because the reliability analysis is nested within the design optimization. Other single-loop or decoupled RBDO formulations have been proposed in order to reduce the computational cost of RBDO. These formulations are of interest in the present research because they facilitate the comparison between RBDO methods and deterministic safety-factor based design. A comparison between traditional deterministic safety-factor based design and RBDO can be made by considering that the safety-factor and conservative values used in place of random variables are effectively converting a probabilistic constraint (e.g. probability of failure) to a conservative deterministic constraint. Wu and Wang proposed a method of converting reliability constraints to approximate deterministic constraints by replacing random variables with the MPP-based deterministic values [5]. This led to a safety-factor based approach for reliability based design [6]. Later, Du and Chen proposed the method of sequential optimization and reliability assessment (SORA) which also relies on converting a probabilistic constraint to an equivalent deterministic constraint [7].



### 2.3.3 RBDO with Epistemic Model Uncertainty

The majority of RBDO methods only consider aleatory parameter uncertainty. Epistemic model uncertainty is of particular interest in the present research. Specialized methods are required for handling epistemic model uncertainty not only because it is a different type of uncertainty (epistemic vs. aleatory) but also because it arises from a different source (model uncertainty vs. input parameter uncertainty). One of the few studies that sought to include model error in RBDO was by Mahadevan and Rebba [9]. This study simply modeled the epistemic model error as a random variable (see Section 2.2 for methods of modeling epistemic model error), however, the findings did show important consequences of epistemic model error. In one example, not considering epistemic model error resulted in a design that was heavier than required because the model overestimated the probability of failure. In another example, not considering epistemic model error resulted in a design that was lighter but did not meet the reliability constraint because the model underestimated the probability of failure. There are two areas for improvement in the method described by Mahadevan and Rebba. First, it may be important to model the epistemic model error as varying with the location in the design space as discussed in Section 2.2. Second, it is important to make a distinction between epistemic and aleatory variables in the reliability assessment. If there is epistemic model error then the true probability of failure is unknown and instead we should calculate a distribution of *possible* probabilities of failure. The distribution of probabilities of failure represents the uncertainty in the probability of failure of the true system.

In order to reduce the computational cost of repeated model evaluations during uncertainty propagation, surrogate models have been proposed as cheap approximations. Studies that use surrogate models in RBDO also encounter a situation of mixed uncertainty. The interesting aspect of these methods in the present research is how these methods handle the epistemic model error that is introduced by the surrogate

approximations. In Section 2.4, the idea that epistemic model error results in a distribution of possible optimums is introduced. There is also a distribution of *possible* RBDO optimums when performing RBDO with epistemic model error. In other words, since the true probability of failure is unknown it is possible that many different designs would satisfy the reliability constraint. However, most surrogate based approaches to RBDO do not consider this uncertainty in the optimum design and instead focus on bounding and reducing the uncertainty in probability of failure.

One EGO inspired algorithm (see EGO in Section 2.4) for RBDO is Efficient Global Reliability Analysis (EGRA) [55]. The EGRA method defines an infill sampling criteria called expected feasibility based on integrating over a region in the immediate vicinity of the constraint boundary. The EGRA method samples the location of the maximum expected feasibility, updates the surrogate model, and repeats this process until the maximum expected feasibility is small. Only after the surrogate model is sufficiently refined is the surrogate used to calculate the probability of failure. Thus, EGRA avoids considering epistemic model error in the reliability assessment by performing many evaluations near the constraint boundary to reduce the epistemic model error to a negligible level. Another method based on surrogate models is the response surface method proposed by Kim and Choi [10]. In this method the prediction interval for the response surface (i.e. epistemic model error) is used to find upper and lower bounds on the reliability index. The prediction interval for the response surface provides an interval of a possible future observation for a given confidence level specified by the engineer. A conservative optimum design is found based on the lower bound of the reliability index. However, to avoid being overly conservative additional sampling is triggered if the upper bound on the reliability index is too high. Another surrogate based approach to RBDO was proposed by Dubourg [56]. In this method probability of failure bounds are estimated by calculating the probability of failure with respect to a conservative and an unconservative Kriging prediction.

### 2.3.4 Uncertainty Reduction Measures

Uncertainty reduction measures, such as testing and quality control, can be used to reduce the uncertainty in the performance and reliability of a final design. However, this uncertainty reduction is often not quantified. Acar et al. found that that certification tests in aircraft design reduce modeling error and result in a much lower calculated probability of failure than using safety factors alone [57]. Acar, Haftka, and Johnson showed that quality control to truncate the tail on the distribution of material properties can be very effective when the a low probability of failure is required [58].

## 2.4 Global Optimization

According to Box and Draper [1], "Essentially, all models are wrong, but some are useful." In general, all models are approximations of the true process and therefore contain some epistemic model uncertainty. In engineering design, many methods consider only uncertainty in model inputs (i.e. parameter uncertainty) and not model uncertainty. In contrast, many global optimization algorithms focus exclusively on epistemic model uncertainty. Some popular global optimization algorithms reduce computational cost by introducing cheap surrogate approximations, however, the surrogate models also introduce significant epistemic model uncertainty. Surrogate based global optimization methods are of interest in the present discussion because the methods acknowledge the effects of high epistemic model error on optimization and explore methods for dealing with this uncertainty. The introduction of epistemic model uncertainty means these algorithms must balance the need to explore regions of high uncertainty and exploit regions where the surrogate predicts high performance. Since all models have some degree of epistemic uncertainty, these methods can be interpreted as representative of a typical design problem where we wish to optimize the true process but instead settle for optimizing a computer model.

In surrogate based global optimization, a typical approach is to fit a surrogate based on an initial design of experiment (DoE) and then sequentially add new points each

iteration to reduce the epistemic model error in regions of interest. These new sample points are called the infill samples and many infill sampling criteria have been proposed. Watson and Barnes proposed three different infill sampling criteria they described as locating threshold-bounded extremes, locating regional extremes, and minimizing surprises [59]. An important aspect of this work by Watson and Barnes was translating engineering objectives in to appropriate sampling criteria. Therefore, the selection of the “best” infill sampling criteria depends on the engineering objective. A very popular method of global optimization known as Efficient Global Optimization (EGO) was proposed by Jones et al. [60]. In EGO the infill sampling criteria is the maximization of the expected improvement. The expected improvement is defined by weighting all the possible improvements by the associated probability density. The EGO method was developed for unconstrained optimization, but Schonlau describes a simple method of adapting the method to constrained optimization problems [61]. Schonlau proposes multiplying the expected improvement by the probability that each constraint is met (i.e. probability of feasibility). An alternative method of handling constraints with EGO is to add a penalty to the infill sampling criteria in the infeasible region [62]. A third alternative is to solve the infill sampling criteria problem as a constrained optimization problem [63]. Parr et al. compares the performance of different infill sampling criteria with constraint handling on analytical examples and as applied to a wing design problem [64].

The Informational Approach to Global Optimization (IAGO) offers a different perspective on infill sampling [65]. Most infill sampling criteria look for likely locations of the optimum  $x^*$  and then sample at this location. In contrast, the IAGO method seeks to choose a new sample based on gaining the most information about the likely location of  $x^*$ . The method relies on estimating the probability density of the possible optimums  $X^*$ . Note that the epistemic model error in the objective function results in a distribution of possible global optimums. In particular, IAGO estimates the distribution

of possible optimum designs conditional on sampling at a new location  $x_c$ . First it is necessary to simulate a possible realization of the true function at this location and then conditional simulations are performed to estimate the distribution of possible optimums conditional on that realization. The process is repeated for many different possible realizations of the function at location  $x_c$ . Although IAGO has only been applied to unconstrained global optimization, we might reason that there is also a distribution of possible optimums for constrained optimization problems under epistemic model error. The concept of a distribution of possible optimums may also be important when performing reliability-based design optimization (RBDO) with epistemic model error.

### CHAPTER 3

#### DECIDING DEGREE OF CONSERVATIVENESS IN INITIAL DESIGN CONSIDERING A FUTURE TEST AND POSSIBLE REDESIGN

$\mathbf{x}$	Design variable vector
$\mathbf{U}$	Aleatory random variable vector
$n$	Safety margin
$e$	Epistemic model error
$f(\cdot, \cdot)$	Objective function
$g(\cdot, \cdot)$	Limit-state function
$q$	Redesign indicator function
$p_{re}$	Probability of redesign
$p_f$	Probability of failure
$\mathbb{E}[\cdot]$	Expected value operator
$\mathbb{P}[\cdot]$	Probability operator
$\text{Var}(\cdot)$	Variance operator

#### *Subscripts*

$L$	Low-fidelity model
$H$	High-fidelity model
$T$	True model
$det$	Deterministic value
$ini$	Initial design
$re$	Design after redesign
$final$	Final design after possible redesign
$lb$	Lower bound
$ub$	Upper bound
$f$	Failure
$U$	Aleatory uncertainty

*E* Epistemic uncertainty

### *Superscripts*

(*i*) Epistemic realization

★ Target value in optimization

### *Accents*

– Mean value

## 3.1 Introduction

Engineering design is an iterative process. Early in the design process engineers often utilize low-fidelity models which may be associated with high uncertainty. Model uncertainty is classified as *epistemic uncertainty* when it arises due to lack of knowledge, it is reducible by gaining more information, and it has only a single true (but unknown) value [31, 66, 67]. In addition, almost all engineering designs are subject to *aleatory uncertainty* (e.g. loading, material properties, etc.). The input parameter uncertainty is classified as aleatory if it is due to natural or inherent variability, it is irreducible, and it is a distributed quantity. In the future when prototypes are tested or high-fidelity simulations are performed, new knowledge will become available that reduces epistemic uncertainty and may result in a decision to change the initial design. Changing the initial design, referred to as *redesign* or *engineering change (EC)*, is an important issue for industry and engineering management [68, 69]. Redesign is often viewed negatively because it is associated with costs and delays, however, it is also an opportunity for design improvement [68].

Research related to redesign, or engineering change, has mostly been performed at the system level requiring a high-level of abstraction. These methods include the Change Prediction Method (CPM) [70], the RedesignIT computer program [71], a pattern-based redesign methodology [72], a combination of a function-behavior-structure

(FBS) linkage model with the CPM method [73], and a Monte Carlo simulation (MCS) based method of estimating redesign risk [74].

At a lower level of abstraction, redesign is typically triggered when an initial design is later revealed to not meet specifications or constraints due to model uncertainty. Roser and Kazmer proposed the flexible design method which allows a designer to minimize total expected costs while considering possible future design changes [75, 76]. Roser et al. demonstrated an economic method for deciding between design changes with different levels of uncertainty and different associated costs [77]. Villanueva et al. simulated the effects of future tests and redesign on an integrated thermal protection system (ITPS) considering the effect of redesign on the uncertainty in the probability of failure [19]. Matsumura et al. compared reliability-based design optimization (RBDO) considering future redesign to traditional RBDO [20]. Villanueva et al. demonstrated the tradeoff between expected design performance and probability of redesign for the ITPS example [21]. Price et al. compared designer versus company perspectives on starting with a higher safety margin and possibly redesigning to improve performance to starting with a lower safety margin and possibly redesigning to improve safety [23]. This study develops a generalized formulation of the previously application specific formulations [19, 21, 23] and explores how the degree of conservativeness in the initial design relates to the expected design performance after possible redesign. In related work, Price et al. introduced a Kriging surrogate to represent epistemic model uncertainty in order to consider spatial variations in model uncertainty in the context of simulating the effects of future tests and redesign [25].

Redesign is often caused by epistemic model uncertainty. If engineers had access to models that were capable of perfectly predicting design performance then the initial design would definitely satisfy design constraints and redesign could largely be avoided. Assuming a known true model, reliability-based design optimization (RBDO) has mostly focused on ensuring a prescribed level of reliability given known aleatory parameter



uncertainty [7, 54, 78]. Therefore, most RBDO formulations are implicitly conditional on the model of the system exactly matching the true physics of the system. Some studies have sought to specifically address the incorporation of model uncertainty into reliability-based design [9, 41, 79]. However, to compensate for all the lack of knowledge (i.e. epistemic model uncertainty) that is present at the initial design stage then the initial design may need to be very conservative. In reality, engineering design is an iterative process where over time designs are tested, experiments are performed, models are improved, and new knowledge is gained that reduces epistemic uncertainty. If there will be a future opportunity to reduce epistemic uncertainty and possibly change the initial design (i.e. redesign), then this may affect the selection of the initial design.

Typically, an initial design will have some *safety margin* relative to design constraints in order to improve safety, but also to provide some insurance against future redesign [80]. When selecting a safety margin for the initial design, designers face a dilemma in whether to start with a larger initial safety margin (i.e. more conservative initial design) and possibly performing redesign to improve performance versus starting with a smaller safety margin (i.e. less conservative initial design) and possibly performing redesign to restore safety. This decision to be more or less conservative in the design process is similar to the question of optimistic versus pessimistic design practices as explored by Thornton [81]. This paper proposes a general method for optimizing the safety margins governing a two-stage deterministic design process in order to control the epistemic uncertainty in the final design, design performance, and probability of failure. The method considers the probability of future redesign while selecting the initial design. This allows for the tradeoff between expected final design performance and redesign risk while still ensuring reliability. The method is demonstrated on a simple bar problem and then on an engine design problem.

The methods are described in Section 3.2. In Section 3.3, the method is applied to the design of a minimum weight uniaxial tension bar and then to the engine design of a

supersonic business jet. The discussions and conclusions are presented in Section 3.4. Limitations of the proposed method and perspectives for future work are presented in Section 3.5.

## 3.2 Methods

The deterministic design process consists of selecting an initial design, testing the initial design, and possibly performing calibration and redesign. The process is controlled by an initial safety margin  $n_{ini}$ , lower and upper bounds on acceptable safety margins  $n_{lb}$  and  $n_{ub}$ , and a redesign safety margin  $n_{re}$ . These safety margins  $\mathbf{n} = \{n_{ini}, n_{lb}, n_{ub}, n_{re}\}$  are optimized as described in Section 3.2.1. The optimizer calls a function to perform a crude Monte Carlo simulation (MCS) of epistemic error realizations as described in Section 3.2.2. The complete design, test, and possible calibration and redesign process is carried out for each realization of epistemic error as described in Section 3.2.3. Probability of redesign, expected probability of failure, and expected design cost are calculated from the MCS as described in Section 3.2.4.

### 3.2.1 Optimization of Safety Margins

The safety margins  $\mathbf{n}$  are optimized to minimize the expected value of the design cost function subject to constraints on expected probability of failure and probability of redesign. The formulation of the optimization problem is

$$\begin{aligned}
 \min \quad & \mathbb{E}_E [\mathbb{E}_U [f(\mathbf{X}_{final}, \mathbf{U})]] \\
 \text{w.r.t} \quad & \mathbf{n} = \{n_{ini}, n_{lb}, n_{ub}, n_{re}\} \\
 \text{s.t.} \quad & \mathbb{E}_E [P_{f,final}] \leq p_f^* \\
 & p_{re} \leq p_{re}^* \\
 & n_{lb} \leq n_{ub} \\
 & \mathbf{n}_{min} \leq \mathbf{n} \leq \mathbf{n}_{max}
 \end{aligned} \tag{3-1}$$

where  $\mathbb{E}_E[\cdot]$  is the expectation with respect to epistemic uncertainty,  $\mathbb{E}_U[\cdot]$  is the expectation with respect to aleatory uncertainty,  $f(\cdot, \cdot)$  is an objective function,  $\mathbf{X}_{final}$

is the vector of final design variables,  $\mathbf{U}$  is a vector of aleatory random variables,  $P_{f,final}$  is the final probability of failure, and  $p_{re}$  is the probability of redesign. The final design and final probability of failure are epistemic random variables. In the objective function, the mean is first calculated with respect to aleatory uncertainty for each design realization and then the expectation is calculated over the means with respect to epistemic uncertainty. The optimization is based on a MCS as seen in Figure 3-1. Solving the optimization problem for different values of  $p_{re}^*$  results in a tradeoff between expected cost and probability of redesign. Covariance Matrix Adaptation Evolution Strategy (CMA-ES) with a penalization strategy to handle the constraints is used to solve the optimization problem[82].

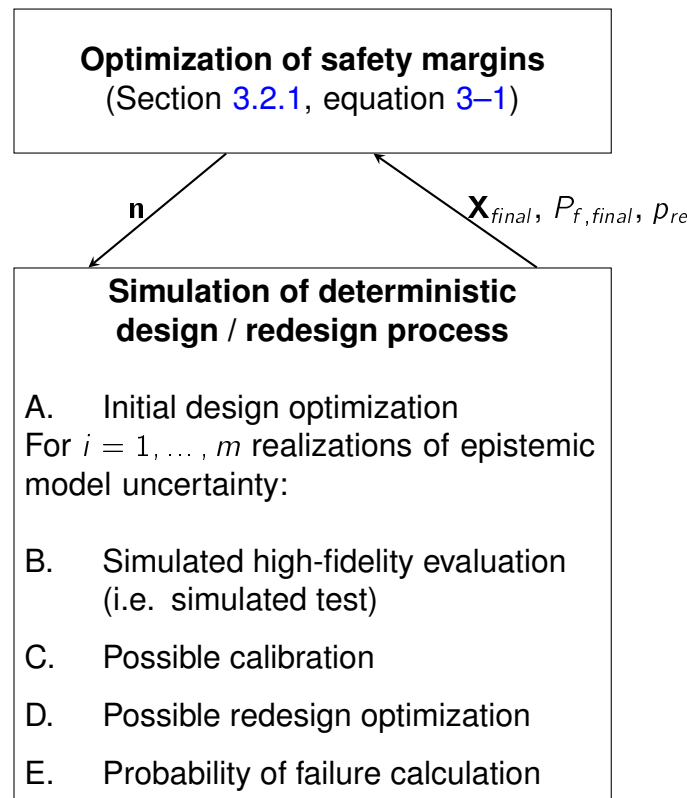


Figure 3-1. The safety margins are optimized based on a MCS of the deterministic design / redesign process

### 3.2.2 Monte-Carlo Simulation of Epistemic Model Error

The epistemic model uncertainty and aleatory parameter uncertainty are treated separately. To represent epistemic model uncertainty we introduce the epistemic random variables  $E_L$  and  $E_H$  to represent the error in the low and high-fidelity models respectively. To simplify the propagation of mixed epistemic model uncertainty and aleatory parameter uncertainty, it is assumed that there is a fixed but unknown bias between the low-fidelity model, the high-fidelity model, and the true model. The assumed relationship between the different fidelity models is

$$g_T(\mathbf{x}, \mathbf{u}) = g_H(\mathbf{x}, \mathbf{u}) + e_H = g_L(\mathbf{x}, \mathbf{u}) + e_L \quad (3-2)$$

where  $\mathbf{x} \in \mathbb{R}^d$  is a vector of design variables,  $\mathbf{u}$  is a vector of aleatory random variables with a realization  $\mathbf{u} \in \mathbb{R}^p$ ,  $g_T(\cdot, \cdot)$  is the true model,  $g_H(\cdot, \cdot)$  is the high-fidelity model,  $g_L(\cdot, \cdot)$  is the low-fidelity model,  $e_H \in \mathbb{R}$  is the true error in the high-fidelity model, and  $e_L \in \mathbb{R}$  is the true error in the low-fidelity model. It is assumed that the possible errors are known based on expert opinion or previous experience. The possible model errors  $E_L$  and  $E_H$  are modeled as two independent uniformly distributed epistemic random variables with  $\text{Var}(E_H) < \text{Var}(E_L)$ .

The true model is predicted based on the distribution of error  $E_L$  as

$$G_T(\mathbf{x}, \mathbf{u}) = g_L(\mathbf{x}, \mathbf{u}) + E_L \quad (3-3)$$

Similarly, the high-fidelity model is predicted as

$$G_H(\mathbf{x}, \mathbf{u}) = g_L(\mathbf{x}, \mathbf{u}) + E_L - E_H \quad (3-4)$$

Let  $g_T^{(i)}(\cdot, \cdot)$  denote a realization of  $G_T(\cdot, \cdot)$  and  $\Omega_E$  denote the epistemic sampling space. It is assumed that there exists an epistemic realization,  $\exists e_L^{(i)} \in \Omega_E$ , such that the realization corresponds to the true process,  $g_T^{(i)}(\cdot, \cdot) = g_T(\cdot, \cdot)$ . This follows from the assumption that the true relationship can be written as shown in equation 3-2 and the

assumption that the epistemic random variable  $E_L$  includes the true model error. The mean of the possible errors is defined as  $\bar{e}_L$  and  $\bar{e}_H$ . The mean prediction with respect to epistemic uncertainty of the high-fidelity model and true model are defined as  $\bar{g}_H(\cdot, \cdot)$  and  $\bar{g}_T(\cdot, \cdot)$  respectively.

A crude Monte Carlo simulation of  $i = 1, \dots, m$  error realizations is performed. In Section 3.2.3, design / redesign process is described conditional on one pair of error samples. The deterministic design / redesign process is repeated for many different error realizations. Based on the MCS, the risk of redesign is estimated. Furthermore, the MCS explores how failing a future test is related to the final design performance and safety.

### 3.2.3 Deterministic Design / Redesign Process

A flowchart of the design / redesign process is shown in Figure 3-2. The design process consists of selecting an initial design, a simulated evaluation of the initial design with a high-fidelity model, possible redesign, and a reliability assessment. In sections 3.2.3.1 to 3.2.3.3 the process is described conditional on the error realizations  $E_L = e_L^{(i)}$  and  $E_H = e_H^{(i)}$

#### 3.2.3.1 Initial design

The selection of the initial design is based on a deterministic safety-margin-based optimization problem

$$\begin{aligned}
 &\min \quad f(\mathbf{x}, \mathbf{u}_{det}) \\
 &\text{w.r.t. } \mathbf{x} \\
 &\text{s.t.} \quad \bar{g}_T(\mathbf{x}, \mathbf{u}_{det}) - n_{ini} \geq 0 \\
 &\quad \mathbf{x}_{min} \leq \mathbf{x} \leq \mathbf{x}_{max}
 \end{aligned} \tag{3-5}$$

where  $\mathbf{u}_{det}$  is a vector of deterministic values that are substituted for aleatory random variables. Note that if the low-fidelity model is believed to be unbiased,  $\bar{e}_L = 0$ , then the mean prediction of the true model is simply the low-fidelity model  $g_L(\cdot, \cdot)$ . The failure

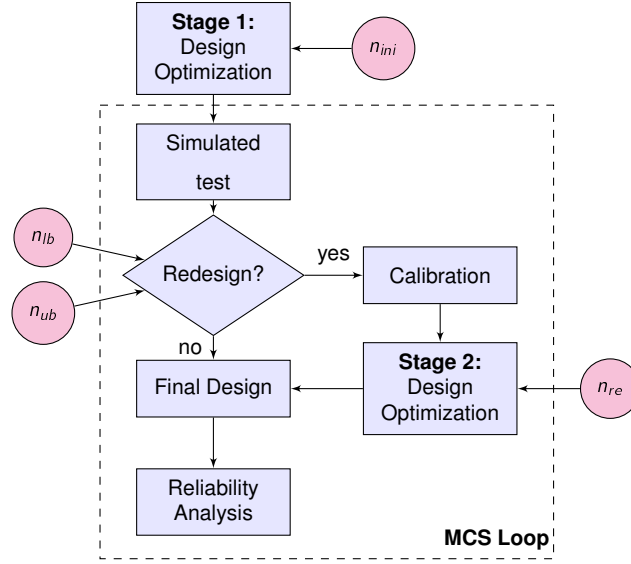


Figure 3-2. Flowchart showing steps in two-stage deterministic design / redesign process. Safety margins  $\mathbf{n} = \{n_{ini}, n_{lb}, n_{ub}, n_{re}\}$  are shown as inputs at relevant steps.

domain is defined with respect to the true (but unknown) model  $g_T(\cdot, \cdot)$  as

$$\Omega_f(\mathbf{x}) = \{\mathbf{u} \in \Omega_U | g_T(\mathbf{x}, \mathbf{u}) < 0\} \quad (3-6)$$

where  $\Omega_U$  is the aleatory sampling space. Let  $\mathbf{x}_{ini}$  denote the optimum design found from Equation 3–5 using initial safety margin  $n_{ini}$ . It is assumed that the conservative values  $\mathbf{u}_{det}$  are based on regulations (e.g. FAR §25.613 [50], FAR§25.303 [2]) and/or previous experience.

### 3.2.3.2 Testing initial design and redesign decision

In the future, the initial design  $\mathbf{x}_{ini}$  will be evaluated with the high-fidelity model to measure the safety margin. In the Monte-Carlo simulation, the test is based on a simulated high-fidelity evaluation  $g_H^{(i)}(\mathbf{x}_{ini}, \mathbf{u}_{det})$ . If  $n_{lb} \leq g_H^{(i)}(\mathbf{x}_{ini}, \mathbf{u}_{det}) \leq n_{ub}$  then the initial design will pass the test and be accepted as the final design. However, if  $g_H^{(i)}(\mathbf{x}_{ini}, \mathbf{u}_{det}) < n_{lb}$  then the design is unsafe and redesign will be performed to improve safety. If  $g_H^{(i)}(\mathbf{x}_{ini}, \mathbf{u}_{det}) > n_{ub}$  then redesign is performed to improve performance because the initial design is too conservative. An indicator function for the redesign

decision is denoted  $q^{(i)}$  which is one for redesign and zero otherwise. Redesign initiated due to a low safety margin ( $g_H^{(i)}(\mathbf{x}_{ini}, \mathbf{u}_{det}) < n_{lb}$ ) is referred to as redesign for safety and redesign initiated due to a high safety margin ( $g_H^{(i)}(\mathbf{x}_{ini}, \mathbf{u}_{det}) > n_{ub}$ ) is referred to as redesign for performance.

### 3.2.3.3 Model calibration

Before redesign, the mean prediction of the true model  $\bar{g}_T(\cdot, \cdot)$  is calibrated based on the test result. The model is calibrated deterministically based on the difference between the prediction and the high-fidelity evaluation of the initial design. The calibrated model is

$$g_{calib}^{(i)}(\mathbf{x}, \mathbf{u}) = \bar{g}_T(\mathbf{x}, \mathbf{u}) + e_{calib}^{(i)} \quad (3-7)$$

where  $e_{calib}^{(i)} = g_H^{(i)}(\mathbf{x}_{ini}, \mathbf{u}_{det}) - \bar{g}_T(\mathbf{x}_{ini}, \mathbf{u}_{det})$ . The calibrated model  $G_{calib}(\cdot, \cdot)$  accounts for changes in the model that might occur during the future calibration. The calibration improves the model when the high-fidelity model is more accurate than the low-fidelity model,  $|e_H^{(i)}| < |e_L^{(i)}|$ . This simple method of calibration works well because of the underlying assumption that the model bias is constant as described in Equation 3-2. Due to the assumption of constant model bias, the error in the low-fidelity model is canceled out during calibration and the calibrated model is simply equal to the high-fidelity model,  $g_{calib}^{(i)}(\cdot, \cdot) = g_H^{(i)}(\cdot, \cdot)$ .

### 3.2.3.4 Redesign

If the test is not passed, redesign will be performed to find a new design using the calibrated model  $g_{calib}^{(i)}(\cdot, \cdot)$  and a new safety margin  $n_{re}$ . The deterministic design problem for selecting a new design after calibration is

$$\begin{aligned} \min \quad & f(\mathbf{x}, \mathbf{u}_{det}) \\ \text{w.r.t.} \quad & \mathbf{x} \\ \text{s.t.} \quad & g_{calib}^{(i)}(\mathbf{x}, \mathbf{u}_{det}) - n_{re} \geq 0 \\ & \mathbf{x}_{min} \leq \mathbf{x} \leq \mathbf{x}_{max} \end{aligned} \quad (3-8)$$

Let  $\mathbf{x}_{re}^{(i)}$  denote the solution to Equation 3–8. The new design  $\mathbf{X}_{re}$  is an epistemic random variable because it is conditional on the unknown outcome of the future high-fidelity evaluation. However, there is no inherent variability (i.e. aleatory uncertainty) in the design choice. The new design is a random variable only because it is unknown at the initial design stage. Note that the feasible design space of the redesign problem Equation 3–8 is different than the feasible design space in the initial design problem Equation 3–5 due to the calibration and the use of a safety margin  $n_{re}$  that may be different than  $n_{ini}$ . Conditional on the outcome of the future test, some designs with improved performance may become accessible during redesign that were previously considered infeasible or some designs that were previously considered reasonable may be revealed to be unsafe.

### 3.2.4 Probabilistic Evaluation

Each set of safety margins  $\mathbf{n}$  results in a probability of redesign  $p_{re}$ , a final probability of failure after possible redesign  $P_{f,final}$  (epistemic random variable), and a final cost  $\mathbb{E}_U[f(\mathbf{X}_{final}, \mathbf{U})]$  (epistemic random variable). Histograms of random variables are obtained based on a crude MCS as described in Section 3.2.2. The expected values with respect to epistemic model uncertainty that are used in Equation 3–1 are obtained using numerical integration.

The probability of redesign is  $p_{re} = \mathbb{E}_E[Q]$ . After possible redesign, the final design is

$$\mathbf{x}_{final}^{(i)} = (1 - q^{(i)}) \mathbf{x}_{ini} + q^{(i)} \mathbf{x}_{re}^{(i)} \quad (3-9)$$

The expected mean design cost after possible redesign is  $\mathbb{E}_E[\mathbb{E}_U[f(\mathbf{X}_{final}, \mathbf{U})]]$ . The expected mean design cost can be written in terms of conditional probabilities as

$$\begin{aligned} \mathbb{E}_E[\mathbb{E}_U[f(\mathbf{X}_{final}, \mathbf{U})]] &= (1 - p_{re})\mathbb{E}_U[f(\mathbf{x}_{ini}, \mathbf{U})] + \\ & p_{re}\mathbb{E}_E[\mathbb{E}_U[f(\mathbf{X}_{re}, \mathbf{U})] | Q = 1] \end{aligned} \quad (3-10)$$



where  $\mathbb{E}_U[f(\mathbf{x}_{ini}, \mathbf{U})]$  is the expected mean design cost conditional on passing the test and  $\mathbb{E}_E[\mathbb{E}_U[f(\mathbf{X}_{re}, \mathbf{U})] | Q = 1]$  is the expected mean design cost conditional on failing the test.

The final safety margin with respect to the high-fidelity model after possible redesign is

$$n_{H,final}^{(i)} = (1 - q^{(i)}) g_H^{(i)}(\mathbf{x}_{ini}, \mathbf{u}_{det}) + q^{(i)} g_H^{(i)}(\mathbf{x}_{re}^{(i)}, \mathbf{u}_{det}) \quad (3-11)$$

where the high-fidelity model is equal to the calibrated model due to the calibration process as described in Section 3.2.3.3. The final safety margin with respect to the true model after possible redesign is

$$n_{T,final}^{(i)} = (1 - q^{(i)}) g_T^{(i)}(\mathbf{x}_{ini}, \mathbf{u}_{det}) + q^{(i)} g_T^{(i)}(\mathbf{x}_{re}^{(i)}, \mathbf{u}_{det}) \quad (3-12)$$

Due to epistemic model uncertainty the true probability of failure is unknown. A realization of the probability of failure for the initial design is

$$p_{f,ini}^{(i)} = \mathbb{P}_U \left[ g_T^{(i)}(\mathbf{x}_{ini}, \mathbf{U}) < 0 \right] \quad (3-13)$$

where  $\mathbb{P}_U[\cdot]$  denotes the probability with respect to aleatory uncertainty. In the probability of failure calculation, epistemic model uncertainty is treated separately from the aleatory uncertainty. There is epistemic uncertainty in the true probability of failure with respect to aleatory uncertainty due to epistemic model uncertainty. In reality, the true probability of failure of the final design does not depend on model fidelity. However, our knowledge of the true probability of failure depends on the uncertainty in our models. To account for model uncertainty, the probability of failure calculation is repeated conditional on different realizations of the true model  $g_T^{(i)}(\cdot, \cdot)$  as shown in

Equation 3–13. After redesign the probability of failure is

$$p_{f, re}^{(i)} = \mathbb{P}_U \left[ g_T^{(i)}(\mathbf{x}_{re}^{(i)}, \mathbf{U}) < 0 \right] \quad (3-14)$$

The design variable  $\mathbf{x}_{re}^{(i)}$  is an epistemic random variable because it is conditional on the outcome of the future test. The final probability of failure after possible redesign is

$$p_{f, final}^{(i)} = (1 - q^{(i)}) p_{f, ini}^{(i)} + q^{(i)} p_{f, re}^{(i)} \quad (3-15)$$

The expected probability of failure after possible redesign is  $\mathbb{E}_E [P_{f, final}]$ . The expected probability of failure can be written in terms of conditional probabilities as

$$\begin{aligned} \mathbb{E}_E [P_{f, final}] &= (1 - p_{re}) \mathbb{E}_E [P_{f, ini} | Q = 0] + \\ &\quad p_{re} \mathbb{E}_E [P_{f, re} | Q = 1] \end{aligned} \quad (3-16)$$

where  $\mathbb{E}_E [P_{f, ini} | Q = 0]$  is the expected probability of failure conditional on passing the test and  $\mathbb{E}_E [P_{f, re} | Q = 1]$  is the expected probability of failure conditional on failing the test. We can see from Equation 3–16 that the expected final probability of failure is a weighted average of the expected probability of failure of the initial design and the expected probability of failure of the possible redesigns.

### 3.3 Test Cases

#### 3.3.1 Uniaxial Tension Test

##### 3.3.1.1 Problem description

In this example we consider the design of a minimum weight bar subject to uniaxial loading. The problem definition is shown in Table 3-1. The design is subject to aleatory uncertainty in loading and material properties. In addition, there is epistemic model uncertainty in the limit-state function describing the yielding of the bar. The uncertain parameters are defined as shown in Table 3-2. The bar is designed to minimize the mass, or equivalently cross sectional area, subject to a stress constraint. The bar is designed using conservative values in place of random loads and material properties. In

Table 3-1. Problem definition for uniaxial tension test example

	Description	Notation
Design variable	Cross sectional area (mm <sup>2</sup> )	$x = a$
Aleatory variables	Applied load, material strength	$\mathbf{U} = \{P, S\}$
Conservative values	Limit load, allowable strength	$\mathbf{u}_{det} = \{1600 \text{ N}, 15.35 \text{ MPa}\}$
Objective function	Cross sectional area (mm <sup>2</sup> )	$f(x) = a$
Limit-state function	Yielding	$g_L(x, \mathbf{U}) = S - P/a$
Target mean reliability		$p_f^* = 1 \times 10^{-5}$

Table 3-2. Uncertain parameters for uniaxial tension test example

Parameter	Classification	Symbol	Mean, $\mu$	C.O.V	Range	Distribution
Applied load	Aleatory	$P$ (N)	1000	0.20	$[-\infty, \infty]$	Normal
Material strength	Aleatory	$S$ (MPa)	20	0.12	$[-\infty, \infty]$	Normal
Error in low-fidelity model	Epistemic	$E_L$ (MPa)	0	–	$[-4.35, 4.35]$	Uniform
Error in high-fidelity model	Epistemic	$E_H$ (MPa)	0	–	$[-2.18, 2.18]$	Uniform

the future, the bar will be tested (e.g. high-fidelity simulation or prototype test) and it will be redesigned if the safety margin with respect to the stress constraint is too high or too low.

The problem follows the general method described in Section 3.2. The limit-state function is a linear function of the aleatory parameters and all aleatory parameters are assumed to be normally distributed. Therefore, the computational cost is reduced by calculating the reliability index analytically for each realization of epistemic model error. Due to the simplicity of the design problem, the optimum deterministic design can be obtained directly by solving for the value of the design variable that satisfies the deterministic constraint.

### 3.3.1.2 Expected performance versus probability of redesign

Tradeoff curves for expected cost,  $\mathbb{E}_E[f(\mathbf{X}_{final})]$ , versus probability of redesign,  $p_{re}$ , are shown in Figure 3-3. The tradeoff curves were obtained by solving Equation

3–1 for several values of the constraint on probability of redesign,  $p_{re}^*$ . The two curves correspond to the special cases of performing redesign only for performance and performing redesign only for safety. It was observed that redesign for performance was the global optimum solution and the optimum safety margins would converge to this solution when allowing for both redesign for safety and performance.

The expected mass of the bar decreases with increasing risk of redesign. When there is zero probability of redesign, the initial design must be conservative enough that the expected probability of failure is less than or equal to the target value of  $1 \times 10^{-5}$ . To meet the target expected probability of failure the initial design must be heavier. This is the design we would obtain if we optimized only  $n_{ini}$  to minimize the weight of the initial design with a constraint on expected probability of failure. Both curves start at this design because the probability of redesign is zero and therefore there is no difference between the redesign strategies. As the probability of redesign increases, redesign can be used to correct the initial design if the high-fidelity model reveals the safety margin is too high or too low.

To explore the simulation in more detail, the points on the tradeoff curve corresponding to 20% probability of redesign were selected. Histograms of the area of the cross section of the bar, safety margin with respect to the high-fidelity model, safety margin with respect to true model, reliability index, and probability of failure for 20% probability of redesign are shown in figures 3-4, 3-5, 3-6, 3-7, 3-8. Statistics on the mass and probability of failure before and after redesign are listed in Table 3-3. When considering only redesign for performance, the initial design is heavier and redesign is performed if the safety margin is revealed to be too high. Observing a high safety margin is correlated with the design being very safe. Redesign for performance has the effect of increasing the probability of failure in order to reduce the mass if the initial design is revealed to be very safe. When considering only redesign for safety, the initial design is lighter and redesign is performed if the safety margin is revealed to be too low.

Table 3-3. Results for uniaxial tension example for 20% probability of redesign

Description	Notation	Redesign for Safety	Redesign for Performance
Probability of redesign	$p_{re}$	0.20	0.20
Cost of initial design	$f(x_{ini})$	155.5	170.7
Expected cost conditional on performing redesign	$\mathbb{E}_E [f(X_{re}) Q = 1]$	191.2	109.4
Expected cost after possibly performing redesign	$\mathbb{E}_E [f(X_{final})]$	162.7	158.4
Expected probability of failure of initial design	$\mathbb{E}_E [P_{f,ini}]$	$2.9 \times 10^{-5}$	$0.9 \times 10^{-5}$
Expected probability of failure of initial design conditional on passing test	$\mathbb{E}_E [P_{f,ini} Q = 0]$	$0.9 \times 10^{-5}$	$1.2 \times 10^{-5}$
Expected probability of failure of new designs conditional on failing test	$\mathbb{E}_E [P_{f,re} Q = 1]$	$1.3 \times 10^{-5}$	$0.4 \times 10^{-5}$
Expected probability of failure after possibly performing redesign	$\mathbb{E}_E [P_{f,final}]$	$1.0 \times 10^{-5}$	$1.0 \times 10^{-5}$

Observing a low safety margin is correlated with the design being unsafe. Redesign for safety has the effect of truncating the tail of the probability of failure distribution corresponding to high probabilities of failure. If the initial design is revealed to be unsafe, the cross sectional area is increased during redesign resulting in a safer, but heavier design.

The redesign decision is based on the safety margin with respect to the high-fidelity model and therefore suffers from the error in the high-fidelity model. The error in the high-fidelity model results in imperfect truncation of the true safety margin and reliability index distributions as shown in figures 3-6, 3-7.

### 3.3.1.3 Expected performance versus level of high-fidelity model error

To explore the effect of the error in the high-fidelity model, the ratio of the standard deviation of the error in the high-fidelity model relative to the standard deviation of the error in the low-fidelity model,  $\sqrt{\text{Var}(E_H)/\text{Var}(E_L)}$ , was varied from zero to one. The standard deviation of the error of the low-fidelity model was held fixed and both

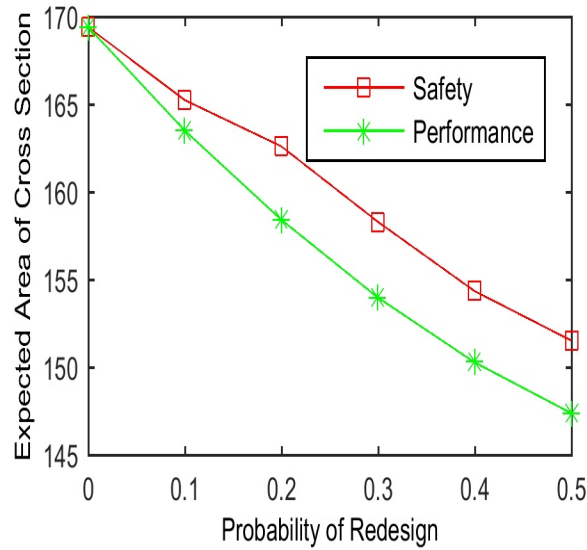


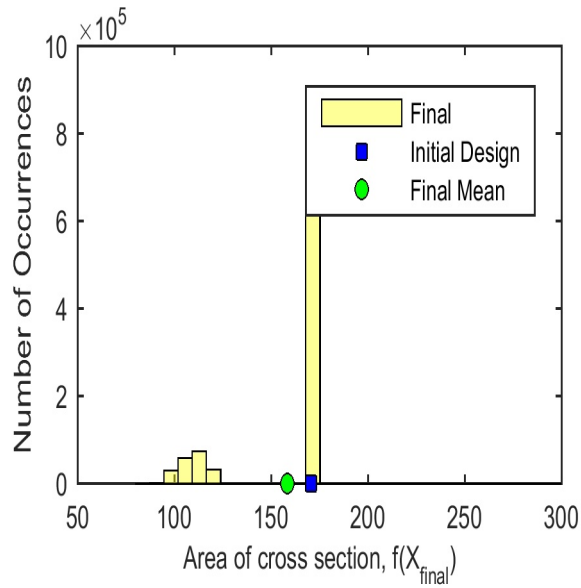
Figure 3-3. Uniaxial tension test - Comparison of expected cross sectional area after possible redesign as a function of probability of redesign for redesign for performance (conservative initial design) versus redesign for safety (ambitious initial design).

distributions had means of zero. An error ratio of zero corresponds to no error in the high-fidelity model and a ratio of one corresponds to having the same error distributions for both models. For each point on the curves, the safety margins were optimized by solving Equation 3-1 for a fixed probability of redesign of 20%. As shown in Figure 3-9, redesign for safety is preferred when the error in the high-fidelity model is low but redesign for performance is preferred when the error in the high-fidelity model is high. Note that for the tradeoff curve shown in Figure 3-3 the ratio of the errors in the models was  $\sqrt{\text{Var}(E_H)/\text{Var}(E_L)} = 0.5$ .

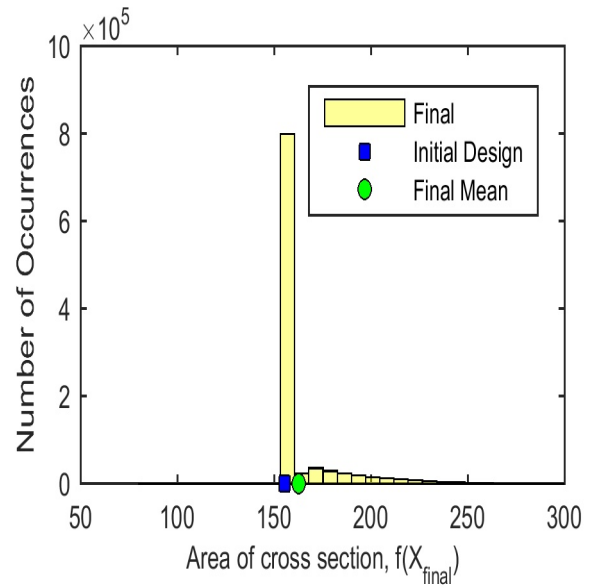
### 3.3.2 Supersonic Business Jet Engine Design

#### 3.3.2.1 Problem description

This example is based on the propulsion discipline design problem from the Sobieski supersonic business jet (SSBJ) problem [83]. The design problem is to minimize engine weight subject to a constraint on the maximum normalized throttle setting. The problem is based on the scaling of a baseline engine to meet a thrust

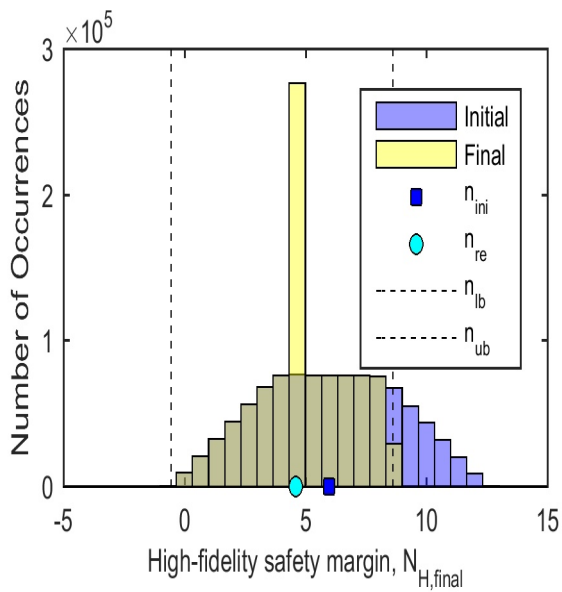


A

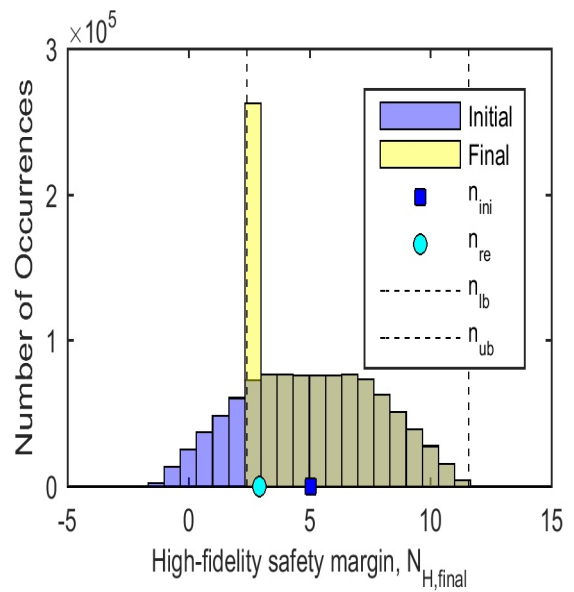


B

Figure 3-4. Uniaxial tension test - Epistemic uncertainty in cross sectional area for 20% probability of redesign.

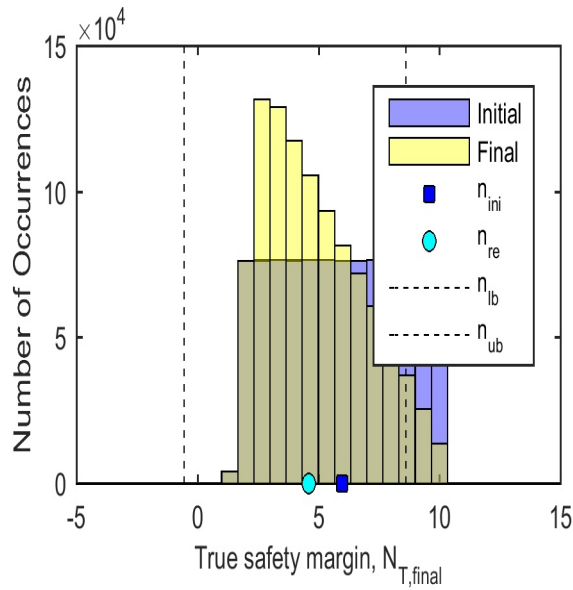


A

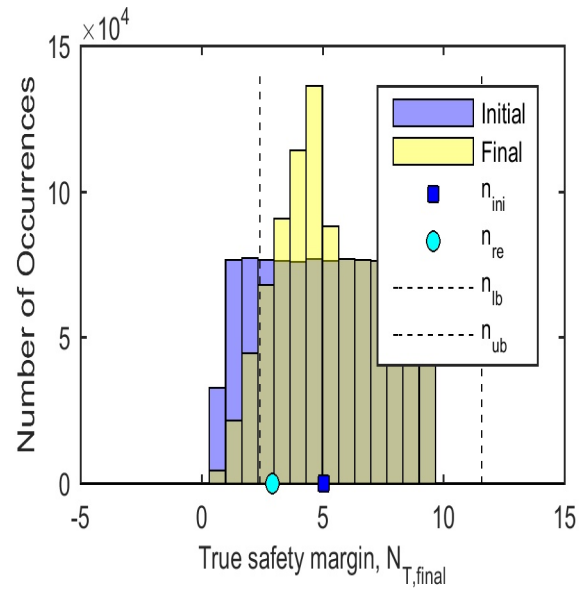


B

Figure 3-5. Uniaxial tension test - Epistemic uncertainty in safety margin with respect to high-fidelity model for 20% probability of redesign. Plots show overlapping transparent histograms.

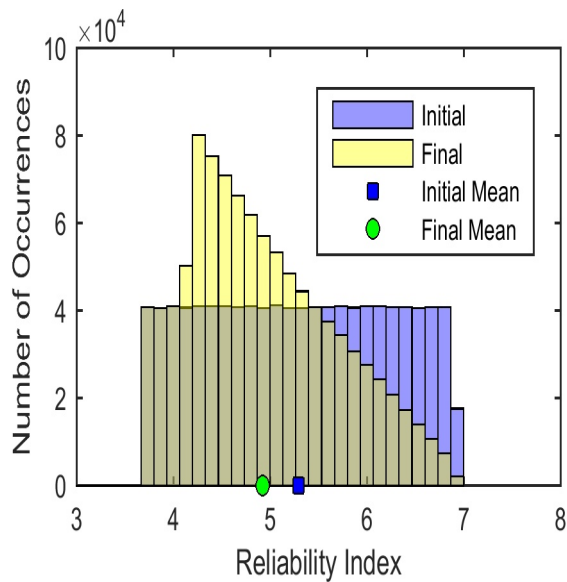


A

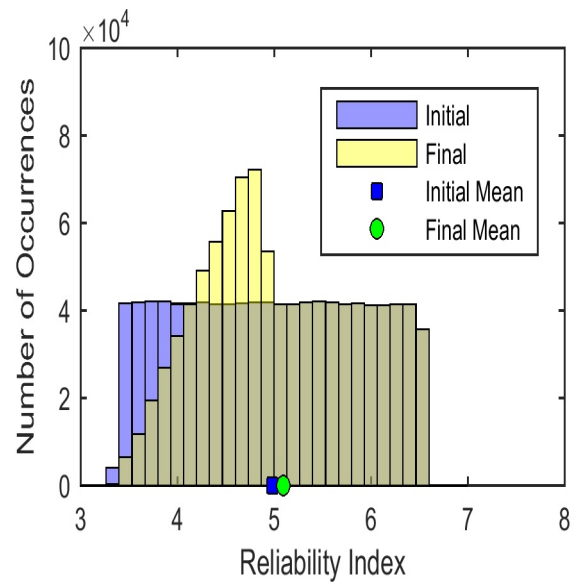


B

Figure 3-6. Uniaxial tension test - Epistemic uncertainty in safety margin with respect to true model for 20% probability of redesign. Plots show overlapping transparent histograms.



A



B

Figure 3-7. Uniaxial tension test - Epistemic uncertainty in reliability index for 20% probability of redesign. Plots show overlapping transparent histograms.



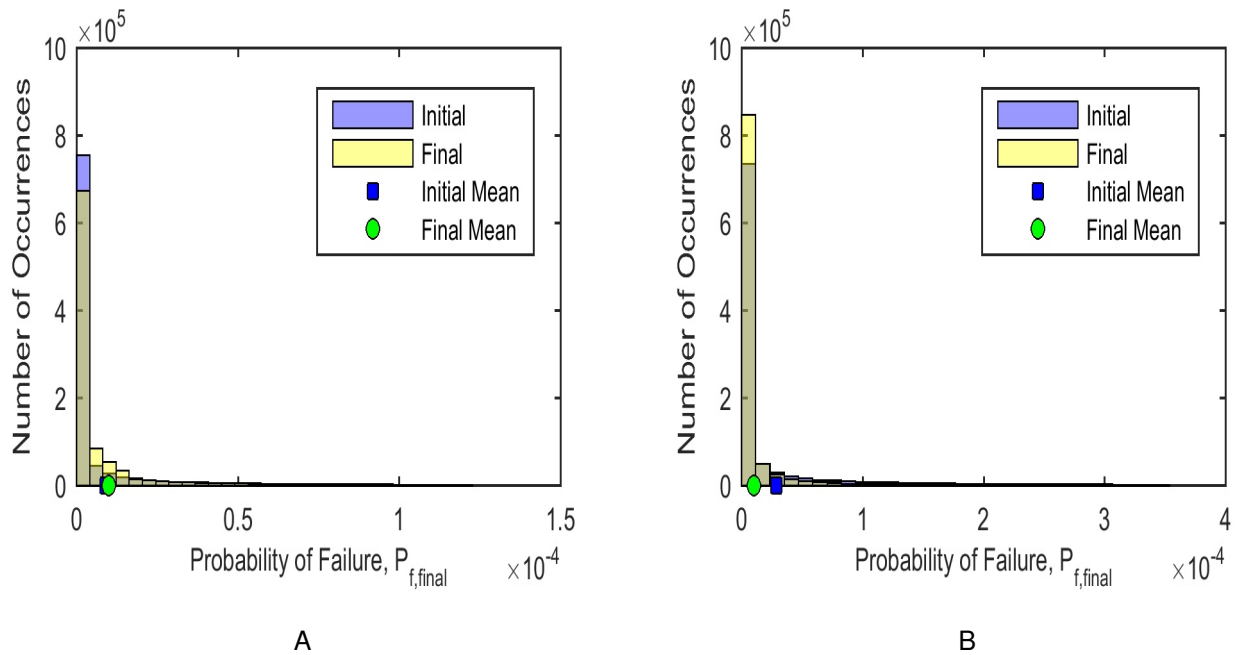


Figure 3-8. Uniaxial tension test - Epistemic uncertainty in failure for 20% probability of redesign. The figures are plotted with different scales to show the change in the tail of the distribution. Plots show overlapping transparent histograms.

requirement. If the engine is designed to provide the required thrust when operating near idle throttle then the resulting engine design is unreasonably large and heavy. If the engine is designed to provide the required thrust when operating at full throttle then the engine design can be smaller and lighter. However, there is epistemic uncertainty in the low-fidelity prediction of the thrust output and therefore it is desirable to have some safety margin to increase the probability that the as-built engine can provide sufficient thrust. In addition, the thrust output of the engine varies with Mach number and altitude. In this example, we consider that the engine is designed to operate for a distribution of altitudes (aleatory uncertainty).

The throttle setting is defined as the ratio of the engine output thrust relative to the maximum available thrust at a given altitude and Mach number. A throttle setting of 1 indicates maximum power at a given altitude and Mach number and a throttle setting of 0.01 is idle thrust. The net available thrust of the engine increases with Mach number

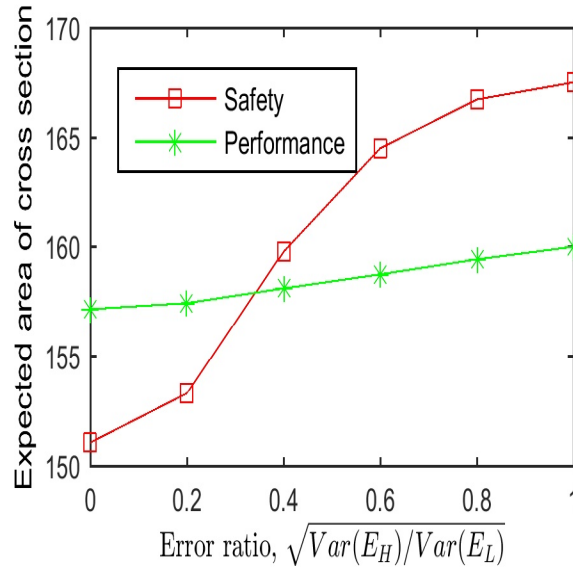


Figure 3-9. Uniaxial tension test - Redesign for safety is preferred when high-fidelity model error is low, but redesign for performance is preferred when high-fidelity model error is high. Plot is for fixed probability of redesign of 20%.

Table 3-4. Problem definition for SSBJ Example

	Description	Notation
Design variable	Throttle	$x$
Aleatory variable	Altitude (ft)	$U = H$
Conservative value	Max altitude	$u_{det} = 56,770 \text{ ft}$
Objective function	Engine weight (lbs)	$f(x) = W_E(x)$
Limit-state function	Maximum throttle	$g_L(x, U) = x_{ub}(H) - x$
Target mean reliability		$p_f^* = 1 \times 10^{-3}$

and decreases with altitude. A non-dimensional throttle setting variable,  $x$ , is created by normalizing the throttle with respect the point of maximum thrust of the baseline engine. The non-dimensional throttle setting is defined as

$$x = S_{out}/S_0 \quad (3-17)$$

where  $S_{out}$  is the output thrust and  $S_0 = 16168 \text{ lbf}$  is the maximum thrust of the baseline engine. If the required thrust  $S_{req}$  is different than the thrust provided by the baseline engine, the baseline engine design is scaled to match the new requirement. In this

Table 3-5. Uncertain Parameters for SSBJ Example

Parameter	Classification	Symbol	Mean, $\mu$	C.O.V	Range	Distribution
Altitude	Aleatory	$H$ (ft)	52500	0.05	[45000,60000]	Truncated Normal
Error in low-fidelity model	Epistemic	$\hat{E}_L$	0	—	[-0.0375,0.0375]	Uniform
Error in high-fidelity model	Epistemic	$\hat{E}_H$	0	—	[-0.0075,0.0075]	Uniform

example, we assume a fixed thrust requirement  $S_{req} = 40000$  lbf. The engine scale factor  $ESF$  is defined as

$$ESF = \frac{S_{req}}{2S_{out}} = \frac{S_{req}}{2 \times S_0} \quad (3-18)$$

where the value of 2 in the denominator reflects the fact that two engines are used on the jet. The weight of the engine  $W_E$  is approximated as following a power law relationship with engine scale factor

$$W_E = 2W_{BE}(ESF)^{1.05} \quad (3-19)$$

where  $W_{BE} = 4360$  lb is the weight of the baseline engine.

A response surface of the engine performance map for the baseline engine calculates maximum available thrust  $S_{avail}$  at a given Mach number  $M$  and altitude  $h$ .

The response surface sets an upper bound on throttle,  $x_{ub}$ , when normalized by  $S_0$

$$\begin{aligned} x_{ub}(M, h) &= \frac{S_{avail}(M, h)}{S_0} \\ &= \frac{1}{S_0} (\alpha_0 + \alpha_1 M + \alpha_2 h + \alpha_3 M^2 + 2\alpha_4 Mh + 2\alpha_5 h^2) \end{aligned} \quad (3-20)$$

where the coefficients are listed in Table 3-6. This response surface models how available thrust decreases with increasing altitude as shown in Figure 3-10.

In this example we are interested in minimizing the weight of the engine subject to a constraint on maximum throttle. The problem definition is shown in Table 3-4. We

Table 3-6. Coefficients for calculating throttle upper bound (Equation 3-20)

Coefficient	Value
$\alpha_0$	$1.1484 \times 10^4$
$\alpha_1$	$1.0856 \times 10^4$
$\alpha_2$	$-5.0802 \times 10^{-1}$
$\alpha_3$	$3.2002 \times 10^3$
$\alpha_4$	$-1.4663 \times 10^{-1}$
$\alpha_5$	$6.8572 \times 10^{-6}$

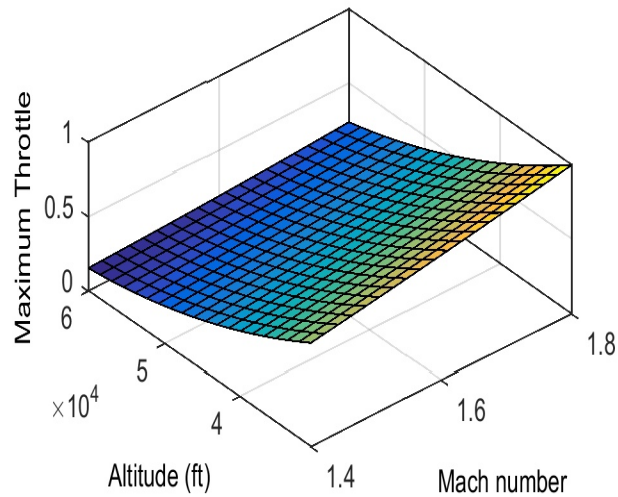


Figure 3-10. A response surface of the engine performance map calculates maximum available thrust at a given Mach number,  $M$ , and altitude,  $h$ . The throttle setting is normalized to one at an altitude of approximately 32000 ft and Mach 1.9.

consider aleatory uncertainty in the altitude and epistemic model uncertainty in the maximum throttle,  $x_{ub}$ , as defined in Table 3-5. The problem follows the general method described in Section 3.2. The engine is designed using a conservative value in place of random altitude. In the future, the engine will be tested (e.g. high-fidelity simulation or prototype test) and it will be redesigned if the safety margin with respect to the throttle constraint is too high or too low. That is, the engine will be redesigned if it provides insufficient thrust or the thrust is so large that it is worth redesigning to use a smaller, lighter engine.

The probability of failure is estimated based on a Monte-Carlo simulation. The throttle should be set to the upper bound to minimize the engine weight. Therefore, deterministic design optimization was avoided by setting the throttle to the upper bound minus the safety margin.

### 3.3.2.2 Expected performance versus probability of redesign

Tradeoff curves for expected cost,  $\mathbb{E}_E[f(\mathbf{X}_{final})]$ , versus probability of redesign,  $p_{re}$ , are shown in Figure 3-11. The tradeoff curves were obtained by solving Equation 3-1 for several values of the constraint on probability of redesign,  $p_{re}^*$ . The two curves correspond to the special cases of performing redesign only for performance and performing redesign only for safety. It was observed that redesign for safety was the global optimum solution and the optimum safety margins would converge to this solution when allowing for both redesign for safety and performance. This result is different from the example in Section 3.3.1 where redesign for performance was preferred. To explore the simulation in more detail, the points on the tradeoff curve corresponding to 20% probability of redesign were selected. Histograms of the throttle setting, weight, safety margin, and probability of failure for 20% probability of redesign are shown in Figure 3-12, 3-14, 3-13, 3-15. Statistics on the mass and probability of failure before and after redesign are listed in Table 3-7.

### 3.3.2.3 Expected performance versus level of high-fidelity model error

The ratio of the standard deviation of the error in the high-fidelity model relative to the standard deviation of the error in the low-fidelity model,  $\sqrt{\text{Var}(E_H)/\text{Var}(E_L)}$ , was varied from zero to one. For each point on the curves, the safety margins were optimized by solving Equation 3-1 for a fixed probability of redesign of 20%. As shown in Figure 3-16, redesign for safety is preferred when the error in the high-fidelity model is low but redesign for performance is preferred when the error in the high-fidelity model is high. The overall trends are similar to those observed for the example in Section 3.3.1.

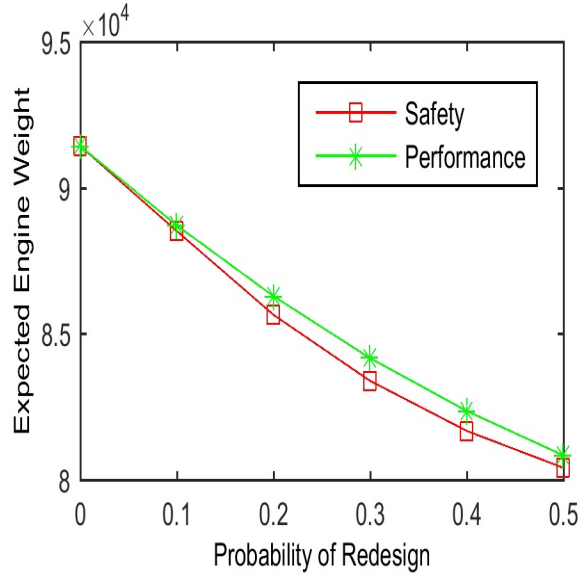


Figure 3-11. SSBJ Engine - Comparison of expected engine weight after possible redesign as a function of probability of redesign for redesign for performance (conservative initial design) versus redesign for safety (ambitious initial design).

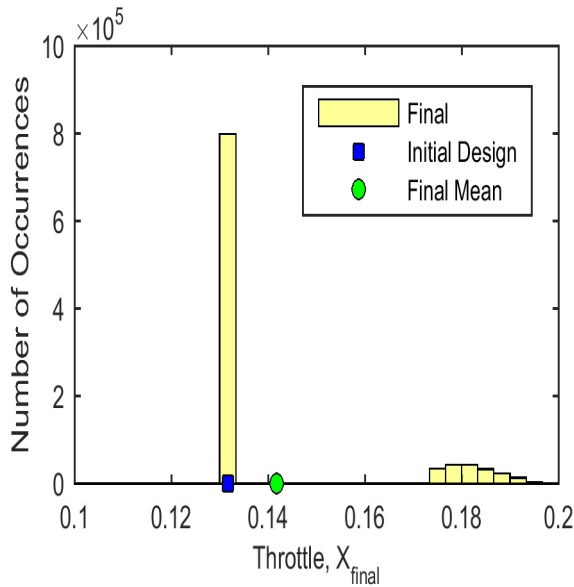
Note that for the tradeoff curve shown in Figure 3-11 the ratio of the errors in the models was  $\sqrt{\text{Var}(E_H)/\text{Var}(E_L)} = 0.2$ .

### 3.4 Discussion and Conclusion

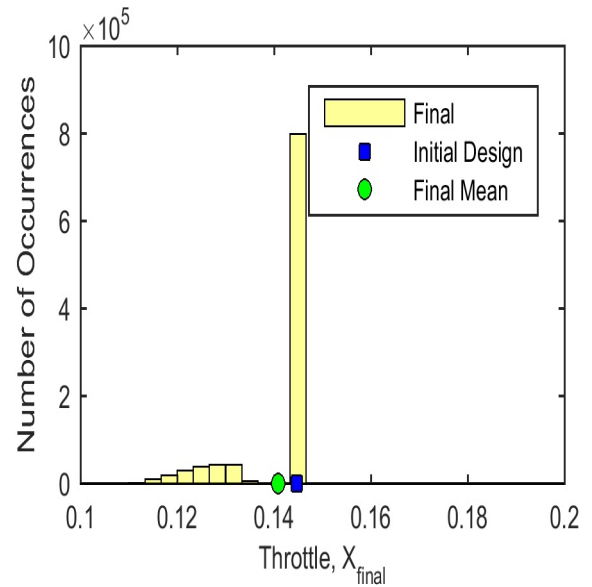
This study presented a generalized formulation of a two-stage safety-margin-based design / redesign process considering the effects of a future test and possible redesign. The safety margins that control the deterministic design / redesign process are optimized to minimize the expected value of the design cost function (i.e. maximize expected performance) while satisfying constraints on probability of redesign and expected probability of failure. The future test result (i.e. high-fidelity evaluation of initial design or prototype test) is an epistemic random variable that is predicted based on the distributions of possible errors in the low and high fidelity models. Future test results are simulated in order to calculate the probability of redesign, the possible designs after calibration and redesign, and the final distribution of probabilities of failure. By considering that the design may change in the future conditional on the outcome of the

Table 3-7. Results for SSBJ example for 20% probability of redesign

Description	Notation	Redesign for Safety	Redesign for Performance
Probability of redesign	$p_{re}$	0.20	0.20
Cost of initial design	$f(x_{ini})$	$8.30 \times 10^4$	$9.16 \times 10^4$
Expected cost conditional on performing redesign	$\mathbb{E}_E [f(X_{re}) Q = 1]$	$9.64 \times 10^4$	$6.52 \times 10^4$
Expected cost after possibly performing redesign	$\mathbb{E}_E [f(X_{final})]$	$8.57 \times 10^4$	$8.63 \times 10^4$
Expected probability of failure of initial design	$\mathbb{E}_E [P_{f,ini}]$	6.94 $10^{-3}$	0.96 $10^{-3}$
Expected probability of failure of initial design conditional on passing test	$\mathbb{E}_E [P_{f,ini} Q = 0]$	1.05 $10^{-3}$	1.20 $10^{-3}$
Expected probability of failure of new designs conditional on failing test	$\mathbb{E}_E [P_{f,re} Q = 1]$	0.80 $10^{-3}$	0.18 $10^{-3}$
Expected probability of failure after possibly performing redesign	$\mathbb{E}_E [P_{f,final}]$	1.00 $10^{-3}$	1.00 $10^{-3}$

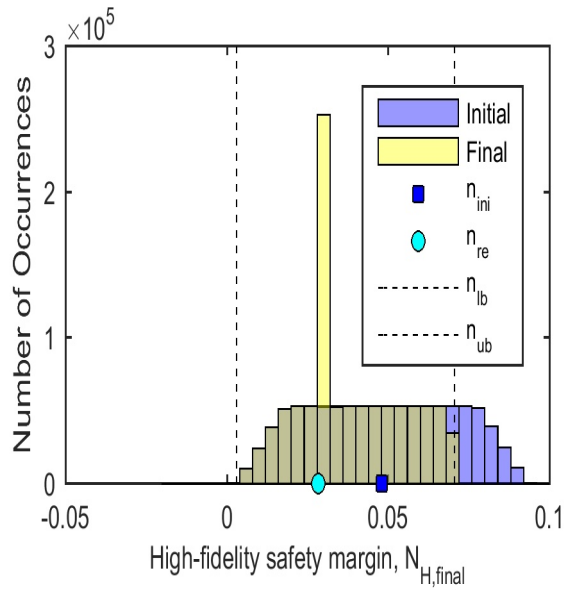


A

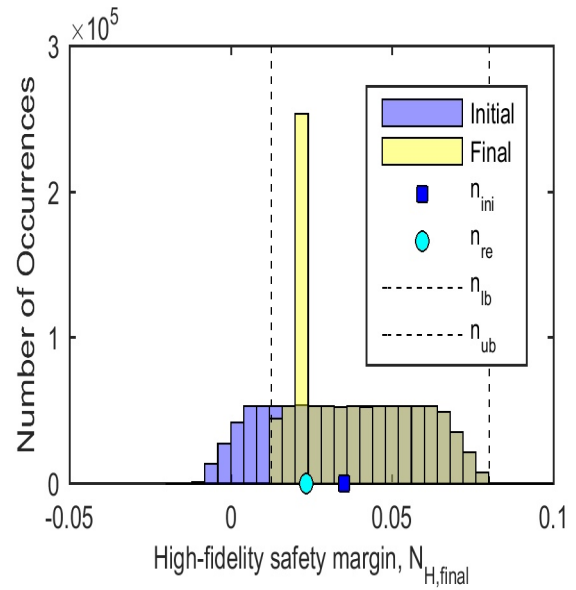


B

Figure 3-12. SSBJ Engine - Epistemic uncertainty in throttle setting for 20% probability of redesign.

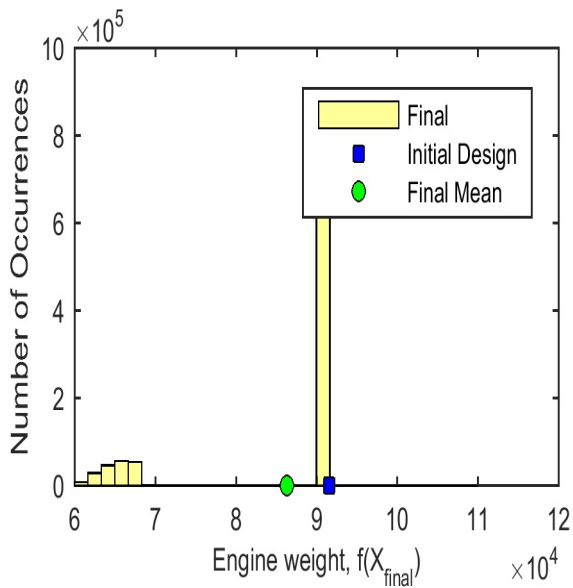


A

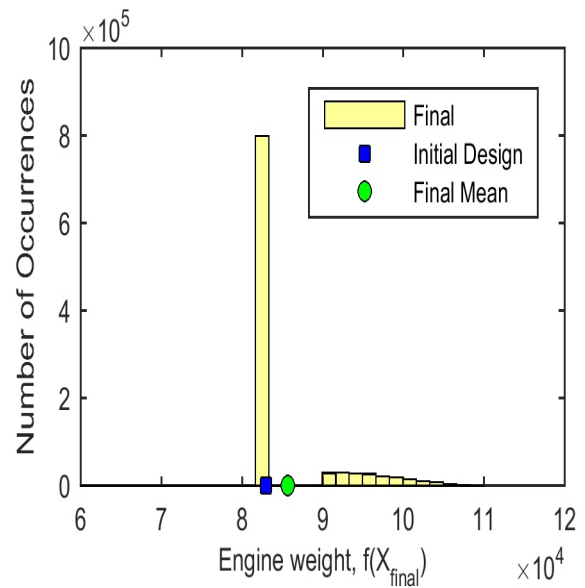


B

Figure 3-13. SSBJ Engine - Epistemic uncertainty in safety margin with respect to high-fidelity model for 20% probability of redesign. Plots show overlapping transparent histograms.



A



B

Figure 3-14. SSBJ Engine - Epistemic uncertainty in engine weight for 20% probability of redesign.



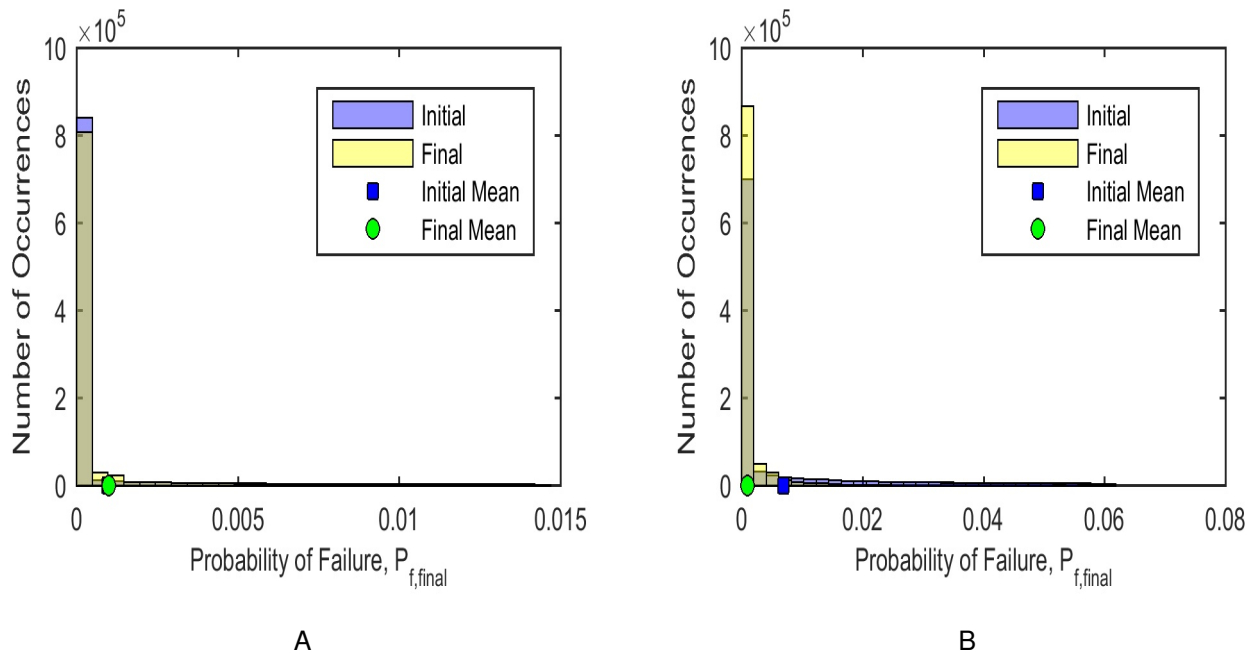


Figure 3-15. SSBJ Engine - Epistemic uncertainty in probability of failure for 20% probability of redesign. The figures are plotted with different scales to show the change in the tail of the distribution. Plots show overlapping transparent histograms.

future test it is possible to trade off between the risk of having to redesign in the future and the associated performance and / or reliability benefits.

When considering epistemic model uncertainty in a design constraint, the designer faces a dilemma in whether to start with a larger initial safety margin (i.e. more conservative initial design) and possibly redesign to improve performance versus starting with a smaller safety margin (i.e. less conservative initial design) and possibly redesigning to restore safety. This study analyzes this decision when there is a fixed but unknown constant bias between the low-fidelity model, high-fidelity model, and true model. In the examples in this study, it is found that the decision of whether to start with a higher initial safety margin and possibly redesign for performance, or to start with a lower initial safety margin and possibly redesign for safety, depends on the ratio of the standard deviation of the uncertainty in the high-fidelity model relative to the standard deviation of uncertainty in the low-fidelity model.

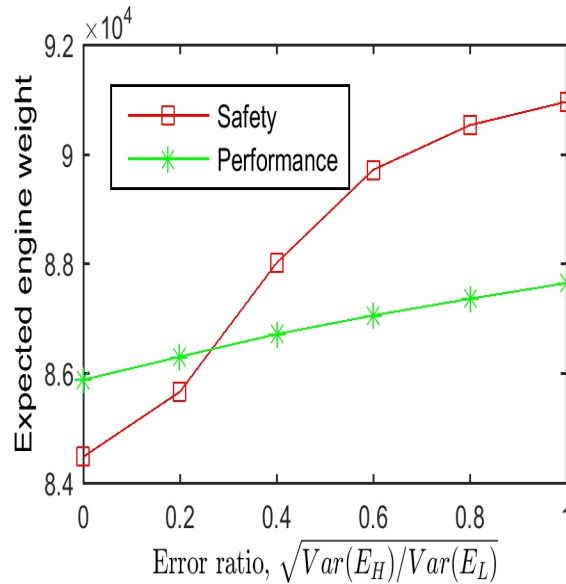


Figure 3-16. SSBJ Engine - Redesign for safety is preferred when high-fidelity model error is low, but redesign for performance is preferred when high-fidelity model error is high. Plot is for fixed probability of redesign of 20%.

It was observed that the redesign for safety strategy was strongly influenced by the amount of error in the high-fidelity model. It is hypothesized that the amount of error in the high-fidelity model has a stronger influence on the redesign for safety strategy because the error interferes with the process of truncating dangerous designs. The benefit of redesign for safety is that it prevents a dangerous initial design from successfully passing the test. This substantially reduces the expected probability of failure which in turn allows the initial design to be less conservative. However, if there is a large amount of error in the high-fidelity model then a dangerous initial design may pass the test unnoticed. Even if this is unlikely, the possibility of a high probability of failure has a significant influence on the mean probability of failure. To compensate, the initial design must be more conservative. On the other hand, when considering redesign for performance it is not a problem if a very safe (i.e. overly conservative) initial design passes the test.

It is observed that redesign for safety and redesign for performance result in different distributions of performance (e.g. weight). Redesign for performance capitalizes on the fact that it may be possible to obtain a substantial improvement in performance if the initial design is revealed to be much too conservative. The performance improvement is large but the probability of obtaining this benefit is small when the probability of redesign is small. The initial design must be more conservative since redesign is only used to improve performance and not to restore safety. Redesign for safety attempts to obtain better initial design performance by allowing for the possibility that redesign may be necessary to restore safety. If the initial design is revealed to be unsafe then it is found a small design change is usually sufficient to restore safety. When the probability of redesign is small the initial design is likely to pass the test and be accepted as the final design. Redesign for safety allows for a better initial design than redesign for performance. However, redesign for performance has the advantage that it may be possible to skip the redesign process when time constraints outweigh the possible performance benefits of redesign.

### **3.5 Limitations and Future work**

This study is based on the assumption that there is a fixed but unknown constant bias between the low-fidelity model, high-fidelity model, and true model. If the model error is constant across the joint design / aleatory space, then the reduction in epistemic model uncertainty does not depend on the location where the high-fidelity model is evaluated. If the model error is not constant, then it may incentivize starting with a lower safety margin in order to have a high-fidelity evaluation close to the limit surface  $g(\mathbf{x}, \mathbf{u}) = 0$ . In related work, a Kriging surrogate is introduced to model epistemic uncertainty in order to account for spatial correlations in model uncertainty [25].

The proposed method may be computationally expensive because it involves a Monte-Carlo simulation (MCS) of a design / redesign process nested inside a global optimization problem. To reduce the computational cost surrogate models can be fit to

the mean probability of failure and mean design cost as a function of the safety margins [25].

In the formulation of the deterministic design optimization problems the aleatory variables  $\mathbf{U}$  are replaced with the conservative deterministic values  $\mathbf{u}_{det}$ . The choice of the conservative deterministic values to use in place of aleatory random variables may have a strong influence on the final results. Future work will investigate optimizing the values  $\mathbf{u}_{det}$  in addition to the safety margins.

In this study, a constraint was placed on the expected probability of failure during the optimization of safety margins. By only constraining the expected probability of failure it is possible to arrive at an optimum set of safety margins that results in some very safe designs but some unsafe designs. To avoid this situation additional constraints should be included that consider the spread of the probability of failure distribution (e.g. superquantile [84]).

CHAPTER 4  
CONSIDERING SPATIAL CORRELATIONS IN THE EPISTEMIC MODEL ERROR  
WHEN SIMULATING A FUTURE TEST AND REDESIGN

**Nomenclature**

$\mathbf{x}$	Design variable vector
$\mathbf{U}$	Aleatory random variable vector
$e(\cdot, \cdot)$	Model error
$f(\cdot)$	Objective function
$g(\cdot, \cdot)$	Limit-state function
$n$	Safety margin
$q$	Redesign indicator function
$p_{re}$	Probability of redesign
$p_f$	Probability of failure
$E_{\Omega}[\cdot]$	Expected value with respect to epistemic uncertainty
$Pr_U[\cdot]$	Probability with respect to aleatory uncertainty

*Subscripts*

$L$	Low-fidelity model
$H$	High-fidelity model
$det$	Deterministic value
$ini$	Initial design
$re$	Design after redesign
$final$	Final design after possible redesign
$lb$	Lower bound
$ub$	Upper bound

*Superscripts*

$(i)$	Realization of epistemic random variable or function
-------	--

- ★ Target value in optimization

### *Accents*

- ^ Epistemic random variables or functions
- Mean prediction of Kriging model

## **4.1 Research Context in Relation to Scope of Dissertation**

In Chapter 3, a method was introduced for predicting the possible outcomes of a future test followed by possible redesign in order to optimize the safety margins controlling a deterministic design process. The method was illustrated on a simple bar design example and on the conceptual design of an engine for a supersonic business jet. However, the method relied on the restrictive assumption that the model bias was constant across the design space. In practice, it may be difficult to support the assumption of constant model bias in the absence of initial test data, but if initial test data is available then the model bias could be corrected before performing the analysis. Therefore, a more general method of modeling and propagating epistemic model uncertainty is needed. In this chapter a Kriging surrogate is used to provide a flexible representation of the epistemic model uncertainty that allows the method to be applicable to a wide range of engineering problems.

## **4.2 Introduction**

At the initial design stage engineers often rely on low-fidelity models that have high uncertainty. This model uncertainty is reducible and is classified as epistemic uncertainty; uncertainty due to variability is irreducible and classified as aleatory uncertainty. Both forms of uncertainty can be implicitly compensated for using conservativeness such as conservative material properties, conservative limit loads, safety margins, and safety factors. However, if the design is too conservative then typically performance will suffer. Traditional safety-factor-based deterministic design

has relied on testing in order to reduce epistemic uncertainty and achieve high levels of safety. Testing is used to calibrate models and prescribe redesign when tests are not passed. After calibration, reduced epistemic model uncertainty can be leveraged through redesign to restore safety or improve design performance; however, redesign may be associated with substantial costs or delays. Integrated optimization of the design, testing, and redesign process can allow the designer to tradeoff between the risk of future redesign and the possible performance and reliability benefits. Previous work has illustrated this tradeoff when there is only a fixed constant model bias [20, 21, 23]. This study builds on previous work by considering spatial correlation in the epistemic model uncertainty. A Kriging surrogate is used to provide a flexible representation of the epistemic model uncertainty that allows the method to be applicable to a wide range of engineering problems.

In this study, the epistemic model uncertainty is treated separately from the aleatory parameter uncertainty in the model inputs. This results in the challenging task of propagating aleatory uncertainty through an uncertain model. Furthermore, in order for the method to be applicable under current safety-factor-based design regulations[2], a traditional deterministic safety-margin-based design approach is considered. Some studies have used the parallels between safety-factor-based design and reliability-based design optimization (RBDO) approaches to reduce computational cost of RBDO [5–7]. However, these studies have not considered epistemic model uncertainty. When there is only epistemic model uncertainty a safety margin balances the need for the final design to be feasible while at the same time not being so conservative that design performances suffer [8]. Few studies have considered the effects of both aleatory parameter uncertainty and epistemic model uncertainty. Mahadevan and Rebba have shown that failing to account for epistemic model uncertainty may lead to an overestimation of reliability and unsafe designs or underestimation of the reliability and designs that are more conservative than needed [9]. Studies that use surrogate

models in RBDO also encounter a situation of mixed uncertainty. However, unlike this study where we are interested in epistemic model uncertainty as a inherent part of the low-fidelity model, these studies are usually motivated by a desire to reduce computational cost. Kim and Choi have shown that when using response surfaces in RBDO the epistemic model uncertainty results in uncertainty in the reliability index and additional sampling can be used to avoid being overly conservative [10].

One of the important aspects of this study is the integration of the design and testing process: the effects of a future test and possible redesign are considered while optimizing the initial design. Since the test will be performed in the future, the test result is an epistemic random variable. Predicting possible test results requires a probabilistic formulation of the relationship between the low-fidelity model prediction, the true value, and the test result. In the context of calibrating computer models, Kennedy and O'Hagan proposed that the true model can be related to a computer model by multiplying by a constant scale parameter and adding a discrepancy function [11]. Similar formulations have subsequently been applied in many other studies[12–17]. These formulations are similar in that they all relate the true model to the low-fidelity model by adding an uncertain discrepancy function. The formulations differ in the representation of the scale parameter. Methods range from omitting the scale parameter [13, 14] to considering an uncertain scaling function [16]. In this study we consider only an uncertain discrepancy function to formulate the relationship between the high-fidelity model and the low-fidelity model. The uncertain discrepancy function is constructed in the joint design and aleatory input space in order to have epistemic model uncertainties that are correlated with respect to design and aleatory inputs.

In addition to the integration of design and testing, this study also seeks to integrate a redesign process. Redesign refers to changing the design variables conditional on the test result. Since the future test result is an epistemic random variable the design variable after redesign is also random variable. Villanueva et al. developed a method for



simulating the effects of future tests and redesign when there is a constant but unknown model bias in the calculation and measurement [19]. In the context of constant model bias, Matsumura et al. compared RBDO considering future redesign to traditional RBDO [20]. Villanueva et al. also studied the tradeoff between future redesign and performance for an integrated thermal protection system [21]. Price et al. compared starting with a more conservative design and possibly redesigning to improve performance to starting with a less conservative design and possibly redesigning to improve safety [23]. These studies have demonstrated that integrated optimization of design, testing, and redesign can be used to manage redesign risk and tradeoff between the probability of future redesign and design performance. However, the assumption of constant model bias in these studies severely limits the types of problems where the method is applicable. In order to apply the method to a broader range of general engineering problems this study uses a Kriging model to represent model uncertainty whose conditional simulations allow uncertainty propagation.

In Section 4.3 the general method of simulating a future test and possible redesign is described. In Section 4.4 the demonstration example of a cantilever beam is described. In Section 4.5 the study is summarized and the implications of the method and results are discussed.

### 4.3 Methods

The design, testing, and redesign process is formulated deterministically in terms of an initial safety margin  $n_{ini}$ , lower and upper bounds on acceptable safety margin  $n_{lb}$  and  $n_{ub}$ , and a redesign safety margin  $n_{re}$ . In Section 4.3.1 the formulation of the optimization of the safety margins is presented. For each set of safety margins, a Monte Carlo simulation (MCS) of epistemic error realizations is performed as described in Section 4.3.2. A single sample in the MCS consists of a complete deterministic design / redesign process as described in Section 4.3.3. The results of the MCS are used to

calculate the probability of redesign, expected probability of failure, and expected design cost as described in Section 4.3.4.

#### 4.3.1 Optimization of Safety Margins

The deterministic design process is controlled by a vector of safety margins  $\mathbf{n} = \{n_{ini}, n_{lb}, n_{ub}, n_{re}\}$ . The safety margins are optimized to minimize expected design cost while satisfying constraints on expected probability of failure and probability of redesign. The optimization of the safety margins is formulated as

$$\begin{aligned} \min_{\mathbf{n}} \quad & E_{\Omega} \left[ f(\hat{\mathbf{X}}_{final}) \right] \\ \text{s.t.} \quad & E_{\Omega} \left[ \hat{P}_{f,final} \right] \leq p_f^* \\ & p_{re} \leq p_{re}^* \end{aligned} \quad (4-1)$$

where  $E_{\Omega}[\cdot]$  is used to denote the expectation with respect to epistemic uncertainty,  $f(\cdot)$  is a cost function,  $\hat{\mathbf{X}}_{final}$  is a distribution of possible final designs,  $\hat{P}_{f,final}$  is a distribution of final probability of failure, and  $p_{re}$  is the probability of redesign. The final design  $\hat{\mathbf{X}}_{final}$  is an epistemic random variable because the design may be modified conditional on the future test result which is unknown at the initial design stage. The final probability of failure is an epistemic random variable because the final design is uncertain and because there is epistemic model uncertainty in the limit-state function  $g(\cdot, \cdot)$ . The tradeoff between expected cost and probability of redesign is captured by solving the single objective optimization problem for several values of the constraint  $p_{re}^*$ .

The global optimization of the safety margins is performed using Covariance Matrix Adaptation Evolution Strategy (CMA-ES) [82] and a penalization strategy to handle the constraints. The optimizer calls a subfunction to perform a MCS of the deterministic design process as shown in Figure 4-1. The MCS of the deterministic design process is used to calculate the distribution of possible final designs, the distribution of final probabilities of failure, and the probability of redesign. To reduce the computational cost of optimizing the safety margins, surrogate models can be fit for the expected cost and

expected probability of failure as a function of the safety margins as described in Section 4.3.1.

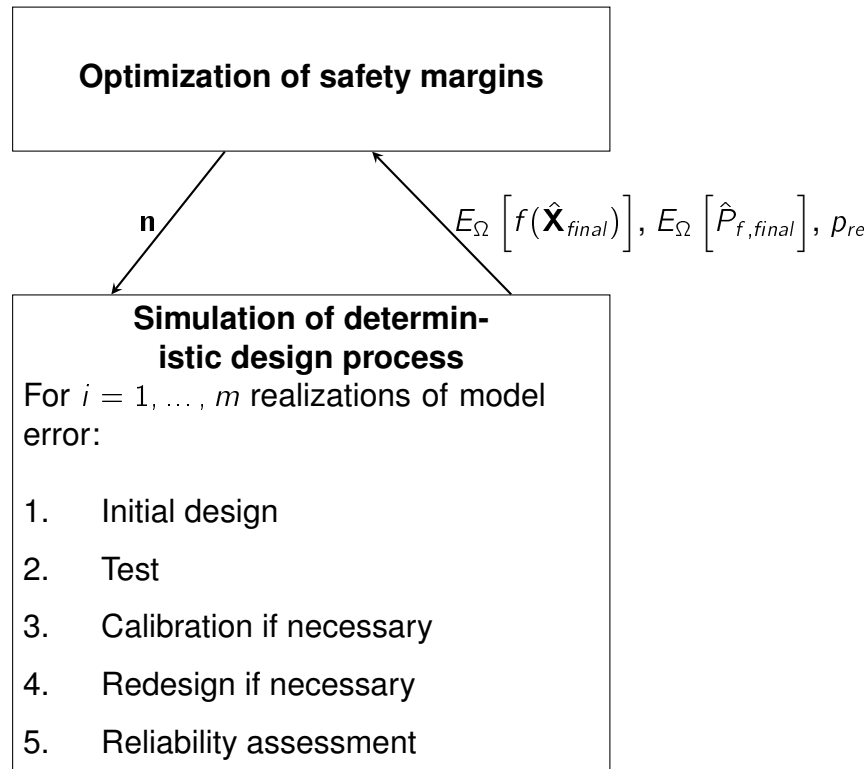


Figure 4-1. The optimization of the safety margins is based on a MCS of the deterministic design process

In this study, we define two different triggers for redesign. We will refer to redesign triggered by a low safety margin (less than  $n_{lb}$ ) as redesign for safety and redesign triggered by a high safety margin (greater than  $n_{ub}$ ) as redesign for performance. To force only redesign for safety the upperbound on acceptable safety margins can be removed from the optimization by setting  $n_{ub} = +\infty$ . To force only redesign for performance, the lowerbound on acceptable safety margins can be removed from the optimization by setting  $n_{lb} = -\infty$ . Considering only redesign for safety or only redesign for performance are special cases of the general formulation where all the safety margins  $\mathbf{n} = \{n_{ini}, n_{lb}, n_{ub}, n_{re}\}$  are optimized simultaneously.

**Surrogate models.** The optimization problem in Equation 4-1 may be prohibitively expensive if a MCS is performed for each evaluation of the objective and constraint

Table 4-1. 95% confidence interval for relative error of surrogate models based on LOOCV

	Mixed	Performance	Safety
Expected probability of failure	$[-33, 25]\%$	$[-17, 13]\%$	$[-17, 14]\%$
Expected cross sectional area	$[-0.12, 0.12]\%$	$[-0.05, 0.07]\%$	$[-0.08, 0.06]\%$

equations. Surrogate models were used to reduce the computational cost of the optimization of the safety margins. Kriging models of the mean final probability of failure  $E_{\Omega} [\hat{P}_{f, final}]$  and mean final design cost  $E_{\Omega} [f(\hat{\mathbf{X}}_{final})]$  were fit as a function of the safety margins  $\mathbf{n} = \{n_{ini}, n_{lb}, n_{ub}, n_{re}\}$ . The mean probability of failure was transformed to a reliability index before fitting the surrogate models. The Kriging models were fit based on a DoE consisting of 400 points generated using Latin hypercube sampling (LHS) and the corner points in the design space. Each point in the DoE required a MCS of epistemic model uncertainty. The sample size of the MCS (i.e. number of conditional simulations) was adapted to reach a target coefficient of variation on the expected final probability of failure of 5% with a maximum sample size of  $m = 5000$ . Kriging with nugget was used in an effort to filter out some of the noise introduced by MCS. A Gaussian covariance function was used and parameters were estimated based on MLE. Three different sets of surrogate models were constructed corresponding to a mixed redesign strategy, redesign for performance, and redesign for safety. The redesign for performance and redesign for safety surrogate models were 3-dimensional surrogate models while the mixed redesign strategy required 4-dimensional surrogates. The error in the surrogate models was estimated based on leave-one-out cross validation (LOOCV). It should be noted that LOOCV may overestimate the error due to the noise filtering effect of Kriging with nugget. Error estimates for the surrogate models are listed in Table 4-1.

#### 4.3.2 Monte-Carlo Simulation of Epistemic Model Error

The epistemic model uncertainty and aleatory parameter uncertainty are treated separately (see [66, 67, 85]). The true relationship between the models is assumed to

be of the form

$$g_H(\mathbf{x}, \mathbf{u}) = g_L(\mathbf{x}, \mathbf{u}) + e(\mathbf{x}, \mathbf{u}) \quad (4-2)$$

where  $\mathbf{x} \in \mathbb{R}^d$  is a vector of design variables,  $\mathbf{U}$  is a vector of aleatory random variables with a realization  $\mathbf{u} \in \mathbb{R}^p$ ,  $g_H(\cdot, \cdot)$  is the high-fidelity model,  $g_L(\cdot, \cdot)$  is the low-fidelity model, and  $e(\cdot, \cdot)$  is the error between the low-fidelity and high-fidelity models. Typically, the error  $e(\cdot, \cdot)$  is unknown. The uncertainty in the model error is represented as a Kriging model  $\hat{E}(\cdot, \cdot)$ . The hat accent on the error is used to differentiate between the random distribution of possible error  $\hat{E}(\cdot, \cdot)$ , and the unknown, deterministic error  $e(\cdot, \cdot)$ . Based on the possible model errors the high-fidelity model is predicted as

$$\hat{G}_H(\mathbf{x}, \mathbf{u}) = g_L(\mathbf{x}, \mathbf{u}) + \hat{E}(\mathbf{x}, \mathbf{u}) \quad (4-3)$$

The Kriging model for the calculation error is constructed in the joint space of the aleatory variables,  $\mathbf{u}$ , and the design variables,  $\mathbf{x}$ . The uncertainty in  $\hat{G}_H(\mathbf{x}, \mathbf{u})$  in Equation 4-3 is only due to epistemic model error  $\hat{E}(\cdot, \cdot)$ . Propagation of aleatory uncertainty  $\mathbf{U}$  through the uncertain model is discussed in Section 4.3.4. For simplicity of notation, we will define the mean of the Kriging prediction for the error as  $\bar{e}(\cdot, \cdot)$  and the mean prediction of the high-fidelity model as

$$\bar{g}_H(\mathbf{x}, \mathbf{u}) = g_L(\mathbf{x}, \mathbf{u}) + \bar{e}(\mathbf{x}, \mathbf{u}) \quad (4-4)$$

The epistemic random function  $\hat{E}(\cdot, \cdot)$  is used to represent the lack of knowledge regarding how well the low-fidelity model matches the high-fidelity model. Assuming initial test data is available, maximum likelihood estimation (MLE) will be used to estimate the parameters of the Kriging model. The prediction  $\hat{G}_H(\cdot, \cdot)$  is viewed as a distribution of possible functions. Samples or trajectories drawn from this distribution that are conditional on initial test data are referred to as conditional simulations. In the absence of test data these realizations are unconditional simulations. These simulations are spatially consistent Monte Carlo simulations. Let  $\hat{g}_H^{(i)}(\cdot, \cdot)$  denote the

$i$ -th realization of  $\hat{G}_H(\cdot, \cdot)$  based on a realization  $\hat{e}^{(i)}(\cdot, \cdot)$  of the Kriging model  $\hat{E}(\cdot, \cdot)$ . A variety of methods exist for generating these conditional simulations [86]. In this study, the conditional simulations are generated directly based on Cholesky factorization of the covariance matrix using the STK Matlab toolbox for Kriging [87] and by sequential conditioning [86].

We can consider a Monte Carlo simulation of  $m$  conditional simulations  $i = 1, \dots, m$  corresponding to  $m$  possible futures. In practice, the sample size  $m$  is increased until the estimated coefficient of variation of the quantity of interest, such as expected probability of failure, is below a certain threshold. Let  $\Omega$  denote the epistemic uncertainty space of the model  $\hat{G}_H(\cdot, \cdot)$ . There is a realization,  $\exists \omega \in \Omega$ , such that the simulation,  $\hat{g}_H^{(\omega)}(\cdot, \cdot)$ , is arbitrarily close to the true model,  $g_H(\cdot, \cdot)$ . The design process conditional on one error realization is described in Section 4.3.3. By repeating the design process for many different error realizations (i.e. for different possible high-fidelity models through Equation 4–3) we can determine the distribution of possible final design outcomes. From the MCS, it is possible to estimate the risk of redesign and to predict how failing a test relates to final design performance or safety. This can in turn be used to optimize the safety margins that govern the deterministic design process.

### 4.3.3 Deterministic Design Process

The deterministic design process is controlled by a vector of safety margins  $\mathbf{n}$ . There is an initial safety margin  $n_{ini}$ , lower and upper bounds on acceptable safety margin  $n_{lb}$  and  $n_{ub}$ , and a redesign safety margin  $n_{re}$ . First, an initial design is found based on deterministic optimization using the mean model prediction and a safety margin  $n_{ini}$ . Then, the optimum design is evaluated using the high-fidelity model to calculate the true safety margin with respect to  $g_H(\cdot, \cdot)$ . Based on the high-fidelity evaluation, the designer will consider the test passed and keep the initial design if the safety margin is greater than  $n_{lb}$  and less than  $n_{ub}$ . The lower bound  $n_{lb}$  is used to initiate redesign when the initial design is revealed to be unsafe. The upper bound  $n_{ub}$

is used to initiate redesign when the initial design is revealed to be so conservative that it is worthwhile to redesign to improve performance. If the test is failed, a calibration process is performed to update the model based on the test result. Finally, if redesign is performed a new design is found by performing deterministic optimization using the calibrated model and a safety margin  $n_{re}$ .

However, the future high-fidelity evaluation of the initial design (i.e. future test) is unknown and therefore modeled as an epistemic random variable. The redesign decision, calibration, and redesign optimum are conditional on a particular test result. In Section 4.3.3.1 to 4.3.3.3, the process is described conditional on the error realization  $\hat{E}(\cdot, \cdot) = \hat{e}^{(i)}(\cdot, \cdot)$ .

#### 4.3.3.1 Initial design

The design problem is formulated as a deterministic safety-margin-based optimization problem

$$\begin{aligned} \min_{\mathbf{x}} \quad & f(\mathbf{x}) \\ \text{s.t.} \quad & \bar{g}_H(\mathbf{x}, \mathbf{u}_{det}) - n_{ini} \geq 0 \end{aligned} \tag{4-5}$$

where  $\bar{g}_H(\cdot, \cdot)$  is the mean of the predicted high-fidelity model,  $n_{ini}$  is the initial safety margin,  $\mathbf{u}_{det}$  is a vector of conservative deterministic values used in place of aleatory random variables, and  $f(\mathbf{x})$  is a known deterministic objective function. We assume the limit-state function is formulated such that failure is defined as  $g(\cdot, \cdot) < 0$ . Let  $\mathbf{x}_{ini}$  denote the optimum design found from Equation 4-5 using initial safety margin  $n_{ini}$ . There is no uncertainty in the initial design  $\mathbf{x}_{ini}$  because the optimization problem is defined using the mean of the model prediction and fixed conservative values,  $\mathbf{u}_{det}$ , are used in place of aleatory random variables.

#### 4.3.3.2 Testing initial design and redesign decision

A possible high-fidelity evaluation,  $\hat{g}_H^{(i)}(\mathbf{x}_{ini}, \mathbf{u}_{det})$ , of the initial design  $\mathbf{x}_{ini}$  is simulated. The test will be passed if  $n_{lb} \leq \hat{g}_H^{(i)}(\mathbf{x}_{ini}, \mathbf{u}_{det}) \leq n_{ub}$ . If the measured safety margin is too low ( $\hat{g}_H^{(i)}(\mathbf{x}_{ini}, \mathbf{u}_{det}) < n_{lb}$ ) then the design is unsafe and redesign should be performed to

restore safety. If the safety margin is too high ( $\hat{g}_H^{(i)}(\mathbf{x}_{ini}, \mathbf{u}_{det}) > n_{ub}$ ) then the design is too conservative and it may be worth redesigning to improve performance. Let  $\hat{q}^{(i)}$  denote an indicator function for the redesign decision that is 1 for redesign and 0 otherwise. We will refer to redesign triggered by a low safety margin as redesign for safety and redesign triggered by a high safety margin as redesign for performance. If the test is not passed then redesign should be performed to select a new design.

#### 4.3.3.3 Calibration and redesign

To obtain the calibrated model, the test realization  $\hat{g}_H^{(i)}(\mathbf{x}_{ini}, \mathbf{u}_{det})$  corresponding to the error instance  $\hat{e}^{(i)}(\mathbf{x}_{ini}, \mathbf{u}_{det})$  is treated as a new data point and the error instance is added to the design of experiment for the error model. The updated mean of the predicted high-fidelity model is

$$\bar{g}_{H,calib}^{(i)}(\mathbf{x}, \mathbf{u}) = E_{\Omega} \left[ \hat{G}_H(\mathbf{x}, \mathbf{u}) | \hat{G}_H(\mathbf{x}_{ini}, \mathbf{u}_{det}) = \hat{g}_H^{(i)}(\mathbf{x}_{ini}, \mathbf{u}_{det}) \right] \quad (4-6)$$

The redesign problem is formulated as a deterministic safety-margin-based optimization problem

$$\begin{aligned} \min_{\mathbf{x}} \quad & f(\mathbf{x}) \\ \text{s.t.} \quad & \bar{g}_{H,calib}^{(i)}(\mathbf{x}, \mathbf{u}_{det}) - n_{re} \geq 0 \end{aligned} \quad (4-7)$$

where the mean of the predicted high-fidelity model  $\bar{g}_{H,calib}^{(i)}(\cdot, \cdot)$  is calibrated conditional on the test result  $\hat{g}_H^{(i)}(\mathbf{x}_{ini}, \mathbf{u}_{det})$  and  $n_{re}$  is a new safety margin that may be different than  $n_{ini}$ . Let  $\hat{\mathbf{x}}_{re}^{(i)}$  denote the optimum design after redesign found from Equation 4-7 using the calibrated model and safety margin  $n_{re}$ .

Comparing the initial design problem in Equation 4-5 to the redesign problem in Equation 4-7, we see that there is a change in the feasible design space. One change is controlled by the safety margin  $n_{re}$ , but there is also a change based on the calibrated model used to calculate the safety margin. For example, if we choose  $n_{ini} = n_{re}$  then it is still possible for the feasible design space to increase or decrease based on the calibration. If the feasible design space increases then some high performance designs



that were considered infeasible before the test may become feasible. Alternatively, the feasible design space may be reduced leading to worse design performance. This relationship between the possible change in feasible design space and the performance is precisely the change we are interested in modeling in order to select the safety margins.

#### 4.3.4 Probabilistic Evaluation

A vector of safety margins  $\mathbf{n}$  is associated with a probability of redesign  $p_{re}$  and a distribution of final designs  $\hat{\mathbf{X}}_{final}$  that translates into a distribution of probability of failure after possible redesign  $\hat{P}_{f,final}$ , and a distribution of design cost  $f(\hat{\mathbf{X}}_{final})$ . The distributions are approximated based on a Monte Carlo simulation of  $m$  error realizations  $i = 1, \dots, m$  as described in Section 4.3.2.

The probability of redesign is  $p_{re} = E_{\Omega} [\hat{Q}]$  where  $\hat{Q}$  is the indicator function for the redesign decision. The final design after possible redesign is

$$\hat{\mathbf{x}}_{final}^{(i)} = (1 - \hat{q}^{(i)}) \mathbf{x}_{ini} + \hat{q}^{(i)} \hat{\mathbf{x}}_{re}^{(i)} \quad (4-8)$$

Recall, that  $\hat{q}^{(i)} = 1$  corresponds to failing the test and performing redesign. The expected design cost after possible redesign is  $E_{\Omega} [f(\hat{\mathbf{X}}_{final})]$ . Since the redesign decision defines a partitioning of the epistemic outcome space, the law of total expectation allows the expectation to be written as

$$E_{\Omega} [f(\hat{\mathbf{X}}_{final})] = (1 - p_{re}) f(\mathbf{x}_{ini}) + p_{re} E_{\Omega} [f(\hat{\mathbf{X}}_{re})] \quad (4-9)$$

where  $f(\mathbf{x}_{ini})$  is the expected design cost conditional on the test being passed and the designer keeping the initial design and  $E_{\Omega} [f(\hat{\mathbf{X}}_{re})]$  is the expected design cost conditional on the test being failed and the designer performing redesign.

The true probability of failure of the final design is unknown since there is epistemic uncertainty in the model  $\hat{G}_H(\cdot, \cdot)$ . A realization of the probability of failure is calculated conditional on an error realization  $\hat{E}(\cdot, \cdot) = \hat{e}^{(i)}(\cdot, \cdot)$ . A realization of the probability of

failure for the initial design is

$$\hat{p}_{f,ini}^{(i)} = Pr_U \left[ \hat{g}_H^{(i)}(\mathbf{x}_{ini}, \mathbf{U}) < 0 \right] \quad (4-10)$$

where  $Pr_U [\cdot]$  denotes the probability with respect to aleatory uncertainty. Note that the epistemic model uncertainty is treated separately from the aleatory uncertainty to distinguish between the quantity of interest, the probability of failure with respect to the high-fidelity model and aleatory uncertainty, and the lack of knowledge regarding this quantity. The error in the low-fidelity model  $\hat{E}(\cdot, \cdot)$  has no impact on the reliability with respect to the high-fidelity model  $g_H(\cdot, \cdot)$ . However, since the high-fidelity model is unknown, the probability of failure calculation is repeated many times conditional on all possible realizations of the high-fidelity model  $\hat{g}_H^{(i)}(\cdot, \cdot)$  as shown in Equation 4-10. A realization of the final probability of failure after possible redesign is

$$\hat{p}_{f,re}^{(i)} = Pr_U \left[ \hat{g}_H^{(i)}(\hat{\mathbf{x}}_{re}^{(i)}, \mathbf{U}) \leq 0 \right] \quad (4-11)$$

After redesign, the design variable  $\hat{\mathbf{x}}_{re}^{(i)}$  is also an epistemic random variable in addition to the limit state function  $\hat{g}_H^{(i)}(\cdot, \cdot)$ . Many different methods are available for calculating the probability of failure. In this study, first order reliability method (FORM) is used to calculate the probability of failure for each epistemic realization. The final probability of failure after possible redesign is

$$\hat{p}_{f,final}^{(i)} = (1 - \hat{q}^{(i)}) \hat{p}_{f,ini}^{(i)} + \hat{q}^{(i)} \hat{p}_{f,re}^{(i)} \quad (4-12)$$

Note that the redesign decision  $\hat{q}^{(i)}$  shapes the final probability of failure distribution because we will have the opportunity in the future to correct the initial design if it fails the deterministic test. The expected probability of failure after possible redesign is  $E_\Omega \left[ \hat{P}_{f,final} \right]$ . As above, the expectation can be written as

$$E_\Omega \left[ \hat{P}_{f,final} \right] = (1 - p_{re}) E_\Omega \left[ \hat{P}_{f,ini} | \hat{Q} = 0 \right] + p_{re} E_\Omega \left[ \hat{P}_{f,re} | \hat{Q} = 1 \right] \quad (4-13)$$

where the  $E_{\Omega} [\hat{P}_{f,ini} | \hat{Q} = 0]$  is the expected probability of failure conditional on the test being passed and the designer keeping the initial design and  $E_{\Omega} [\hat{P}_{f,re} | \hat{Q} = 1]$  is the expected probability of failure conditional on the test being failed and the designer performing redesign.

## 4.4 Demonstration Example

### 4.4.1 Overview

The demonstration problem is adapted from an example by Wu et al. [6]. The example is the design of a cantilever beam to minimize mass subject to a constraint on tip displacement. The original problem involved the design of a long slender beam and therefore used Euler-Bernoulli beam theory. In this example, the length of the beam is reduced such that shear stress effects become important and Timoshenko beam theory is more accurate. The low-fidelity model of the tip displacement is formulated based on Euler-Bernoulli beam theory and the high-fidelity model is formulated based on Timoshenko beam theory. The design optimization (equations 4–5 and ??) is performed using sequential quadratic programming (SQP).

The low-fidelity model of the limit state function is

$$g_L(\mathbf{x}, \mathbf{U}) = d^* - \frac{4I^3}{ewt} \sqrt{\left(\frac{F_Y}{t^2}\right)^2 + \left(\frac{F_X}{w^2}\right)^2} \quad (4-14)$$

where  $\mathbf{x} = \{w, t\}$  are the design variables and  $\mathbf{U} = \{F_X, F_Y\}$  are the aleatory variables.

The high-fidelity model of the limit state function is

$$g_H(\mathbf{x}, \mathbf{U}) = d^* - \sqrt{(d_x(\mathbf{x}, \mathbf{U}))^2 + (d_y(\mathbf{x}, \mathbf{U}))^2} \quad (4-15)$$

where  $d_x$  and  $d_y$  are given by equations 4–16 and 4–17. The problem parameters are described in Table 4-2.

$$d_x(\mathbf{x}, \mathbf{U}) = \left( \frac{3IF_X}{2gwt} + \frac{4I^3F_X}{ewt^3} \right) \quad (4-16)$$

$$d_y(\mathbf{x}, \mathbf{U}) = \left( \frac{3IF_Y}{2gwt} + \frac{4I^3F_Y}{ew^3t} \right) \quad (4-17)$$

Table 4-2. Parameters for cantilever beam example

	Parameter	Notation	Value
Design variables, $\mathbf{x}$	Width of cross section	$w$	$2.5 \leq w \leq 5.5$ in
	Thickness of cross section	$t$	$1.5 \leq t \leq 4.5$ in
Aleatory variables, $\mathbf{U}$	Horizontal load	$F_X$	$F_X \sim N(500, 100^2)$ lbs
	Vertical load	$F_Y$	$F_Y \sim N(1000, 100^2)$ lbs
Constants	Elastic modulus	$e$	$29 \times 10^6$ psi
	Shear modulus	$g$	$11.2 \times 10^6$ psi
	Length of beam	$l$	10 in
	Allowable tip displacement	$d^*$	$2.25 \times 10^{-3}$ in
	Conservative aleatory values	$\mathbf{u}_{det}$	$\{664.5, 1164.5\}$ lbs
	Target mean probability of failure	$p_f^*$	$1.35 \times 10^{-3}$

The objective function is the cross-sectional area of the beam

$$f(\mathbf{x}) = wt \quad (4-18)$$

#### 4.4.2 Error Model

It is assumed that some preliminary test data is available for constructing the surrogate model  $\hat{E}(\mathbf{x}, \mathbf{U})$ . In this example, the preliminary test data corresponds to evaluations of  $g_H(\cdot, \cdot)$  at the 16 corner points of the joint design-aleatory space. The corner points were selected for illustration purposes in order to ensure there is reasonably high epistemic model uncertainty for points inside the design domain. In practice, other designs of experiments (DoE) could be used or any available test data could be used to construct the error model. The design space is defined according to the bounds on  $\mathbf{x}$  in Table 4-2 and bounds on  $\mathbf{U}$  corresponding to  $-2\sigma$  to  $+7\sigma$ . Based on this DoE the parameters for the Kriging error model are estimated using maximum likelihood estimation (MLE). A Gaussian covariance function was selected for the Kriging model. The error model is constructed in the joint space of design variables,  $\mathbf{x}$ , and

aleatory variables,  $\mathbf{U}$ . Recall, the design optimization problem is formulated using fixed conservative values,  $\mathbf{U} = \mathbf{u}_{det}$ . In Figure 4-2, the design optimization problem is shown along with the 95% confidence interval of model uncertainty. In Figure 4-2, the reliability analysis is shown for the optimum design found using  $n_{ini} = 0$  along with the 95% confidence interval of model uncertainty. Selecting a different design by using a different safety margin will alter the plot shown in Figure 4-2. However, the plot is provided as an example to show how the model uncertainty results in a wide confidence interval in the aleatory space. The wide confidence intervals in aleatory space will result in high uncertainty in the probability of failure. The mean and variance of the model error vary with design variables,  $\mathbf{x}$ , and aleatory variables,  $\mathbf{U}$  as shown in Figure 4-3. The variance is zero at the corners of the design space since these points correspond to sample locations in the DoE. Although the absolute values of the error appear small, the error is significant relative to the model predictions of tip displacement. For example, the allowable tip displacement in this example is  $d^* = 2.25 \times 10^{-3}$  inches.

#### 4.4.3 Results

Tradeoff curves for expected cost versus probability of redesign are shown in Figure 4-4. For zero probability of redesign, the problem reduces to finding an initial safety margin,  $n_{ini}$ , that minimizes the mass of the initial design,  $f(\mathbf{x}_{ini})$ , while ensuring that the mean probability of failure for the initial design,  $E_{\Omega} [\hat{P}_{f,ini}]$ , satisfies the reliability constraint. With increasing probability of redesign, redesign can be used to improve safety if the initial design is revealed to be dangerous or improve performance if the initial design is revealed to be too conservative. Redesign for safety allows for a lighter initial design because the initial design will be corrected if the tip displacement is later revealed to be too high (i.e. unsafe). If redesign is required, the final beam will become heavier during redesign because making the beam stiffer (i.e. safer) results in a mass increase. Redesign for performance starts with a heavier initial design and redesign will be performed if the tip displacement of the initial design is later revealed to be too low

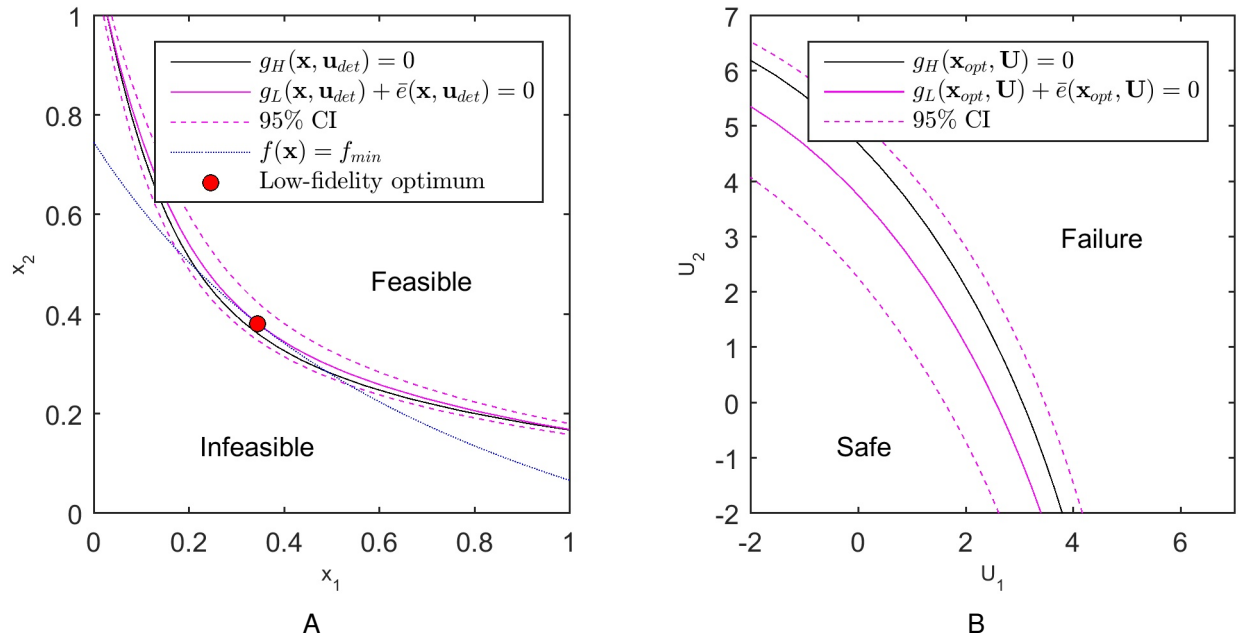


Figure 4-2. The figure on the left shows the design optimization when using a safety margin  $n_{ini} = 0$  and fixed conservative values  $\mathbf{u}_{det}$  in place of aleatory variables  $\mathbf{U}$ . The figure on the right shows the reliability of the optimum design found on the left by plotting the limit-state function in standard normal space.

(i.e. very conservative or safe). If redesign is required, the final design can be made lighter during redesign because the beam can be made less stiff. It is observed that redesign for safety results in a lower mean mass than redesign for performance. It is also observed that a mixed redesign strategy offers a slight improvement over redesign for safety. However, as indicated by the error bars it is not clear if this difference is a result of bias in the surrogate models used when optimizing the safety margins.

The simulation results can be explored in more detail by looking at a single point on the tradeoff curve. The safety margins corresponding to 20% probability of redesign were selected for more detailed investigation. Figure 4-5 shows the distribution of possible high-fidelity safety margins for the initial design that are predicted based on the model error. Both distributions capture the true safety margin if we were to evaluate the initial design using the high-fidelity model. In the case of redesign for

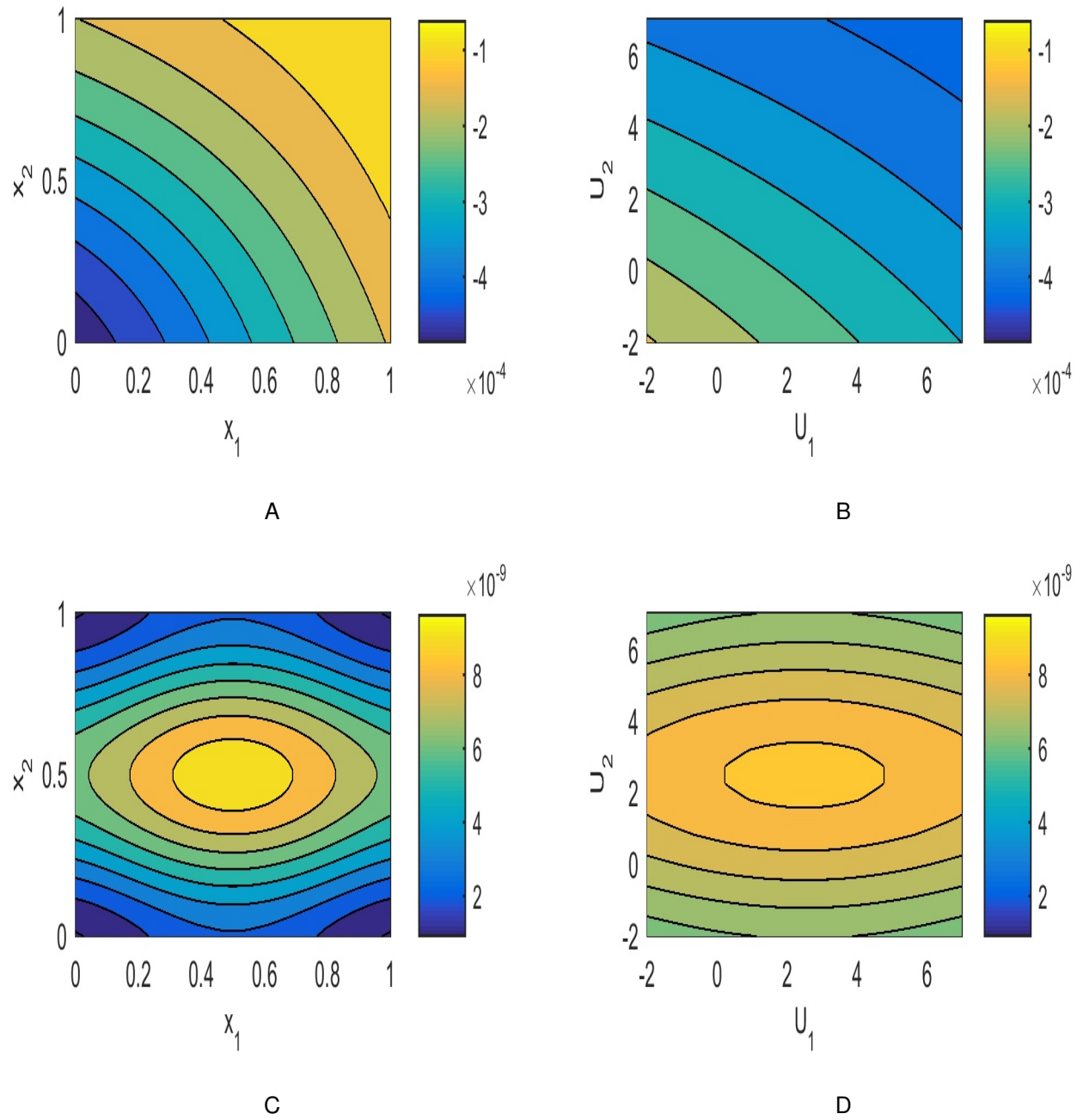


Figure 4-3. On the left, the mean and variance of the error are plotted in a normalized design space with fixed conservative values  $\mathbf{u}_{det}$  in place of aleatory variables  $\mathbf{U}$ . On the right, the mean and variance of the error are plotted in standard normal aleatory space for optimum design found using  $n_{ini} = 0$ . The error is in inches.

performance, we see that the true safety margin is greater than  $n_{ub}$  and therefore redesign would be required. If we calibrate using the true high-fidelity evaluation and perform redesign the true safety margin is now very close to  $n_{re}$  which agrees with the predicted change in the safety margin. Figure 4-6 shows the joint distributions of the design variables corresponding to the width and thickness of the beam cross section. The peak in the distributions corresponds to the initial design,  $\mathbf{x}_{ini}$ . The safety margins have been optimized such that there is an 80% probability that the design will not require any changes after the future test. The other designs in the figure correspond to failing the future test and performing redesign. Figure 4-7 shows the distributions of cross-sectional area corresponding to the designs in Figure 4-6. The mass is reduced if redesign for performance is required and the mass is increased if redesign for safety is required. We can see in the distribution of cross sectional area for redesign for performance that the predicted mass reduction after redesign is close to the true value. Comparing the safety margin distributions in Figure 4-5 to the reliability index distributions in Figure 4-8 we observe similar distribution shapes. Both distributions capture the true reliability index of the initial design as calculated with respect the high-fidelity model. After redesign for performance the true reliability index is reduced in order to reduce the mass of the beam. The true reliability index after redesign falls within the predicted distribution of possible final reliability indexes. Histograms of the most-probable point (MPP) are shown in Figure 4-9. The fixed deterministic values we selected  $\mathbf{u}_{det}$  are slightly outside the distribution of possible MPP's. However, the values are not totally unreasonable since they are much closer to the center of the distribution than, for example, the mean of the distributions which is located at  $[0, 0]$ .

#### 4.5 Discussion and Conclusions

In this study we described a method for the optimization of a safety-margin-based design process that allows the designer to tradeoff between the expected design performance and probability of redesign. Previous studies on the optimization of safety



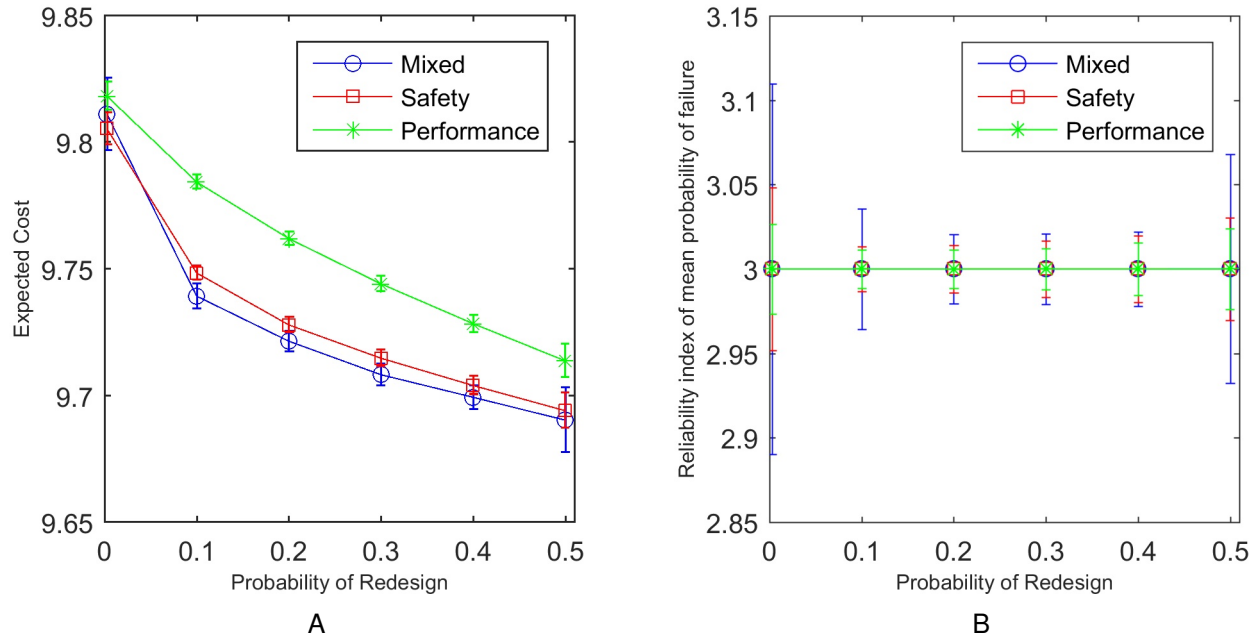


Figure 4-4. Tradeoff curves for expected cost (cross sectional area in square inches) as a function of probability of redesign. The curve labeled “mixed” corresponds to simultaneous optimization of  $\mathbf{n} = \{n_{ini}, n_{lb}, n_{ub}, n_{re}\}$ . The curve labeled “safety” corresponds to optimizing  $\{n_{ini}, n_{lb}, n_{re}\}$  with  $n_{ub} = +\infty$ . The curve labeled “performance” corresponds to optimizing  $\{n_{ini}, n_{ub}, n_{re}\}$  with  $n_{lb} = -\infty$ . Error bars are based on surrogate models used during optimization.

margins when considering future redesign required an assumption of constant model bias [20, 21, 23]. However, in engineering design problems the model bias may vary with the design variables as well as the aleatory variables, such as in the case of the cantilever beam example. This study improves on previous work by introducing a Kriging model as a more general model of the epistemic uncertainty in the low-fidelity model. The Kriging model offers several practical benefits over the previous method. In particular, the Kriging model easily allows for the incorporation of preliminary high-fidelity data and a simple calibration of the model when new high-fidelity data becomes available. The Kriging error model captures the intuitive idea that the variance of the model error is greatest in unexplored regions and a minimum at existing data points. The Kriging model also provides several theoretical improvements of the method. One

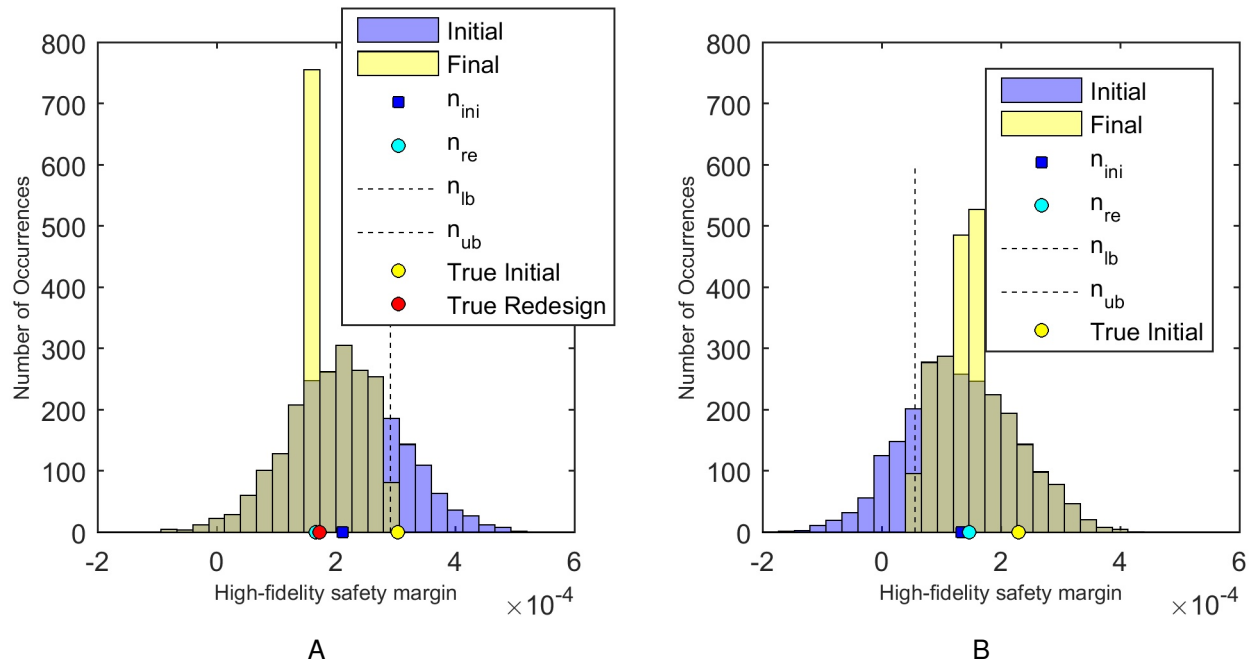


Figure 4-5. Histograms of possible safety margin distributions for 20% probability of redesign. Plots show overlapping transparent histograms.

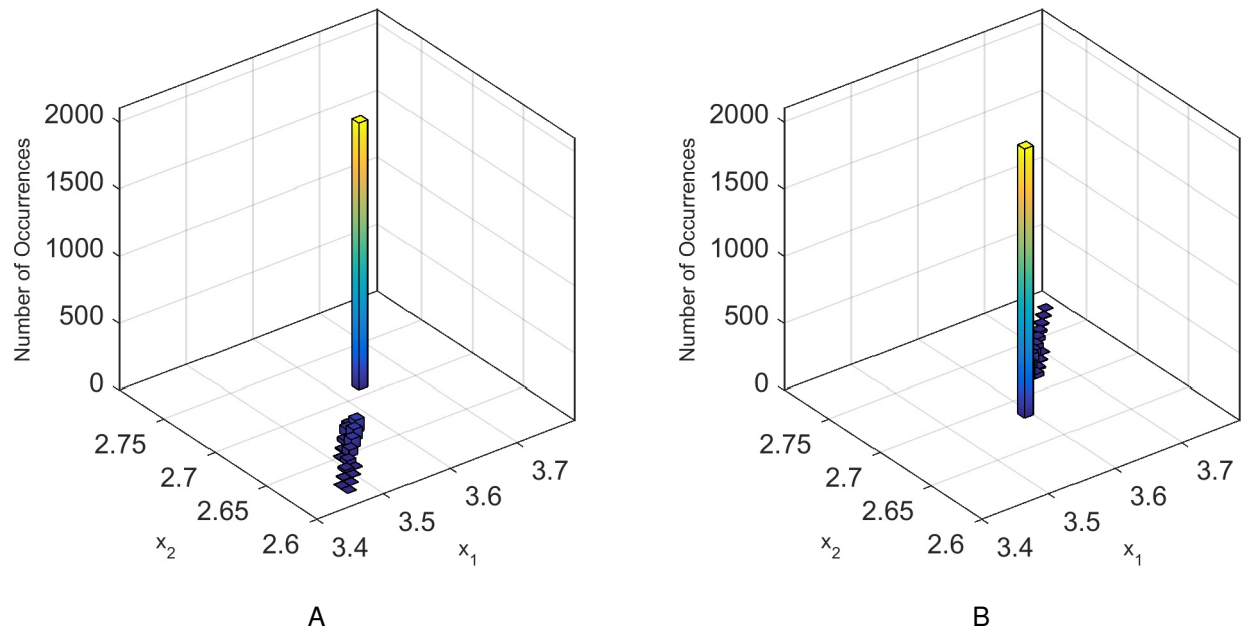


Figure 4-6. Joint distribution of design variables for possible final designs for 20% probability of redesign. Peak is located at initial design.

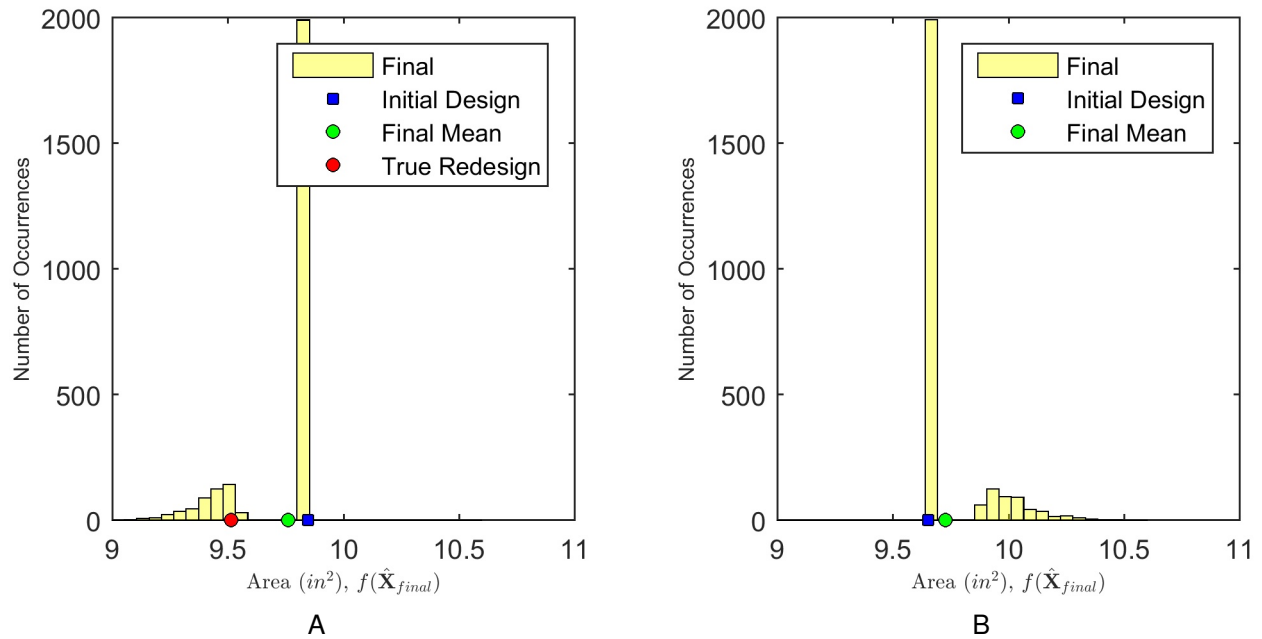


Figure 4-7. Histograms of cross-sectional area distributions for 20% probability of redesign.

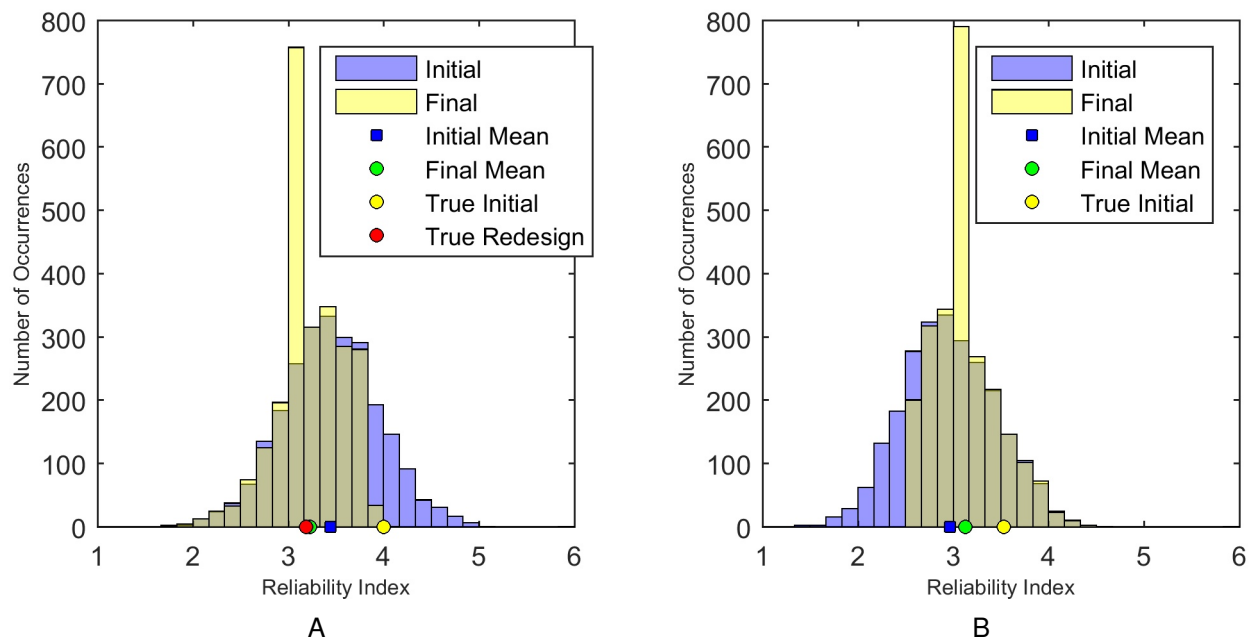


Figure 4-8. Histograms of reliability index distributions for 20% probability of redesign. Plots show overlapping transparent histograms.

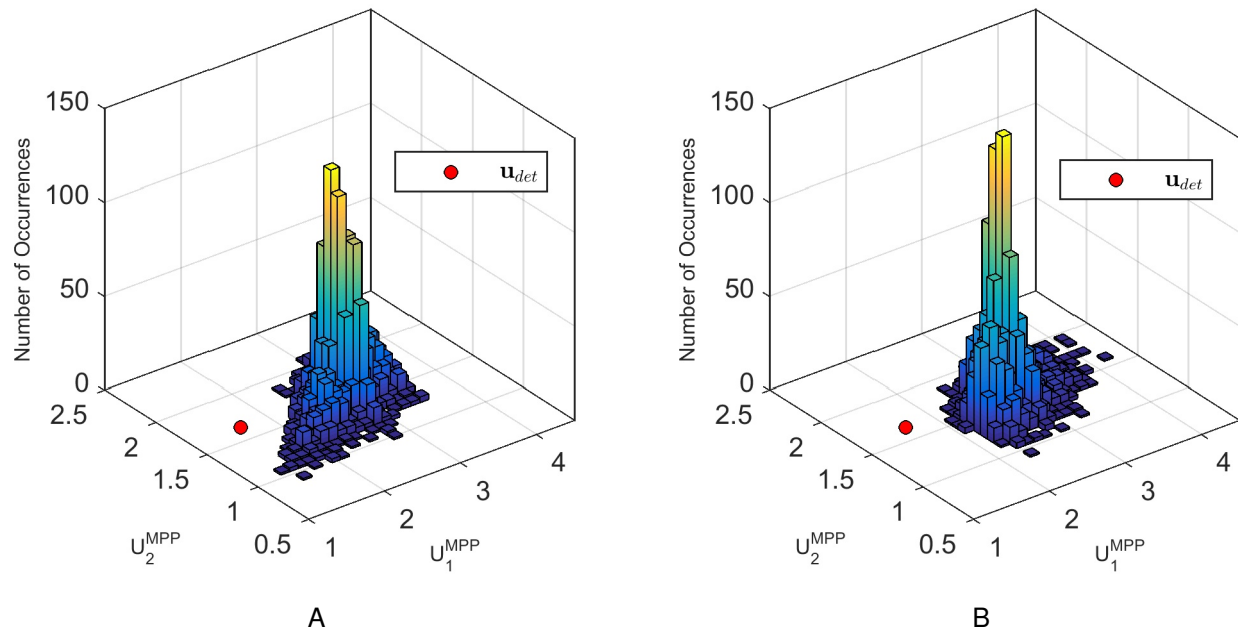


Figure 4-9. Joint distribution of possible most probable points (MPP's) for 20% probability of redesign.

benefit is that it is likely that there exists a realization taken from the Kriging model that is arbitrarily close to the actual error between the low and high-fidelity models. Therefore, it is likely that there also exists a realization of the probability of failure that is close to the true probability of failure with respect to the high-fidelity model. In addition, it is likely the Kriging model will converge to the true error as more high-fidelity evaluations (or tests) are performed. If the Kriging model converges to the true error, then the distribution of probability of failure will also converge to the true probability of failure with respect to the high-fidelity model. Previous work was not capable of modeling the convergence of the model error because under the assumption of constant model bias only a single high-fidelity evaluation was necessary to remove all epistemic uncertainty.

The method was applied to a simple cantilever beam design problem of minimizing the mass, or equivalently cross-sectional area, subject to a constraint on tip-displacement. Only a few high-fidelity evaluations were needed to construct the Kriging model that was used to provide the distribution of model uncertainty. A distribution of probability of

failure was obtained through the combination of FORM and a MCS of error realizations (i.e. conditional simulations). It was shown that the distribution of possible reliability indexes captured the true reliability index of the initial design with respect to the high-fidelity model. Furthermore, it was shown that the predicted change in reliability after redesign agreed with the actual redesign outcome when the high-fidelity model was evaluated and redesign was performed. The safety margins governing a deterministic design process were optimized to tradeoff between the probability of redesign and the expected mass of the final design. It was shown that the predicted mass reduction (i.e. performance improvement) agreed with the actual change in performance after evaluating the high-fidelity model and performing redesign. For this example, it was found that it was better to start with a less conservative, lighter design and implement a test and redesign process that would restore safety if the initial design was later revealed by the high-fidelity model to be unsafe. This process was contrasted with starting with a more conservative, heavier design and implementing a test and redesign process that would improve design performance if the initial design was later revealed by the high-fidelity model to be too conservative. A mixed design strategy where redesign would restore safety or improve performance conditional on the results of the high-fidelity evaluation was found to be comparable to the redesign for safety approach. It is hypothesized that the best redesign strategy is problem dependent. In general, there is no need to specify a redesign for safety or redesign for performance a priori because when allowed to control all the safety margins the optimizer will converge to the best redesign strategy.

## CHAPTER 5

### SOUNDING ROCKET DESIGN UNDER MIXED EPISTEMIC MODEL UNCERTAINTY AND ALEATORY PARAMETER UNCERTAINTY

#### 5.1 Research Context in Relation to Scope of Dissertation

In Chapter 3, a method was introduced for predicting the possible outcomes of a future test followed by possible redesign in order to optimize the safety margins controlling a deterministic design process. In Chapter 4, the method was modified to remove the restrictive assumption of constant model bias and the method was demonstrated on a simple cantilever beam design example. The cantilever beam example was useful for illustrating the method, but it is much simpler than typical engineering design problems. In this chapter, a sounding rocket design example is used to illustrate the method on a complex design problem. The sounding rocket design example is significantly more complex than previous examples due to the:

1. Increased computational cost of the models
2. Increased number of design variables
3. Multi-disciplinary design considerations
4. Design variables that are unique to the high-fidelity model
5. Epistemic uncertainty in the objective function
6. Additional deterministic design constraints.

The method from Chapter 4 is modified to reduce the computational cost so the method is more readily applicable to realistic design problems. The constraint on mean probability of failure from chapters 3 and 4 is replaced with a more conservative quantile constraint to ensure that some very safe designs do not cancel out the risk of obtaining a dangerous final design. The cantilever beam example is revisited to illustrate the changes to the method before applying the method to the sounding rocket design example.

## 5.2 Introduction

At the initial design stage engineers usually rely on low-fidelity models that have high epistemic uncertainty. Uncertainty is typically classified as aleatory or epistemic [31, 37, 67]. Epistemic uncertainty is due to lack of knowledge, is reducible by gaining more information, and has a fixed but unknown value. Aleatory uncertainty is due to variability, is irreducible, and is a distributed quantity. In engineering design, a system is typically designed to be robust with respect to aleatory variables such as environmental conditions or material variability. The robustness of the system to aleatory uncertainty may be controlled implicitly through safety margins, safety factors[2], and conservative design values[50] or explicitly through reliability-based design methods. However, there are relatively few design methods that consider epistemic model uncertainty [9, 10, 79]. If there is high epistemic model uncertainty, then there may be significant epistemic uncertainty (i.e. lack of knowledge) regarding the reliability of the as-built system. Errors in low-fidelity models, which may be considered indicative of errors in reliability estimates, are often revealed in the future when higher fidelity simulations are performed or prototypes are tested. If improved modeling reveals significant discrepancies between low and high-fidelity simulations or between simulations and prototypes, redesign may be required to correct the initial design.

Redesign, also known as engineering change, is the process of revising an initial design conditional on new knowledge[69]. Typically, redesign is performed if a low-fidelity model is revealed to have unconservative bias that may indicate an unsafe initial design. Redesign is also beneficial when an initial design is revealed to be overly conservative such that the design performance can be significantly improved. Redesign provides an opportunity for design improvement, however, it is often viewed as a problem in industry because redesign may be associated with substantial costs and delays [68]. Designers could benefit from controlling the probability of future redesign and trading off between the probability of redesign and design performance[21].

However, predicting how the reliability and performance may change conditional on future redesign is a complex and computationally expensive task.

Even without considering redesign, there is significant computational cost involved in mixed epistemic and aleatory uncertainty propagation. For example in a two level Monte-Carlo simulation (MCS), for each epistemic realization sampled in the outer loop many aleatory realizations are sampled and propagated through design models in the inner loop in order to calculate a distribution, or family, of distributions [66]. Two-level uncertainty propagation is computationally costly, but provides the complete distribution of probability of failure which can be used to calculate a variety of useful statistics, such as confidence intervals[67]. Alternatively, a model with epistemic model uncertainty could be replaced with a conservative prediction, such as mean plus  $k$  standard deviation offset, in order to avoid the expensive two-level uncertainty propagation[10, 56]. However, the former approach allows for precise reliability statements such as “we believe with  $1-\alpha$  confidence that the probability of failure is less than  $p_f^\alpha$ ” whereas the interpretation of the latter approach is less straightforward and may only yield “pseudo-confidence bounds[56]”. The reliability assessment becomes more complex when we consider that the design variables are epistemic random variables. That is, if there is some probability of future redesign then the final design is an epistemic random variable because it is unknown (e.g. incomplete, imprecise, or uncertain specification) at the initial design stage.

In this study, we propose a design method that considers mixed epistemic model uncertainty and aleatory parameter uncertainty and includes the possibility of future redesign. It will be shown that redesign acts as a type of quality control measure for epistemic uncertainty by implementing design changes in response to extreme epistemic realizations. In the proposed method, aleatory and epistemic uncertainties in the reliability assessment are handled sequentially rather than in a nested fashion. In a preliminary step, traditional RBDO is performed with respect to aleatory parameter



uncertainty using the mean low-fidelity model in order to find the most probable point (MPP) of the aleatory random variables with respect to the mean low-fidelity model. In subsequent steps, aleatory random variables are fixed at this MPP and a  $k$  standard deviation offset is used as a safety margin with respect to epistemic model uncertainty. An initial design is found based on deterministic optimization using a standard deviation offset  $k_{ini}$ . In the future, the initial design will be tested (i.e. the high-fidelity model will be evaluated at the initial design) and the redesign decision will be based on the observed discrepancy between the low and high-fidelity models. If the observed discrepancy is less than  $k_{lb}$  or above  $k_{ub}$  then redesign will be performed. During redesign a possibly different standard deviation offset  $k_{re}$  is used. The outcome of the future high-fidelity evaluation (i.e. future test) is unknown at the initial design stage and therefore the design process is repeated in a MCS. The MCS allows for the calculation of the probability of redesign and a prediction of how future redesign is related to final design performance and reliability. The standard deviation offsets  $\mathbf{k} = \{k_{ini}, k_{lb}, k_{ub}, k_{re}\}$  governing the design process are optimized to minimize the expected value of the objective function while satisfying constraints on reliability and probability of redesign. In contrast to previous work on simulating the effects of a future test and redesign[19–21], this study accounts for spatial correlations in epistemic model uncertainty by using a Kriging model to represent model uncertainty and significantly reduces the computational cost by proposing a computationally cheap approximation of the reliability constraint. After the optimization of the standard deviation offsets, the complete probability of failure distribution is recovered through two-level uncertainty propagation.

In Section 5.3 the general method of simulating a future test and possible redesign is described. In Section 5.4 the method is demonstrated on a cantilever beam bending example and then a multidisciplinary sounding rocket design problem. In Section 5.5 the study is summarized and the implications of the method and results are discussed.

### 5.3 Methods

In Section 5.3.1, the conservative values that will be used in place of aleatory random variables are found based on preliminary RBDO. In Section 5.3.2, the formulation of the optimization of the standard deviation offsets is presented. The Monte Carlo simulation (MCS) of epistemic error realizations is described in Section 5.3.3. A single sample in the MCS consists of a complete deterministic design / redesign process as described in Section 5.3.4. In Section 5.3.5, the calculation of the expected objective function value, probability of redesign, and probability of the probability of failure exceeding a target value are described.

#### 5.3.1 Preliminary Reliability-Based Design Optimization (RBDO)

Preliminary reliability-based design optimization (RBDO) is performed using the mean low-fidelity model of the limit-state function and considering only aleatory uncertainty. In subsequent steps, aleatory random variables are fixed at the MPP as the design is optimized deterministically. The preliminary RBDO problem is formulated as

$$\begin{aligned}
 &\min \quad \mathbb{E}_U [f(\mathbf{x}, \mathbf{U})] \\
 &\text{w.r.t } \mathbf{x} \\
 &\text{s.t.} \quad \mathbb{P}_U [\bar{g}(\mathbf{x}, \mathbf{U}) \leq 0] \leq p_f^*
 \end{aligned} \tag{5-1}$$

where  $\mathbb{E}_U[\cdot]$  is an expectation operator with respect to aleatory uncertainty,  $\mathbb{P}_U[\cdot]$  is a probability operator with respect to aleatory uncertainty,  $f(\cdot, \cdot)$  is the objective function,  $\mathbf{x} \in \mathbb{R}^d$  is a vector of design variables,  $\mathbf{U}$  is a vector of aleatory random variables with a realization  $\mathbf{u} \in \mathbb{R}^p$ ,  $\bar{g}_H(\cdot, \cdot)$  is the mean limit-state function, and  $p_f^*$  is the target probability of failure. The formulation of the search for the MPP of the RBDO optimum  $\mathbf{x}_{RBDO}$  is

$$\begin{aligned}
 &\min \quad ||\mathbf{u}|| \\
 &\text{w.r.t } \mathbf{u} \\
 &\text{s.t.} \quad \bar{g}(\mathbf{x}_{RBDO}, \mathbf{u}) \geq 0
 \end{aligned} \tag{5-2}$$

Since the RBDO problem does not consider epistemic model uncertainty in the limit-state function there is a high probability that the resulting optimum could be very unsafe or very conservative. However, the computational cost of the optimization problem is much lower than formulating an optimization with full two-level mixed epistemic / aleatory uncertainty propagation. The task of locating a design that is conservative with respect to epistemic model uncertainty, but not overly so, will be addressed in the remainder of the proposed method.

### 5.3.2 Optimization of Standard Deviation Offsets

The optimization of the standard deviation offsets (i.e. safety margins) is formulated as

$$\begin{aligned}
& \min \quad \mathbb{E}_E [\mathbb{E}_U [f(\mathbf{X}_{final}, \mathbf{U})]] \\
& \text{w.r.t } \mathbf{k} = \{k_{ini}, -k_{lb}, k_{ub}, k_{re}\} \\
& \text{s.t.} \quad \mathbb{P}_E [P_f(\mathbf{X}_{final}) \geq p_f^*] \leq \alpha \\
& \quad \quad p_{re} \leq p_{re}^* \\
& \quad \quad 0 \leq \mathbf{k} \leq 4
\end{aligned} \tag{5-3}$$

where  $\mathbb{E}_E[\cdot]$  an expectation operator with respect to epistemic uncertainty,  $\mathbf{X}_{final}$  is a vector of final optimum design variables,  $\mathbb{P}_E[\cdot]$  is a probability operator with respect to epistemic uncertainty,  $P_f(\cdot)$  is the probability of failure with respect to aleatory uncertainty,  $p_f^*$  is the target probability of failure,  $1 - \alpha$  is the desired confidence level, and  $p_{re}$  is the probability of redesign. The final design,  $\mathbf{X}_{final}$ , is uncertain because we consider the possibility that the design may need to be redesigned in the future conditional on the outcome of a high-fidelity evaluation of the initial design. The probability of failure,  $P_f(\cdot)$ , is uncertain because there is epistemic model uncertainty in the limit-state function and because the design is uncertain. The tradeoff between the expected objective function value and probability of redesign is captured by solving the single objective optimization problem for several values of the constraint  $p_{re}^*$ . The

global optimization is performed using Covariance Matrix Adaptation Evolution Strategy (CMA-ES) [82] with a penalization strategy to handle the constraints.

The computational cost of the standard deviation offsets optimization problem is high due to the mixed epistemic and aleatory uncertainty in the reliability constraint. To reduce the computational cost, the reliability constraint is approximated as

$$\mathbb{P}_E [P_f(\mathbf{X}_{final}) \geq p_f^*] \approx \mathbb{P}_E [G_H(\mathbf{X}_{final}, \mathbf{u}_{det}) \leq 0] \quad (5-4)$$

where  $\mathbf{u}_{det}$  is a vector of fixed conservative values used in place of aleatory variables corresponding to the MPP as found in 5-1, 5-2 and  $G_H(\cdot, \cdot)$  is an uncertain limit-state function. The true probability on the left-hand side of 5-4 requires two-level uncertainty propagation, but the approximation on the right only considers epistemic uncertainty and is therefore only requires single level uncertainty propagation. The approximation is inspired by studies on reliability-based design considering only aleatory uncertainty where the reliability constraint is converted to an equivalent deterministic constraint [5-7]. There are two elements that contribute the the error in the proposed approximation. First, the MPP is an epistemic random variable due to model uncertainty so any single point estimate will incur some degree of error. Second, the final design is an epistemic random variable and will differ from  $\mathbf{x}_{RBDO}$  where the MPP search was performed. It is assumed that the MPP with respect to the mean limit-state function  $\bar{g}(\cdot, \cdot)$  is a reasonable approximation of the mean MPP with respect to the realizations of the uncertain limit-state function  $G(\cdot, \cdot)$ . That is, it is assumed the MPP of the mean is close to the mean of the MPP's. Furthermore, it is assumed that the distribution of final designs  $\mathbf{X}_{final}$  will be centered near  $\mathbf{x}_{RBDO}$ . The approximation is introduced to reduced the cost of the optimization of the standard deviation offsets. The full two-level uncertainty propagation is performed for the optimum standard deviation offsets in order to recover the full probability of failure distribution and assess the accuracy of the approximation.

### 5.3.3 Monte-Carlo Simulation of Epistemic Model Error

The epistemic model uncertainty and aleatory parameter uncertainty are treated separately (see [66, 67, 85]). The true relationship between the different fidelity models is assumed to be of the form

$$g_H(\mathbf{x}, \mathbf{u}) = g_L(\mathbf{x}, \mathbf{u}) + e(\mathbf{x}, \mathbf{u}) \quad (5-5)$$

where  $g_H(\cdot, \cdot)$  is the high-fidelity model,  $g_L(\cdot, \cdot)$  is the low-fidelity model, and  $e(\cdot, \cdot)$  is the error between the low-fidelity and high-fidelity models. Typically, the error  $e(\cdot, \cdot)$  is unknown. The uncertainty in the model error is represented as a Kriging model  $E(\cdot, \cdot)$ . Based on the possible model errors the high-fidelity model is predicted as

$$G_H(\mathbf{x}, \mathbf{u}) = g_L(\mathbf{x}, \mathbf{u}) + E(\mathbf{x}, \mathbf{u}) \quad (5-6)$$

The Kriging model for the error is constructed in the joint space of the aleatory variables,  $\mathbf{u}$ , and the design variables,  $\mathbf{x}$ . The uncertainty in  $G_H(\mathbf{x}, \mathbf{u})$  in 5-6 is only due to epistemic model error  $E(\cdot, \cdot)$ . Propagation of aleatory uncertainty  $\mathbf{U}$  through the uncertain model is discussed in Section 5.3.5. For simplicity of notation, we will define the mean of the Kriging prediction for the error as  $\bar{e}(\cdot, \cdot)$  and the standard deviation as  $\sigma_E(\cdot, \cdot)$ . The mean prediction of the high-fidelity model is

$$\bar{g}_H(\mathbf{x}, \mathbf{u}) = g_L(\mathbf{x}, \mathbf{u}) + \bar{e}(\mathbf{x}, \mathbf{u}) \quad (5-7)$$

with standard deviation  $\sigma_G(\cdot, \cdot) = \sigma_E(\cdot, \cdot)$ .

The epistemic random function  $E(\cdot, \cdot)$  is used to represent the lack of knowledge regarding how well the low-fidelity model matches the high-fidelity model. Assuming initial test data is available, maximum likelihood estimation (MLE) will be used to estimate the parameters of the Kriging model. The prediction  $G_H(\cdot, \cdot)$  is viewed as a distribution of possible functions. Samples or trajectories drawn from this distribution that are conditional on initial test data are referred to as conditional simulations. In

the absence of test data these realizations are unconditional simulations. These simulations are spatially consistent Monte Carlo simulations. Let  $g_H^{(i)}(\cdot, \cdot)$  denote the  $i$ -th realization of  $G_H(\cdot, \cdot)$  based on a realization  $e^{(i)}(\cdot, \cdot)$  of the Kriging model  $E(\cdot, \cdot)$ . A variety of methods exist for generating these conditional simulations [86]. In this study, the conditional simulations are generated directly based on Cholesky factorization of the covariance matrix using the STK Matlab toolbox for Kriging [87] and by sequential conditioning [86].

We can consider a Monte Carlo simulation of  $m$  conditional simulations  $i = 1, \dots, m$  corresponding to  $m$  possible futures. In practice, the sample size  $m$  is increased until the estimated coefficient of variation of the quantity of interest is below a certain threshold. Let  $\Omega$  denote the epistemic uncertainty space of the model  $G_H(\cdot, \cdot)$ . There is a realization,  $\exists \omega \in \Omega$ , such that the simulation,  $g_H^{(\omega)}(\cdot, \cdot)$ , is arbitrarily close to the high-fidelity model,  $g_H(\cdot, \cdot)$ . The design process conditional on one error realization is described in Section 5.3.4. By repeating the design process for many different error realizations (i.e. for different possible high-fidelity models through 5–6) we can determine the distribution of possible final design outcomes.

#### 5.3.4 Deterministic Design Process

The deterministic design process is controlled by a vector of standard deviation offsets  $\mathbf{k}$ . The design process consists of finding an initial design, testing the initial design by evaluating it with the high-fidelity model, and possible calibration and redesign. The future high-fidelity evaluation of the initial design (i.e. future test) is unknown and therefore modeled as an epistemic random variable. The redesign decision, calibration, and redesign optimum are conditional on a particular test result. In Section 5.3.4.1, Section 5.3.4.2, Section 5.3.4.3 the process is described conditional on the error realization  $E(\cdot, \cdot) = e^{(i)}(\cdot, \cdot)$ .

### 5.3.4.1 Initial design

The design problem is formulated as a deterministic optimization problem

$$\begin{aligned}
 & \min \quad f(\mathbf{x}, \mathbf{u}_{det}) \\
 & \text{w.r.t } \mathbf{x} \\
 & \text{s.t.} \quad \bar{g}_H(\mathbf{x}, \mathbf{u}_{det}) - k_{ini}\sigma_G(\mathbf{x}, \mathbf{u}_{det}) \geq 0
 \end{aligned} \tag{5-8}$$

where  $\bar{g}_H(\cdot, \cdot)$  is the mean of the predicted high-fidelity model,  $k_{ini}$  is the initial standard deviation offset,  $\mathbf{u}_{det}$  is a vector of conservative deterministic values used in place of aleatory random variables, and  $\sigma_G(\cdot, \cdot)$  is the standard deviation of the limit-state function with respect to epistemic model uncertainty. We assume the limit-state function is formulated such that failure is defined as  $g_H(\cdot, \cdot) < 0$ . Let  $\mathbf{x}_{ini}$  denote the optimum design found from 5–8. There is no uncertainty in the initial design  $\mathbf{x}_{ini}$  because the optimization problem is defined using the mean of the model prediction and fixed conservative values,  $\mathbf{u}_{det}$ , are used in place of aleatory random variables.

### 5.3.4.2 Testing initial design and redesign decision

A possible high-fidelity evaluation,  $g_H^{(i)}(\mathbf{x}_{ini}, \mathbf{u}_{det})$ , of the initial design  $\mathbf{x}_{ini}$  is simulated. The test will be passed if  $n_{lb} \leq g_H^{(i)}(\mathbf{x}_{ini}, \mathbf{u}_{det}) \leq n_{ub}$  where  $n_{lb}$  and  $n_{ub}$  correspond to lower and upper bounds on acceptable safety margins. The redesign decision can be formulated in terms of standard deviation offsets as  $k_{lb} \leq z_{ini}^{(i)} \leq k_{ub}$  where

$$z_{ini} = \frac{G_H(\mathbf{x}_{ini}, \mathbf{u}_{det}) - \bar{g}(\mathbf{x}_{ini}, \mathbf{u}_{det})}{\sigma_G(\mathbf{x}_{ini}, \mathbf{u}_{det})} \tag{5-9}$$

If the observed safety margin is too low ( $g_H^{(i)}(\mathbf{x}_{ini}, \mathbf{u}_{det}) < n_{lb}$ ) then the design is unsafe and redesign should be performed to restore safety. If the observed safety margin is too high ( $g_H^{(i)}(\mathbf{x}_{ini}, \mathbf{u}_{det}) > n_{ub}$ ) then the design is too conservative and it may be worth redesigning to improve performance. Let  $q^{(i)}$  denote an indicator function for the redesign decision that is 1 for redesign and 0 otherwise. We will refer to redesign triggered by a low safety margin as redesign for safety and redesign triggered by a

high safety margin as redesign for performance. If the test is not passed then redesign should be performed to select a new design.

### 5.3.4.3 Calibration and redesign

To obtain the calibrated model, the test realization  $g_H^{(i)}(\mathbf{x}_{ini}, \mathbf{u}_{det})$  corresponding to the error instance  $e^{(i)}(\mathbf{x}_{ini}, \mathbf{u}_{det})$  is treated as a new data point and the error instance is added to the design of experiment for the error model. The redesign problem is formulated as a deterministic optimization problem

$$\begin{aligned} \min \quad & f(\mathbf{x}, \mathbf{u}_{det}) \\ \text{w.r.t } \quad & \mathbf{x} \\ \text{s.t.} \quad & \bar{g}_{H,calib}^{(i)}(\mathbf{x}, \mathbf{u}_{det}) - k_{re}\sigma_{G,calib}^{(i)}(\mathbf{x}, \mathbf{u}_{det}) \geq 0 \end{aligned} \tag{5-10}$$

where the mean of the predicted high-fidelity model  $\bar{g}_{H,calib}^{(i)}(\cdot, \cdot)$  and the standard deviation  $\sigma_{G,calib}^{(i)}(\cdot, \cdot)$  are calibrated conditional on the test result  $g_H^{(i)}(\mathbf{x}_{ini}, \mathbf{u}_{det})$  and  $k_{re}$  is a new standard deviation offset. Let  $\mathbf{x}_{re}^{(i)}$  denote the optimum design after redesign found from 5-10. Comparing the initial design problem in 5-8 to the redesign problem in 5-10, we see that there is a change in the feasible design space due to the change in the standard deviation offset and calibration. Note that the calibration is conditional on obtaining the high-fidelity evaluation  $g_H^{(i)}(\mathbf{x}_{ini}, \mathbf{u}_{det})$  in the future. That is, if we obtain the evaluation  $g_H^{(i)}(\mathbf{x}_{ini}, \mathbf{u}_{det})$ , we can obtain the calibrated model  $\bar{g}_{H,calib}^{(i)}(\cdot, \cdot)$ , and we will select an improved design  $\mathbf{x}_{re}^{(i)}$ .

### 5.3.5 Probabilistic Evaluation

The final design after possible redesign is

$$\mathbf{x}_{final}^{(i)} = (1 - q^{(i)}) \mathbf{x}_{ini} + q^{(i)} \mathbf{x}_{re}^{(i)} \tag{5-11}$$

where  $q^{(i)} = 1$  corresponds to failing the test and performing redesign. The expected objective function value after possible redesign is  $\mathbb{E}_E [\mathbb{E}_U [f(\mathbf{X}_{final}, \mathbf{U})]]$ . The probability of



redesign is calculated analytically as

$$p_{re} = \Phi(k_{lb}) + (1 - \Phi(k_{ub})) \quad (5-12)$$

where  $\Phi(\cdot)$  is the standard normal cumulative distribution function (cdf).

The optimization of the standard deviation offsets is based on a computationally cheap approximation of the reliability constraint as described in Section 5.3.2. The key benefit of the proposed approximation is that the probability can be calculated analytically. The probability of a negative safety margin conditional on passing the test and keeping the initial design is

$$\mathbb{P}_E [G(\mathbf{x}_{ini}, \mathbf{u}_{det}) \leq 0 | Q = 0] = \Phi_T(-k_{ini}) \quad (5-13)$$

where  $\Phi_T(\cdot)$  is the normal cdf truncated to the interval  $[-k_{lb}, k_{ub}]$ . The probability conditional on performing redesign is

$$\mathbb{P}_E [G(\mathbf{X}_{re}, \mathbf{u}_{det}) \leq 0 | Q = 1] = \Phi(-k_{re}) \quad (5-14)$$

The final probability of a negative safety margin after possible redesign is

$$\mathbb{P}_E [G(\mathbf{X}_{final}, \mathbf{u}_{det}) \leq 0] = (1 - p_{re})\Phi_T(-k_{ini}) + p_{re}\Phi(-k_{re}) \quad (5-15)$$

After solving the optimization problem in 5-3, the full two-level mixed aleatory / epistemic uncertainty propagation is performed to recover the probability of failure distribution and check the accuracy of the proposed approximation. The probability of failure of the final design is unknown since there is epistemic uncertainty in the model  $G_H(\cdot, \cdot)$ . A realization of the probability of failure is calculated conditional on an error realization  $E(\cdot, \cdot) = e^{(i)}(\cdot, \cdot)$ . A realization of the probability of failure of the initial design is

$$p_f^{(i)}(\mathbf{x}_{ini}) = \mathbb{P}_U [g_H^{(i)}(\mathbf{x}_{ini}, \mathbf{U}) < 0] \quad (5-16)$$

where  $\mathbb{P}_U[\cdot]$  denotes the probability with respect to aleatory uncertainty. Note that the epistemic model uncertainty is treated separately from the aleatory uncertainty to distinguish between the quantity of interest, the probability of failure with respect to the high-fidelity model and aleatory uncertainty, and the lack of knowledge regarding this quantity. The error in the low-fidelity model  $E(\cdot, \cdot)$  has no impact on the reliability with respect to the high-fidelity model  $g_H(\cdot, \cdot)$ . However, since the high-fidelity model is unknown, the probability of failure calculation is repeated many times conditional on many different realizations of the high-fidelity model  $g_H^{(i)}(\cdot, \cdot)$  through 5–16. A realization of the final probability of failure after possible redesign is

$$p_f^{(i)}(\mathbf{x}_{re}^{(i)}) = \mathbb{P}_U \left[ g_H^{(i)}(\mathbf{x}_{re}^{(i)}, \mathbf{U}) \leq 0 \right] \quad (5-17)$$

After redesign, the design variable  $\mathbf{x}_{re}^{(i)}$  is also an epistemic random variable in addition to the limit state function  $g_H^{(i)}(\cdot, \cdot)$ . Many different methods are available for calculating the probability of failure. In this study, first order reliability method (FORM) is used to calculate the probability of failure for each epistemic realization. The final probability of failure after possible redesign is

$$p_f^{(i)}(\mathbf{x}_{final}^{(i)}) = (1 - q^{(i)}) p_f^{(i)}(\mathbf{x}_{ini}) + q^{(i)} p_f^{(i)}(\mathbf{x}_{re}^{(i)}) \quad (5-18)$$

Note that the redesign decision  $q^{(i)}$  shapes the final probability of failure distribution because we will have the opportunity in the future to correct the initial design if it fails the deterministic test. The probability of the probability of failure of the final design exceeding the target probability of failure is estimated by MCS as

$$\mathbb{P}_E [P_f(\mathbf{X}_{final}) \geq p_f^*] \approx \frac{1}{m} \sum_{i=1}^m I \left[ p_f^{(i)}(\mathbf{x}_{final}^{(i)}) \geq p_f^* \right] \quad (5-19)$$

where  $I[\cdot]$  is an indicator function. The computational cost of the full two-level mixed aleatory / epistemic uncertainty propagation is high and therefore only performed after the optimization of the standard deviation offsets. For example, more than  $m = 1900$

probability of failure calculations are necessary to estimate a probability of the order  $\alpha = 0.05$  with a 10% coefficient of variation.

## 5.4 Test Cases

### 5.4.1 Cantilever Beam Bending Example

#### 5.4.1.1 Problem description

The first example is the design of a cantilever beam to minimize mass subject to a constraint on tip displacement adapted from an example by Wu et al [6]. The beam is subject to independent aleatory random loads in the horizontal and vertical directions. The original problem involved the design of a long slender beam and therefore used Euler-Bernoulli beam theory. In this example, the length of the beam is reduced such that shear stress effects become important and Timoshenko beam theory is more accurate. The Timoshenko beam model plays the role of a computationally expensive high-fidelity model (e.g. finite element analysis) and the Euler-Bernoulli beam model plays the role of an inexpensive low-fidelity model. The beam is optimized to ensure with 95% confidence that the reliability index of the final design after possible redesign is greater than 3.

The low-fidelity model of the limit state function is

$$g_L(\mathbf{x}, \mathbf{U}) = d^* - \frac{4I^3}{ewt} \sqrt{\left(\frac{F_Y}{t^2}\right)^2 + \left(\frac{F_X}{w^2}\right)^2} \quad (5-20)$$

where  $\mathbf{x} = \{w, t\}$  are the design variables and  $\mathbf{U} = \{F_X, F_Y\}$  are the aleatory variables.

The high-fidelity model of the limit state function is

$$g_H(\mathbf{x}, \mathbf{U}) = d^* - \sqrt{(d_x(\mathbf{x}, \mathbf{U}))^2 + (d_y(\mathbf{x}, \mathbf{U}))^2} \quad (5-21)$$

where  $d_x$  and  $d_y$  are given by 5-22 and 5-23. The problem parameters are described in Table 5-1.

$$d_x(\mathbf{x}, \mathbf{U}) = \left( \frac{3IF_X}{2gwt} + \frac{4I^3F_X}{ewt^3} \right) \quad (5-22)$$

Table 5-1. Parameters for cantilever beam example

	Parameter	Notation	Value
Design variables, $\mathbf{x}$	Width of cross section	$w$	$2.5 \leq w \leq 5.5$ in
	Thickness of cross section	$t$	$1.5 \leq t \leq 4.5$ in
Aleatory variables, $\mathbf{U}$	Horizontal load	$F_X$	$N(500, 100^2)$ lbs
	Vertical load	$F_Y$	$N(1000, 100^2)$ lbs
Constants	Elastic modulus	$e$	$29 \times 10^6$ psi
	Shear modulus	$g$	$11.2 \times 10^6$ psi
	Length of beam	$l$	10 in
	Allowable tip displacement	$d^*$	$2.25 \times 10^{-3}$ in
	Conservative aleatory values	$\mathbf{u}_{det}$	$\{744.7, 1173.5\}$ lbs
	Target probability of failure	$p_f^* = \Phi(-\beta^*)$	$1.35 \times 10^{-3} = \Phi(-3)$
	Target confidence level	$1 - \alpha$	0.95

$$d_y(\mathbf{x}, \mathbf{U}) = \left( \frac{3lF_Y}{2gwt} + \frac{4l^3F_Y}{ew^3t} \right) \quad (5-23)$$

The objective function is the cross-sectional area of the beam

$$f(\mathbf{x}) = wt \quad (5-24)$$

which is proportional to the mass of the beam.

#### 5.4.1.2 Application of the proposed method

**Step 1: Quantifying the model uncertainty.** The first step is to quantify the uncertainty in the low-fidelity model. A Kriging model is constructed for the discrepancy between the low and high-fidelity models based on evaluations at the corner points in the joint design-aleatory space (4 beam designs each with 4 loading conditions). To demonstrate the method, the corner points were chosen in order to ensure high model uncertainty. In practice, the model could also be constructed based on data from previous designs. The Kriging model improves the prediction from the low-fidelity model, but more importantly it provides confidence intervals for the model uncertainty. In Figure 5-2, the confidence intervals arising due to model uncertainty are shown in the design space and aleatory space.

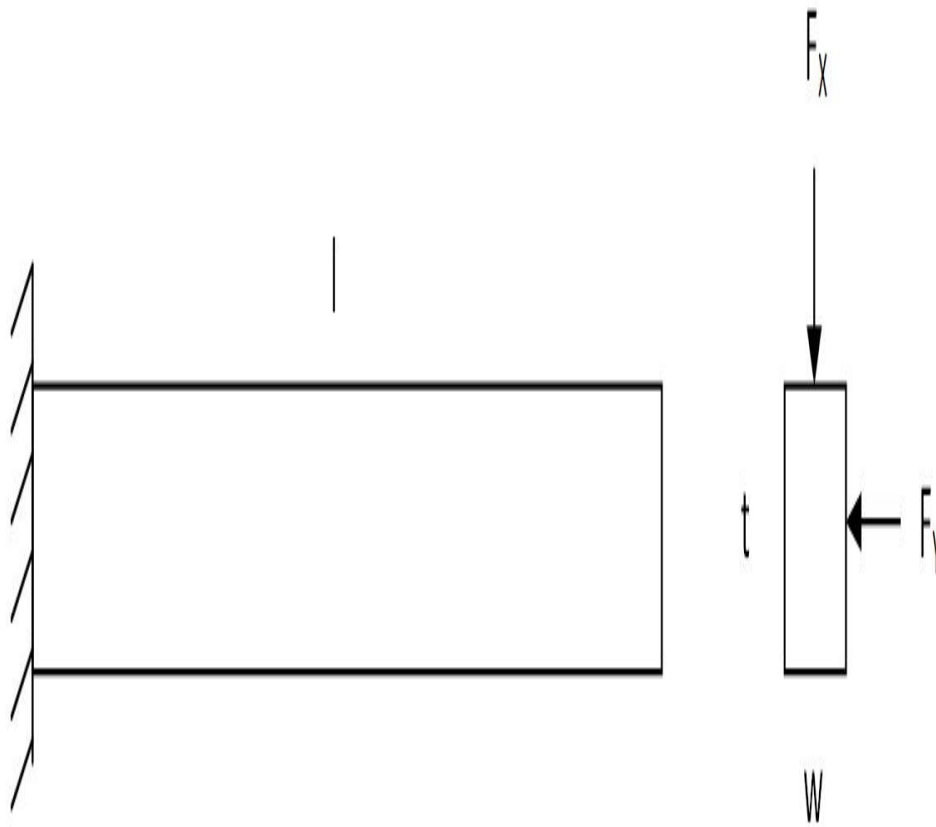


Figure 5-1. The beam is subject to horizontal and vertical tip loads

**Step 2: Selecting fixed conservative values for aleatory variables.** Next, aleatory random variables  $\mathbf{U}$  are replaced with fixed conservative values  $\mathbf{u}_{det}$ . The conservative values are found by solving the RBDO problem in 5-1. The RBDO is performed with respect to aleatory uncertainty conditional on the mean low-fidelity model. By solving the optimization problem in 5-1, we select conservative values  $\mathbf{u}_{det} = \{744.7, 1173.5\}$  lbs. These values correspond to approximately the 99th and 96th percentiles of the loads. The RBDO problem only requires single level uncertainty propagation since epistemic model uncertainty is fixed at the mean prediction.

**Step 3: Optimization of safety margins (i.e. standard deviation offsets)**

. In the third step, the optimum standard deviation offsets are found by solving 5-3

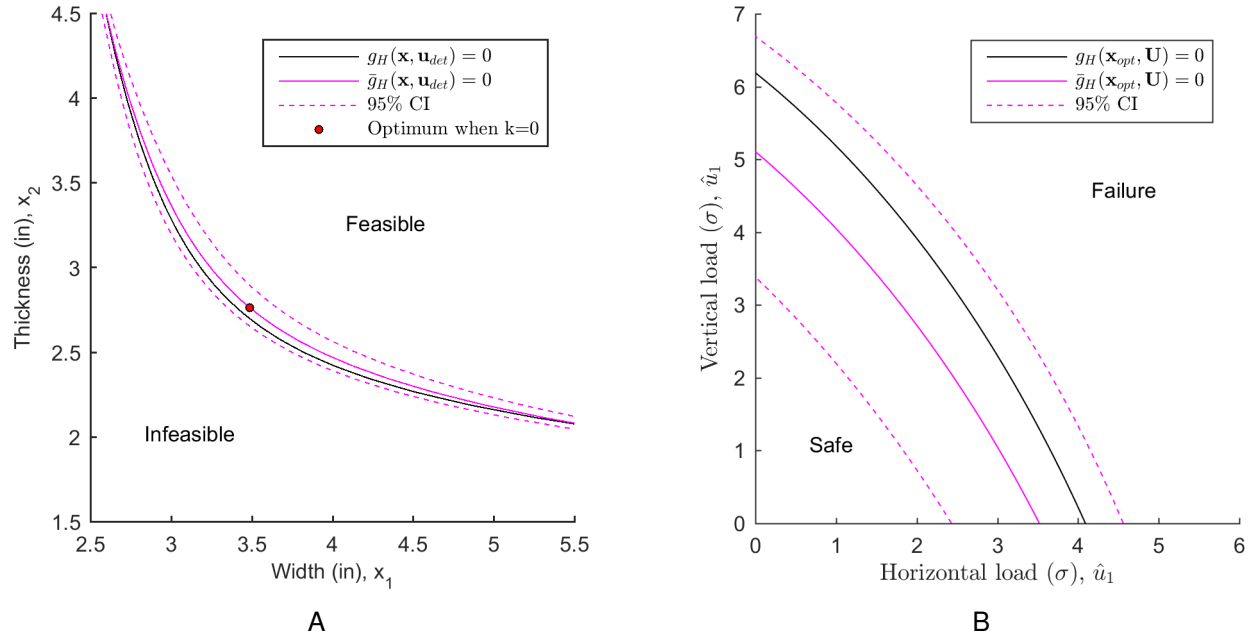


Figure 5-2. The figure on the left shows the design optimization with standard deviation offset  $k = 0$  and fixed conservative values  $\mathbf{u}_{det}$  in place of aleatory variables. The figure on the right shows the limit-state function in standard normal space for the optimum design found on the left. The reliability index is the distance in standard normal space from the origin to the limit-state.

using CMA-ES with a penalized objective function. Recall that standard deviation offsets of model uncertainty are used during the design / redesign process as safety margins against model uncertainty. Inside the MCS, the design optimization (5–8, 5–10) is performed using sequential quadratic programming (SQP). By varying the constraint on the probability of redesign  $p_{re}^*$  we obtain a curve for the expected cross sectional area versus probability of redesign as shown in Figure 5-3. The tradeoff curve is used to determine how much risk of redesign is acceptable given the expected performance improvement. For illustration, we will select the optimum safety margins  $\mathbf{k} = \{0.71, 0.89, 2.25, 3.00\}$  corresponding to 20% probability of redesign for more detailed study.

**Step 4: Full two-level mixed uncertainty propagation.** In the fourth step, the full two-level mixed uncertainty propagation is performed for the selected optimum

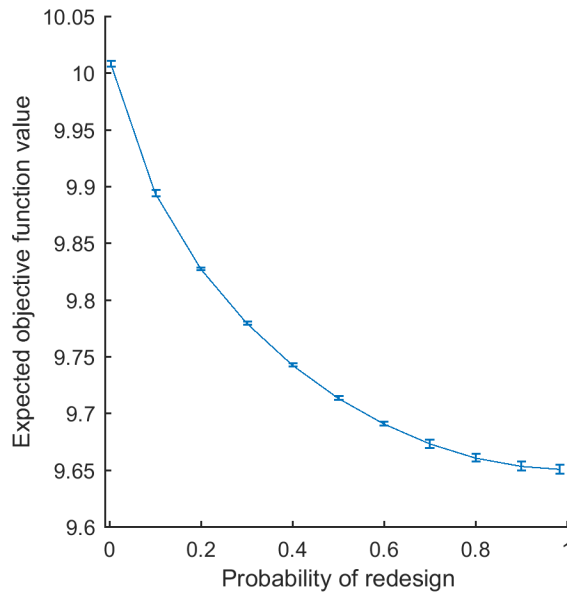


Figure 5-3. Tradeoff curve for expected cross sectional area versus probability of redesign

safety margins. The full two-level mixed uncertainty propagation is used to recover the probability of failure distribution and obtain detailed results for the MCS of the design/redesign process. In the previous step involving the optimization of the safety margins, aleatory variables were fixed and only epistemic model uncertainty was considered. In the full two-level mixed uncertainty propagation, the probability of failure is calculated using first order reliability method (FORM) for each realization of epistemic model uncertainty (i.e. Kriging conditional simulation)

**Step 5: Post-processing of simulation results.** Finally, post-processing is performed for the data gathered in the MCS.

First, we examine the safety margin distribution and the reliability index distribution shown in Figure 5-4. The safety margin distribution in Figure 5-4 shows the possible constraint violations with respect to epistemic model uncertainty conditional on the fixed conservative values  $\mathbf{u}_{det}$ . The beam will be redesigned if the safety margin is less than  $-0.16 \times 10^{-4}$  inches or greater than  $2.8 \times 10^{-4}$  inches. It can be observed that if redesign is required, we expect to have much more precise control over the tip displacement of

the beam due to the knowledge gained from the future test. Redesign acts as a type of quality control measure by initiating design changes in response to observing an extreme safety margin. We can compare the safety margin distribution and reliability index distributions in Figure 5-4. There is a strong correlation between the observed safety margin and the reliability index (correlation coefficient 0.999). As a result, the safety margin based redesign criteria is very useful for identifying overly conservative or unsafe designs. The safety margin is strongly correlated with the reliability index because the safety margin is calculated with respect to the MPP of the mean low-fidelity model. As shown in Figure 5-5, the conservative values  $\mathbf{u}_{det}$  provide a reasonable point estimate of the MPP distribution. The standard deviation offsets have been optimized based on the computationally cheap approximation of the reliability constraint in 5-4 such that the probability of a negative safety margin after possible redesign is 5%. After performing the full two-level mixed uncertainty propagation, the probability of the probability of failure exceeding the target value of  $1.35 \times 10^{-3}$  is estimated to be in the range of 5% to 7% (95% confidence interval with  $m = 2500$ ). In other words, we have between 93% and 95% confidence that the probability of failure of the final design after possible redesign will be less than  $p_f^* = 1.35 \times 10^{-3}$ .

Second, we examine the optimum design variable distribution and the cross sectional area distribution shown in Figure 5-6. The design variable distribution in Figure 5-6 shows how the design variables will change if redesign is required in the future. The peak corresponds to the initial design since there is an 80% probability the initial design will be accepted as the final design. The distribution of design variables can be used to plan for future design changes. The cross sectional area distribution corresponding to the designs is shown in Figure 5-6. Although the change in the mean area due to all possible design changes is relatively small, the realizations of the area corresponding to redesign may be significantly different than the initial area. For example, if redesign for performance is required the area is reduced by about 6.4%, however, there is only



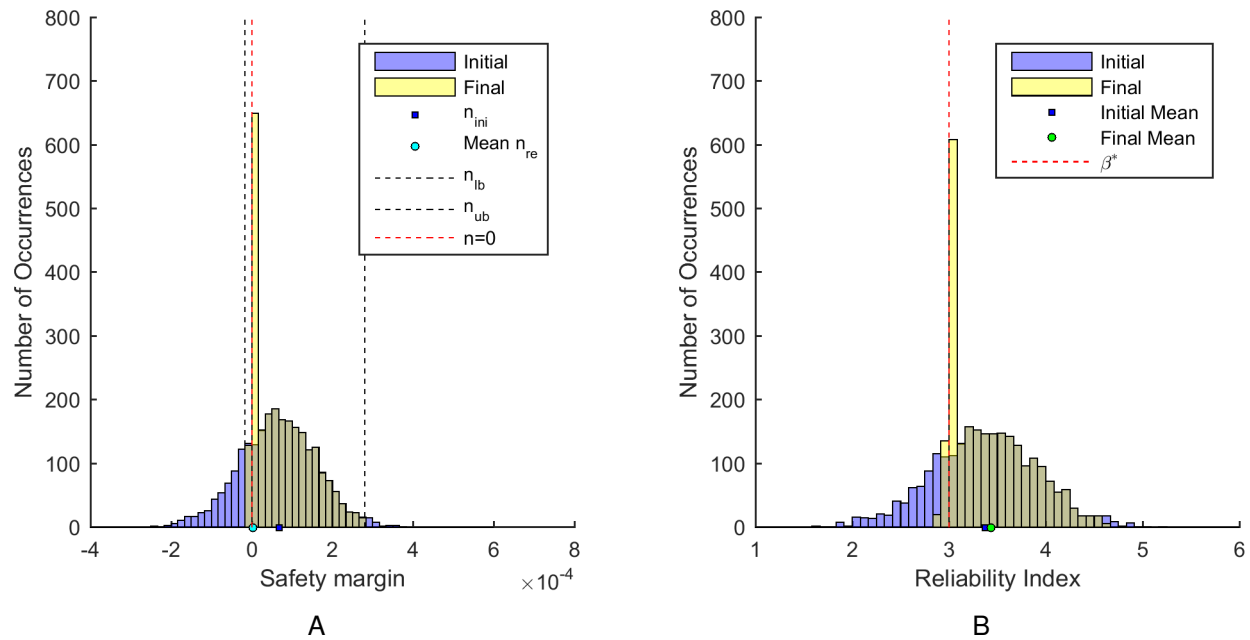


Figure 5-4. Distribution of safety margin and reliability index for 20% probability of redesign. Plots show overlapping transparent histograms.

about a 1% chance of redesign for performance. On the other hand, there is about a 19% chance of redesign for safety which is associated with an increase in area of approximately 2%.

## 5.4.2 Multidisciplinary Sounding Rocket Design Example

### 5.4.2.1 Problem description

The sounding rocket design example is based on a multidisciplinary design optimization (MDO) problem. The sounding rocket has a single cryogenic liquid hydrogen fueled gas generator engine. The intertank and thrust frame are made from a composite material. The thrust vector control (TVC) system is electromechanical. The avionics and electrical power system have no redundancies. The rocket is designed for vertical integration. The design structure matrix for the sounding rocket example is shown in Figure 5-7. There are four disciplines corresponding to propulsion, structures (sizing and weights estimation), aerodynamics, and trajectory simulation. There are five design variables corresponding to the mass of propellant  $M_P$ , initial thrust to weight

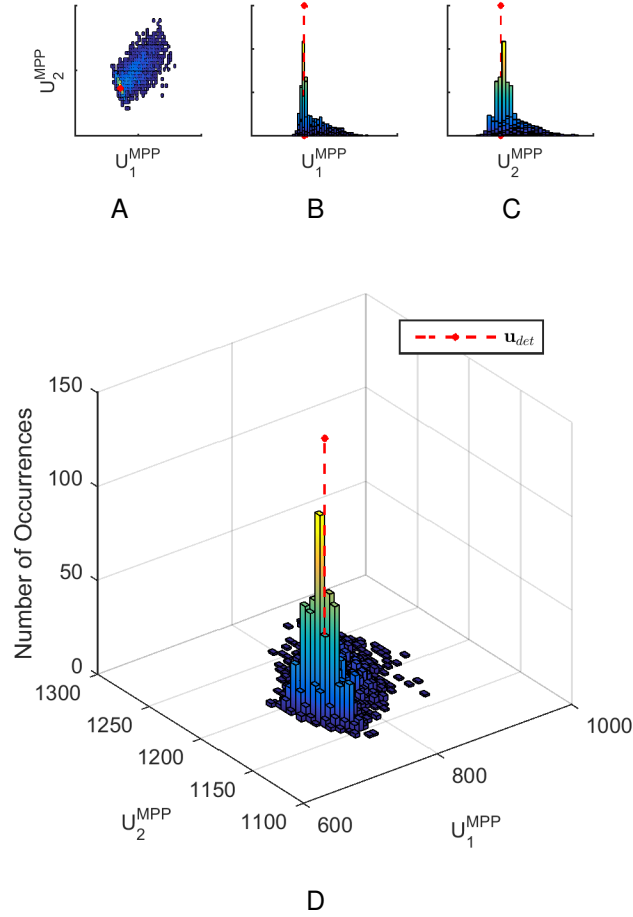


Figure 5-5. Distribution of most probable point (MPP) for 20% probability of redesign.

ratio  $T/W$ , engine chamber pressure  $p_{cc}$ , mixture ratio  $\alpha_P$ , and diameter  $D$ . The engine efficiency factor  $\eta$  is considered to be an aleatory random variable. The outputs are the total mass  $M_{tot}$ , final altitude at the end of the propulsion phase  $r_{final}$ , and length to diameter ratio  $L/D$ . The design problem is to minimize the total mass while satisfying constraints on the final altitude and the length to diameter ratio. The constraint on the length to diameter ratio is purely deterministic and is therefore simply included as an additional design constraint in the design optimization problems in 5–8, 5–10. There is aleatory uncertainty in the final altitude and total mass (GLOW) due to the aleatory uncertainty in the engine efficiency factor  $\eta$ .

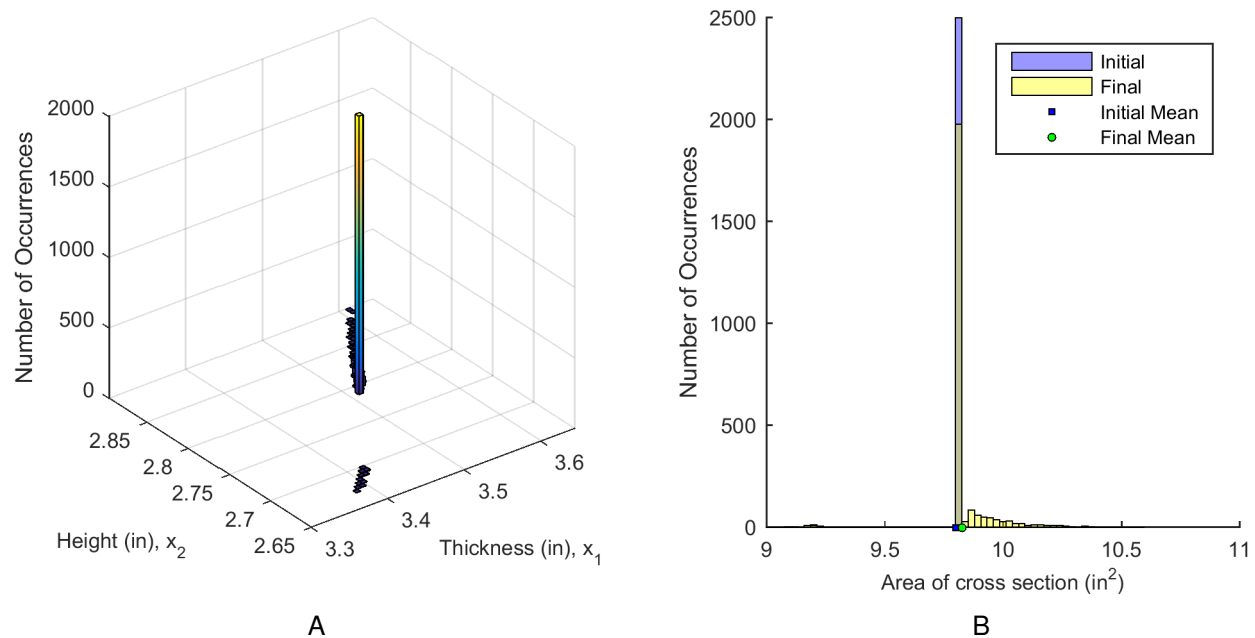


Figure 5-6. Distribution of optimum design variables and design performance for 20% probability of redesign. Peak is located at initial design.

There is a coupling between the structures and aerodynamic disciplines in that the maximum axial acceleration and maximum dynamic pressure are related to the total mass. The structure must be sized to withstand the loads, but changes in the total mass are related to the loads through trajectory and aerodynamics. There is a coupling between structures and propulsion in that the inert mass fraction is related to the thrust through the thrust to weight ratio. The engine mass and thrust frame mass must be designed for a given thrust, but because the thrust to weight ratio is specified beforehand changes in mass alter the thrust. A fixed point iteration is performed to satisfy the coupling constraints with respect to the maximum axial load, maximum dynamic pressure, and inert mass fraction. There is a loop between aerodynamics and trajectory because the drag coefficient varies with Mach number.

#### 5.4.2.2 Standard atmosphere models

The atmosphere model includes variations of the speed of sound, atmospheric pressure, and air density as a function of altitude. The speed of sound varies as a

### Design Variables:

$M_p$ : propellant mass  
 $T/W$ : thrust to weight ratio  
 $p_{cc}$ : chamber pressure  
 $\alpha_p$ : mixture ratio  
 $D$ : diameter  
 $\eta$ : engine efficiency factor

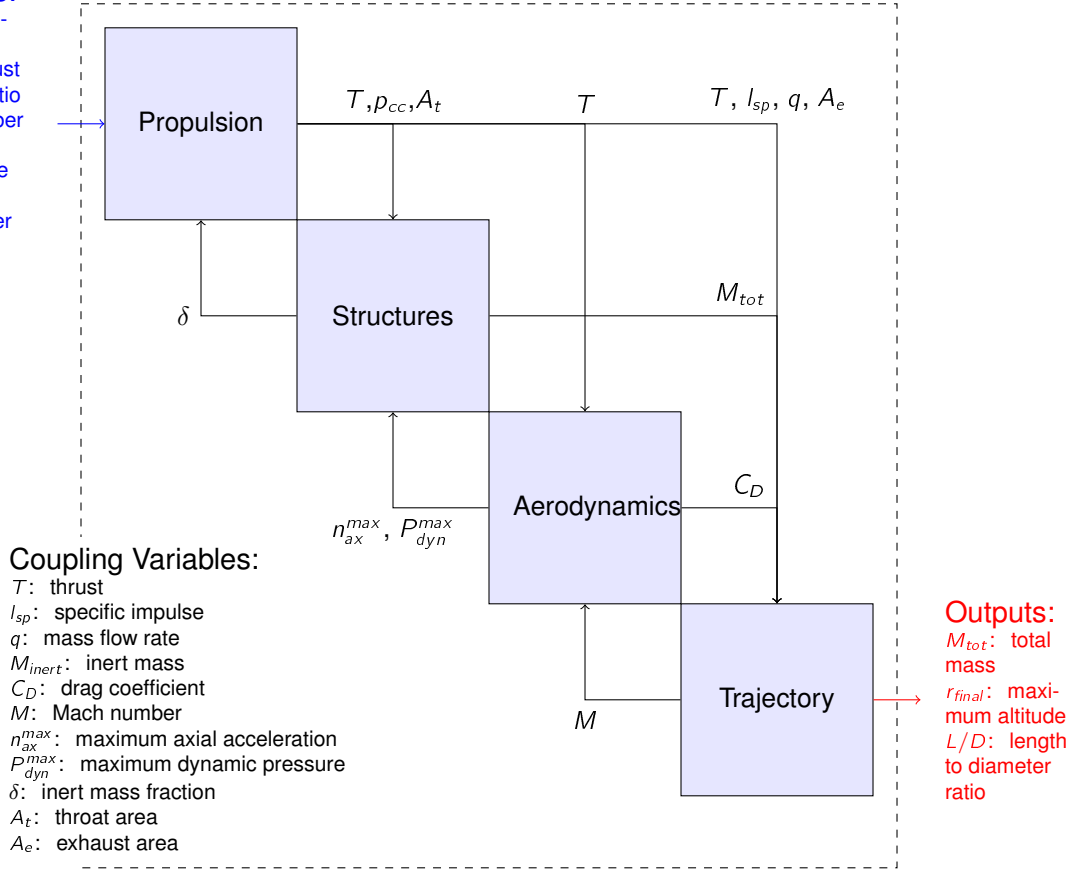


Figure 5-7. Design structure matrix for sounding rocket design example. There are couplings between propulsion/structures, aerodynamics/structures, and trajectory/aerodynamics.

function of altitude

$$c(r) = \begin{cases} c_1(r) & r - R_E < 122 \times 10^3 \text{ m} \\ 303.1416 \text{ m/s} & r - R_E \geq 122 \times 10^3 \text{ m} \end{cases} \quad (5-25)$$

where

$$c_1(r) = \beta_6 x^6 + \beta_5 x^5 + \beta_4 x^4 + \beta_3 x^3 + \beta_2 x^2 + \beta_1 x + \beta_0 \quad (5-26)$$

and  $x = r - R_E$  is the altitude in meters relative to the radius of the earth  $R_E$ . The coefficients are listed in Table 5-2 and the variation in the speed of sound is plotted in

Table 5-2. Coefficients for calculating speed of sound as a function of altitude (5–25)

Coefficient	Value
$\beta_0$	$3.4394 \times 10^2$
$\beta_1$	$-6.3990 \times 10^{-3}$
$\beta_2$	$2.2964 \times 10^{-7}$
$\beta_3$	$-8.9126 \times 10^{-13}$
$\beta_4$	$-5.7391 \times 10^{-17}$
$\beta_5$	$7.6283 \times 10^{-22}$
$\beta_6$	$-2.7182 \times 10^{-27}$

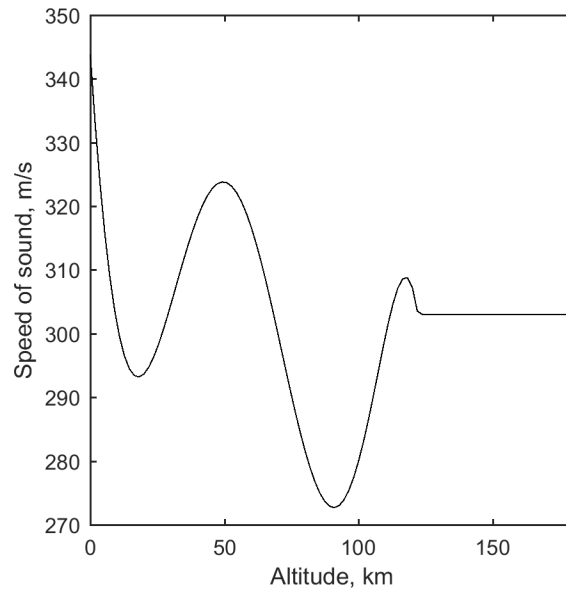


Figure 5-8. Speed of sound as a function of altitude (5–25)

Figure 5-8. The atmospheric pressure (Pa) decreases with altitude

$$P_a(r) = p_0 \exp(-p_{ref}(r - R_E)) \quad (5-27)$$

where  $p_0 = 1.0437 \times 10^5$  and  $p_{ref} = 1.4589 \times 10^{-4}$ . The density of the air ( $\text{kg}/\text{m}^3$ ) decreases with altitude

$$\rho(r) = \rho_0 \exp\left(-\frac{r - R_E}{h_{ref}}\right) \quad (5-28)$$

where  $\rho_0 = 1.22557$  and  $h_{ref} = 7254.24$ .

### 5.4.2.3 Discipline models

The discipline models are based on the dissertation of Castellini, “Multidisciplinary design optimization for expendable launch vehicles” [88]. Full details of the models can be found in the dissertation. The discipline models are briefly summarized here.

**Propulsion.** The propulsion discipline calculates the performance characteristics of the engine based on NASA computer program CEA (Chemical Equilibrium with Applications) for calculating chemical equilibrium compositions and properties of complex mixtures [89, 90]. In order to reduce computational cost, Kriging surrogate models were fit to the characteristic velocity ( $C_*$ ) and thrust coefficient ( $C_T$ ) as a function of mixture ratio, chamber pressure, and nozzle expansion ratio. The surrogate models were constructed based on a design of experiment consisting of 500 points generated using Latin-hypercube sampling. The Kriging models used a Gaussian covariance function and zero order trend functions. Kriging models were constructed in Matlab using DACE (Design and Analysis of Computer Experiments) Matlab toolbox [91]. Any epistemic model uncertainty introduced by the Kriging surrogates in the propulsion discipline is not included in the analysis. The specific impulse is calculated as

$$I_{sp} = \frac{C_* C_T \eta}{g_0} \quad (5-29)$$

where  $C_*$  is the Kriging prediction of the characteristic velocity,  $C_T$  is the the Kriging prediction of the thrust coefficient,  $\eta$  is an efficiency factor, and  $g_0$  is the standard acceleration due to gravity. The single efficiency factor represents the combined degrading effects of chamber and nozzle losses as well as mass flow losses. The throat area is calculated as

$$A_t = \frac{T}{C_T p_{cc}} \quad (5-30)$$

where  $T$  is the thrust and  $p_{cc}$  is the chamber pressure. The exhaust area is calculated as

$$A_e = \varepsilon A_t \quad (5-31)$$

Table 5-3. Inputs and outputs of propulsion discipline

Inputs		Outputs	
Chamber pressure	$p_{cc}$	Mass flow rate	$q$
Mixture ratio	$\alpha_P$	Specific impulse	$I_{sp}$
Nozzle expansion ratio	$\varepsilon$	Throat area	$A_t$
Thrust	$T$	Exhaust area	$A_e$

where  $\varepsilon$  is the nozzle expansion ratio. The mass flow rate is calculated as

$$q = \frac{T}{C_* C_T} = \frac{T}{I_{sp} g_0} \quad (5-32)$$

**Structures.** The structures discipline calculates the total inert mass of the rocket and the total length of the rocket. For this example, the structures discipline is defined as the combination of sizing and weights estimation. The weights estimation includes engine mass, thrust frame mass, tank mass including thermal protection system, thrust vector control (TVC), and avionics and electrical power system. The thrust frame and tanks are designed using structural safety margins of  $SSM = 1.1$ . All weight estimation relationships (WER's) are based on the dissertation of Castellini [88]. The total mass of the rocket is calculated as

$$M_{tot} = M_{inert} + M_P + M_{PL} \quad (5-33)$$

where  $M_{inert}$  is the total inert mass,  $M_P$  is the propellant mass, and  $M_{PL}$  is the payload mass. The total inert mass is calculated as

$$M_{inert} = M_{eng} + M_{TF} + M_{FT} + M_{OxT} + M_{TPS,OxT} + M_{TPS,FT} + M_{avio} + M_{EPS} + M_{intertank} + M_{PLF} \quad (5-34)$$

where  $M_{eng}$  is the engine,  $M_{TF}$  is the thrust frame,  $M_{FT}$  is the fuel tank,  $M_{OxT}$  is the oxidizer tank,  $M_{TPS,OxT}$  is the thermal protection for the oxidizer tank,  $M_{TPS,FT}$  is the thermal protection for fuel tank,  $M_{avio}$  is the avionics,  $M_{EPS}$  is the electrical power system,  $M_{intertank}$  is the intertank, and  $M_{PLF}$  is the payload fairing.

**Mass of tanks and intertank** The mass of the fuel and oxidizer tanks are usually the largest part of the structural mass of liquid propulsion rockets [88]. The WER's for

Table 5-4. Inputs and outputs of structures discipline

Inputs		Outputs	
Thrust	$T$	Total inert mass	$M_{inert}$
Chamber pressure	$p_{cc}$	Total Length	$L$
Mixture ratio	$\alpha_P$		
Nozzle expansion ratio	$\varepsilon$		
Throat area	$A_t$		
Maximum axial acceleration	$n_{ax}^{max}$		
Maximum dynamic pressure	$P_{dyn}^{max}$		
Diameter	$D$		
Mass of propellant	$M_P$		
Mass of payload fairing	$M_{PLF}$		

Table 5-5. Notation used in weights estimation

$M_{tot}$	Total
$M_{inert}$	Total inert
$M_P$	Propellant
$M_{PL}$	Payload
$M_{PLF}$	Payload fairing
$M_{eng}$	Engine (including TVC and nozzle)
$M_{TVC}$	Thrust vector control (TVC)
$M_{nozzle}$	Nozzle
$M_{TF}$	Thrust frame
$M_{FT}$	Fuel tank
$M_{OxT}$	Oxidizer tank
$M_{TPS,OxT}$	Thermal protection system - Oxidizer tank
$M_{TPS,FT}$	Thermal protection system - Fuel tank
$M_{avio}$	Avionics
$M_{EPS}$	Electrical power system
$M_{intertank}$	Intertank

the tank masses are a linear regression for fuels and a slightly non-linear power law regression of the tank volume for oxidizers. The mass of the fuel tanks is

$$M_{FT} = \prod_{j=1}^6 k_j \cdot ((V_F \cdot 35.315) \cdot 0.4856 + 800) \cdot 0.4536 \quad (5-35)$$

where  $V_F$  is the volume of the fuel tank and  $k_j$  are coefficients to account for load parameters and discrete design variables. The mass of the oxidizer tank is

$$M_{OxT} = \prod_{j=1}^6 k_j \cdot ((V_{Ox} \cdot 35.315)^{1.04} \cdot 1.0850 + 700) \cdot 0.4536 \quad (5-36)$$



Table 5-6. Coefficients for tank mass WER's

Description		
$k_1$	Structural material	$k_1 = \begin{cases} 1 & \text{Al-Li alloy} \\ 0.9 & \text{Composite} \end{cases}$
$k_2$	Common bulkhead or intertank	$k_2 = \begin{cases} S_{tot} - 1.5S_{dome}/S_{tot} & \text{Common bulkhead} \\ 1 & \text{Intertank} \end{cases}$
$k_3$	Horizontal or vertical integration	$k_3 = \begin{cases} (1/30) \cdot (L/D) + (29/30) & \text{Horizontal} \\ 1 & \text{Vertical} \end{cases}$
$k_4$	Max dynamic pressure	$k_4 = (P_{dyn}^{max})^{0.16} / 5.76404$
$k_5$	Axial acceleration	$k_5 = (SSM \cdot n_{ax}^{max})^{0.15} / 1.29134$
$k_6$	Tank pressure	$k_6 = 1.3012 + 1.4359 \times 10^{-6} \cdot p_{tanks} / 2.7862$

where  $V_{Ox}$  is the volume of the oxidizer tank. The coefficients used in the mass WER's are described in Table 5-6. The mass of the thermal protection system is approximated as a linear function of the tanks surface area

$$M_{TPS,OxT/FT} = k_{ins} S_{OxT/FT} \quad (5-37)$$

with  $k_{ins} = 0.9765$  for liquid oxygen tanks and  $k_{ins} = 1.2695$  for liquid hydrogen tanks. The mass of the intertank is approximated as a two dimensional linear function of the lateral surface and the diameter

$$M_{IT} = k_{SM} \cdot k_1 S_{IT} \cdot (D_{IT} \cdot 3.2808)^{k_2} \quad (5-38)$$

where  $k_{SM} = 1$  for aluminum alloys or  $k_{SM} = 0.7$  for composites,  $k_1 = 5.4015$ , and  $k_2 = 0.5169$ .

*Propulsion system and thrust frame* The engine mass for cryogenic propulsion and gas generator feed is approximated as a function of the thrust as

$$M_{eng} = a T^b + M_{nozzle} + M_{TVC} \quad (5-39)$$

where  $a = 7.54354 \times 10^{-3}$ ,  $b = 0.885635 \times 10^{-1}$ ,  $c = 20.2881$ , and  $M_{nozzle}$  is the mass of the nozzle, and  $M_{TVC}$  is the mass of the thrust vector control system. The mass of an electromechanical thrust vector control system is approximated as a function of the thrust

as

$$M_{TVC} = 0.1078 \cdot (T \times 10^{-3}) + 43.702 \quad (5-40)$$

The thrust frame mass<sup>1</sup> is approximated as a function of the thrust and maximum axial acceleration as

$$M_{TF} = (0.013 N_{eng}^{0.795} T^{0.579} + 0.01 N_{eng} (M_{eng}/0.45)^{0.717}) \quad (5-41)$$

$$0.45 (1.5 \cdot SSM \cdot n_{ax}^{max} \cdot g_0) \cdot k_{SM}$$

where  $k_{SM} = 1$  for aluminum alloys or  $k_{SM} = 0.62$  for composites and  $N_{eng} = 1$  for this example.

*Avionics and electrical power system* The mass of the avionics system is approximated as

$$M_{avio} = k_{RL} (246.76 + 1.3183 S_{tot}) (1 - 0.75) \quad (5-42)$$

where  $k_{RL} = 0.7$  for no redundancy,  $k_{RL} = 1$  for critical components redundancy, or  $k_{RL} = 1.3$  for full redundancy. The mass of the electrical power system is approximated as

$$M_{EPS} = k_{RL} 0.405 M_{avio} (1 - 0.18) \quad (5-43)$$

**Aerodynamics.** Given the instantaneous velocity, altitude, and total mass of the rocket the aerodynamics discipline calculates the drag force, dynamic pressure, and axial acceleration. The aerodynamics discipline analysis is based on Missile DATCOM [93]. In order to reduce computational cost, the drag coefficient is calculated as a function of the Mach number based on PCHIP (piecewise cubic hermite interpolating polynomial) interpolation between values in a table of Missile DATCOM evaluations. The interpolation between data points for the drag coefficient as a function of Mach number is shown in Figure 5-9.

---

<sup>1</sup> WER from [88] is corrected to match original source [92] and Ariane 5 Vulcain engine data point

Table 5-7. Inputs and outputs of aerodynamics discipline

Inputs		Outputs	
Velocity	$V(t)$	Drag force	$F_D(t)$
Altitude	$r(t)$	Dynamic pressure	$P_{dyn}(t)$
Total mass	$m(t)$	Axial acceleration	$n_{ax}(t)$
Diameter	$D$		
Exhaust area	$A_e$		

The Mach number is calculated as

$$M = \frac{V}{c(r)} \quad (5-44)$$

where the speed of sound  $c(r)$  varies as a function of altitude according to 5-25. The axial accelerations in g's is calculated as

$$n_{ax} = \frac{1}{mg_0} (T - F_D) \quad (5-45)$$

where  $F_D = 0.5\rho(r)V^2C_D A$  is the drag force and the air density  $\rho(r)$  decreases with altitude according to 5-28. The thrust is calculated as

$$T = I_{sp}g_0 q - A_e P_a(r) \quad (5-46)$$

where  $A_e$  is the exhaust area and the air pressure  $P_a(r)$  decreases with altitude according to 5-27. The dynamic pressure is calculated as

$$P_{dyn} = 0.5\rho(r)V^2 \quad (5-47)$$

**Trajectory.** The trajectory discipline calculates the altitude, velocity, and total mass as a function of time. The trajectory discipline analysis is based on a two dimensional model. The equations of motion are

$$\begin{aligned} \dot{r} &= V \\ \dot{V} &= \frac{1}{m} (-F_D + T - \frac{GM_E m}{r^2}) \\ \dot{m} &= -q \end{aligned} \quad (5-48)$$

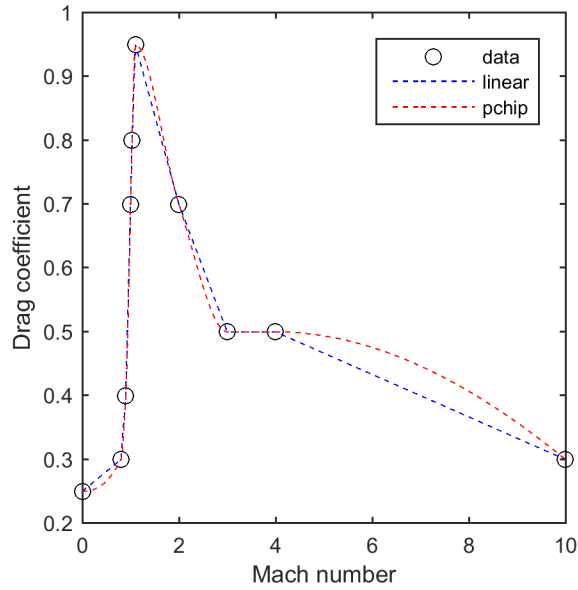


Figure 5-9. Drag coefficient as a function of Mach number based on Missile DATCOM. PCHIP interpolation is used between data points.

where  $r$  is the radius,  $V$  is the norm of the velocity vector,  $F_D$  is the drag force,  $T$  is the thrust,  $G$  is the gravitational constant,  $M_E$  is the mass of the earth, and  $m$  is the mass of the rocket. Equations of motion are derived assuming the flight path angle ( $\gamma$ ) and pitch angle ( $\theta$ ) are both 90 degrees. The trajectory discipline is coupled with the aerodynamics discipline. During ODE integration, the trajectory discipline calls the aerodynamics discipline to update the instantaneous values of the thrust and drag force.

The time at which maximum dynamic pressure occurs is obtained by finding the point at which the rate of change of the dynamic pressure crosses zero axis from positive to negative. The derivative of the dynamic pressure is

$$\frac{dP_{dyn}}{dt} = \rho V \frac{dV}{dt} + 0.5 \frac{d\rho}{dt} V^2 \quad (5-49)$$

where the derivative of the air density in 5-28 is

$$\frac{d\rho}{dt} = -\frac{\rho_0}{h_{ref}} \frac{dr}{dt} \exp\left(-\frac{r - R_E}{h_{ref}}\right) \quad (5-50)$$

Table 5-8. Inputs and outputs of trajectory discipline

Inputs		Outputs	
Total mass	$M_{tot}$	Final altitude	$r_{final}$
Thrust	$T(t)$	Velocity	$v(t)$
Drag force	$F_D(t)$	Altitude	$r(t)$
Thrust duration	$t_{burn}$	Total mass	$m(t)$

#### 5.4.2.4 Low-fidelity model

A low-fidelity approximation is introduced for the inert mass fraction as a function of the mass of propellant. The low-fidelity model is based on a curve fit of the model provided in the “Handbook of Cost Engineering and Design of Space Transportation” [94]. Table 5-9 lists the data that was read from the figure (approximated visually). A second order polynomial was fit to the inert mass fraction as a function of the log of propellant

$$\delta_L = (1.5879 \log(M_P)^2 - 36.1554 \log(M_P) + 217.8084)/100 \quad (5-51)$$

The design curve is for rockets that are much larger than the sounding rocket we are investigating in this design example. Therefore, we will extrapolate outside of the range of the design curve using the polynomial curve fit. The extrapolation may introduce significant error on top of the already questionable accuracy of the low-fidelity model. The low-fidelity mass model is a 1-dimensional function. However, in the fully coupled system the mass depends on all 6 design-aleatory variables. To visualize the accuracy of the low-fidelity model, a cloud of 10,000 different designs was generated in the 6-dimensional design-aleatory space using Latin-hypercube sampling. Fixed point iterations were performed for each of the designs to enforce coupling constraints between disciplines. In Figure 5-11, the 10,000 designs are projected onto a 1-dimensional plane in order to compare with the 1-dimensional low-fidelity model. It is observed that the low-fidelity model captures the overall trend, but there is significant error. Furthermore, there appears to be significant scatter in the design points around the mean trend line. This is because different designs are being projected onto the

Table 5-9. Data read from design curve

Mass of propellant (kg)	Inert Mass Fraction
10,000	0.195
20,000	0.155
30,000	0.138
40,000	0.130
50,000	0.125

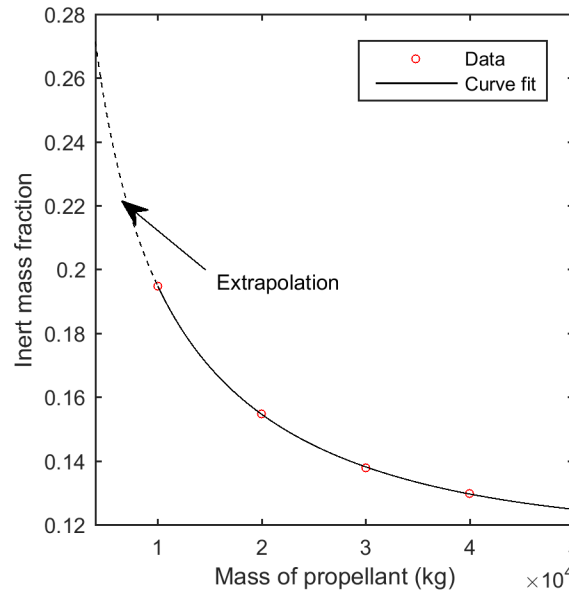


Figure 5-10. A second order polynomial was fit to the inert mass fraction as a function of the log of the propellant mass. The model is extrapolated to the region of interest for sounding rocket design.

1-dimensional plane. The low-fidelity model is incapable of representing this variation with respect to design variables other than the mass of propellant. For the low-fidelity model,  $r^2 = 0.81$  indicating the the model explains about 81% of the variation.

#### 5.4.2.5 Application of the proposed method

**Step 1: Quantifying the model uncertainty.** The first step is to quantify the uncertainty in the low-fidelity model. The low-fidelity model of the inert mass fraction is related to the high-fidelity model (i.e. coupled system) as

$$\delta_H(\mathbf{x}, u) = \delta_L(M_P) + E(\mathbf{x}, u) \quad (5-52)$$

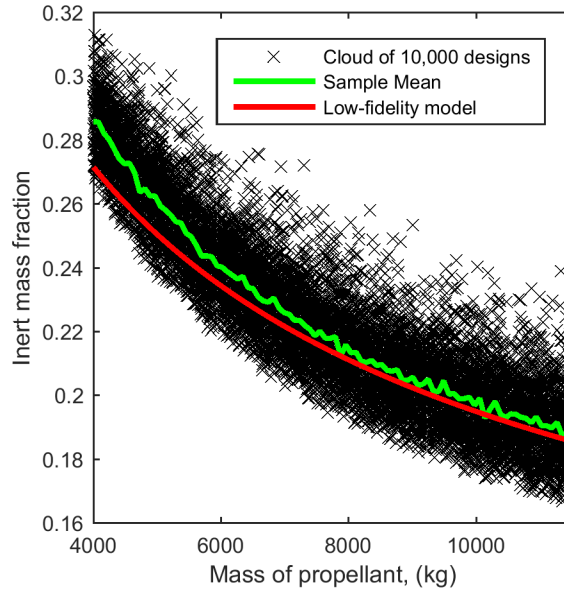


Figure 5-11. A cloud of 10,000 designs in 6-dimensions is projected onto a one dimensional plane and compared to the low-fidelity model prediction

where  $\mathbf{x} = \{M_P, T/W, p_{cc}, \alpha_P, D\}$  is the vector of design variables,  $u = \eta$  is a realization of the aleatory random variable  $U$ ,  $\delta_H(\cdot, \cdot)$  is the inert mass fraction when coupling constraints are satisfied,  $\delta_L(\cdot)$  is the low-fidelity model given by Equation 5-51, and  $E(\cdot, \cdot)$  is the Kriging model of the discrepancy between the two models. By introducing the low-fidelity model the propulsion/structures and the aerodynamics/structures couplings are removed. In effect, the coupling constraints are incorporated into the construction of the error model  $E(\cdot, \cdot)$ . Removing the couplings eliminates the need for fixed point iterations and allows the sounding rocket design to be represented as a simple feed forward system. This may substantially reduce the computational cost of uncertainty propagation relative to performing fixed point iterations for every realization of aleatory uncertainty. However, the low-fidelity model may introduce significant epistemic model uncertainty, particularly when the Kriging model is constructed based on only a small set of initial data (i.e. small design of experiment). The epistemic model uncertainty results in additional uncertainty in the final altitude and GLOW.

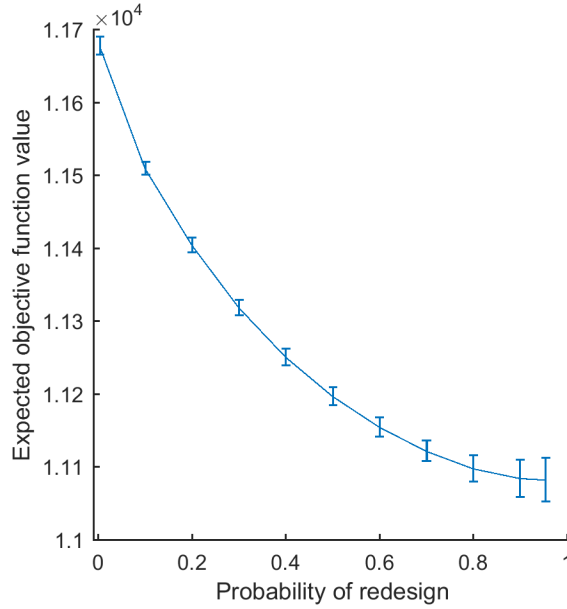


Figure 5-12. Tradeoff curve for expected GLOW versus probability of redesign

**Step 2: Selecting fixed conservative values for aleatory variables.** Next, the aleatory random variable  $U$  is replaced with a fixed conservative value  $u_{det}$ . Instead of solving the RBDO problem in 5-1, the 5th percentile of the engine efficiency is used for the conservative value. The 5th percentile was selected because the altitude is nearly a linear function of the engine efficiency and the target probability of failure is  $p_f^* = 0.05$ .

**Step 3: Optimization of safety margins (i.e. standard deviation offsets).** In the third step, the optimum standard deviation offsets are found by solving 5-3 using CMA-ES with a penalized objective function. Inside the MCS, the design optimization (5-8, 5-10) is performed using sequential quadratic programming (SQP). By varying the constraint on the probability of redesign  $p_{re}^*$  we obtain a curve for the expected GLOW versus probability of redesign as shown in Figure 5-12. The tradeoff curve is used to determine how much risk of redesign is acceptable given the expected performance improvement. For illustration, we will select the optimum safety margins  $\mathbf{k} = \{0.78, 0.96, 1.87, 2.29\}$  corresponding to 20% probability of redesign for more detailed study.



**Step 4: Full two-level mixed uncertainty propagation.** In the fourth step, the full two-level mixed uncertainty propagation is performed for the selected optimum safety margins. The full two-level mixed uncertainty propagation is used to recover the probability of failure distribution and obtain detailed results for the MCS of the design/redesign process. For each realization of epistemic model uncertainty (i.e. Kriging conditional simulation) the probability of failure is calculated using first order reliability method (FORM).

**Step 5: Post-processing of simulation results.** Finally, post-processing is performed for the data gathered in the MCS.

First, we examine the safety margin distribution and the probability of failure distribution shown in Figure 5-13. The safety margin distribution in Figure 5-13 shows the possible constraint violations with respect to epistemic model uncertainty conditional on the fixed conservative values  $u_{det}$ . The rocket will be redesigned if the safety margin is less than  $-0.6$  kilometers or greater than  $9.5$  kilometers (relative to target of  $150$  km assuming conservative engine efficiency). Redesign acts as a type of quality control measure by initiating design changes in response to observing an extreme safety margin. We can compare the safety margin distribution to the probability of failure distribution in Figure 5-13. There is a strong correlation between the observed safety margin and the probability of failure (correlation coefficient  $-0.65$ ). As a result, the safety margin based redesign criteria is very useful for identifying overly conservative or unsafe designs. The correlation coefficient is not as strong as in the beam example because the aleatory uncertainty in the engine efficiency is bounded. Due to the bounded aleatory uncertainty the correlation between safety margin and probability of failure breaks down when the safety margin is less than the point corresponding to 100% probability of failure or the safety margin is greater than the point corresponding to 0% probability of failure. The standard deviation offsets have been optimized based on the computationally cheap approximation of the reliability constraint in 5-4 such that the

probability of a negative safety margin after possible redesign is 5%. After performing the full two-level mixed uncertainty propagation, the probability of the probability of failure exceeding the target value of  $p_f^* = 0.05$  is found to be in agreement with the target value of  $\alpha = 0.05$ .

Second, we examine the optimum design variable distribution shown in Figure 5-14 and the GLOW and dry mass distributions shown in Figure 5-15. The design variable distribution is 5-dimensional so the marginal distributions are shown. The peak corresponds to the initial design since there is an 80% probability the initial design will be accepted as the final design. The distribution of design variables is useful for planning for future design changes. It is observed that the chamber pressure does not change during redesign. The optimum chamber pressure is always the upper bound of 120 bars regardless of the outcome of the future high-fidelity evaluation. The change in diameter is relatively small with a change on the order of  $\pm 1\%$  if redesign is required. However, the propellant mass may change substantially. The mass of propellant may decrease approximately 12% if redesign for performance is required or increase by 4% if redesign for safety is required. The relative change in GLOW due to redesign is similar to the relative change in propellant mass as seen in Figure 5-15. The dry mass distribution is shown in Figure 5-15. If redesign for safety is required, the dry mass will increase by about 2%. If redesign for performance is required, the dry mass will decrease by about 7%. Since underestimating the mass corresponds to overestimating the altitude, and vice versa, redesign tends to increase the mass of heavier mass realizations or decrease the mass of lighter mass realizations by adjusting the propellant mass accordingly.

## 5.5 Discussion Conclusions

At the initial design stage, engineers often must rely on low-fidelity models with high epistemic model uncertainty. One approach to high epistemic model uncertainty is to add a safety margin, such as a  $k$  standard deviation offset, to design constraints

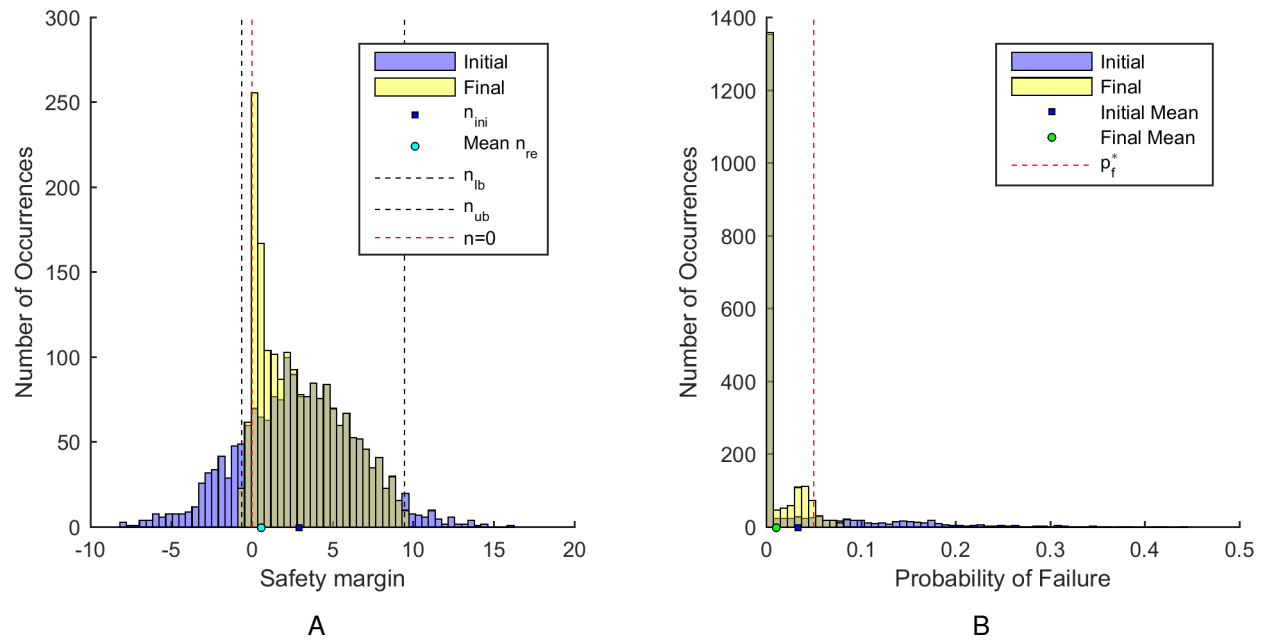


Figure 5-13. Distributions of safety margin and probability of failure for 20% probability of redesign. Plots show overlapping transparent histograms.

to ensure the optimum design is well within the safe design space. If the safety margin is large then the designer has more confidence that the design is safe, but design performance suffers. If the safety margin is small then the design space is larger and designs with better performance become accessible, but the designer has less confidence in the safety of the design. If there will be an opportunity in the future to evaluate the design using higher fidelity modeling (or to perform a test on a prototype), then this provides an opportunity to redesign (i.e. correct or modify) a design that is revealed to be too conservative or unsafe.

In this study we propose a safety-margin-based method for design under mixed epistemic model uncertainty and aleatory parameter uncertainty. The method is based on a two stage design process where an initial design is selected based on low-fidelity modeling, but there will be an opportunity in the future to evaluate the design with a high-fidelity model and if necessary calibrate the low-fidelity model and perform redesign. The design optimization is performed deterministically based on fixing

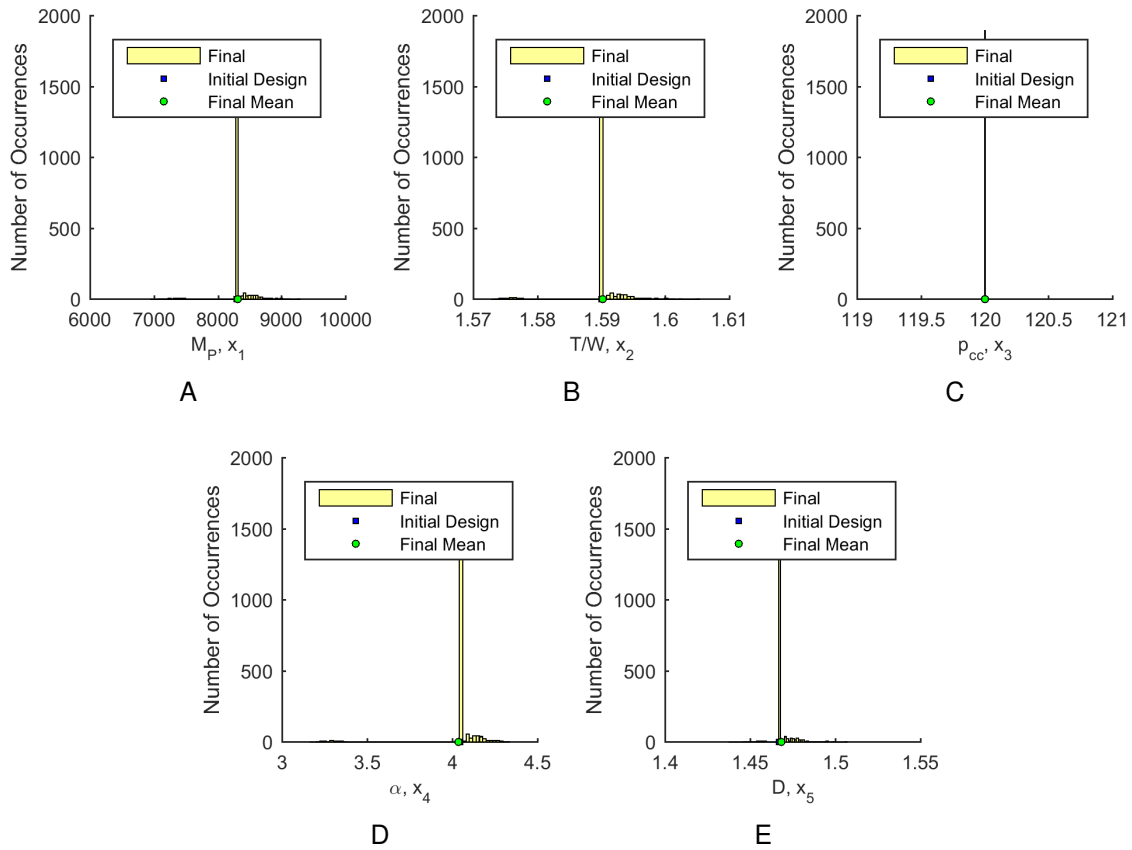


Figure 5-14. Distribution of optimum design variables for 20% probability of redesign. Plots show marginal distributions of 5-dimensional joint distribution.

the aleatory variables at the MPP of the mean low-fidelity model and applying a  $k$  standard deviation offset to constraint functions to compensate for model uncertainty. A MCS is performed with respect to epistemic model uncertainty based on conditional simulations of a Kriging model. By repeating the deterministic design process for many different realization of model uncertainty it is possible to predict how future redesign may change the design performance and reliability. It is shown that future redesign acts similar to quality control measures in truncating extreme values of epistemic model uncertainty. The simulation allows the designer to tradeoff between the expected design performance and the risk of future redesign while still achieving a specified confidence level in the reliability of the final design. It is found that redesign for safety is particularly effective at truncating high probabilities of failure and therefore allows for

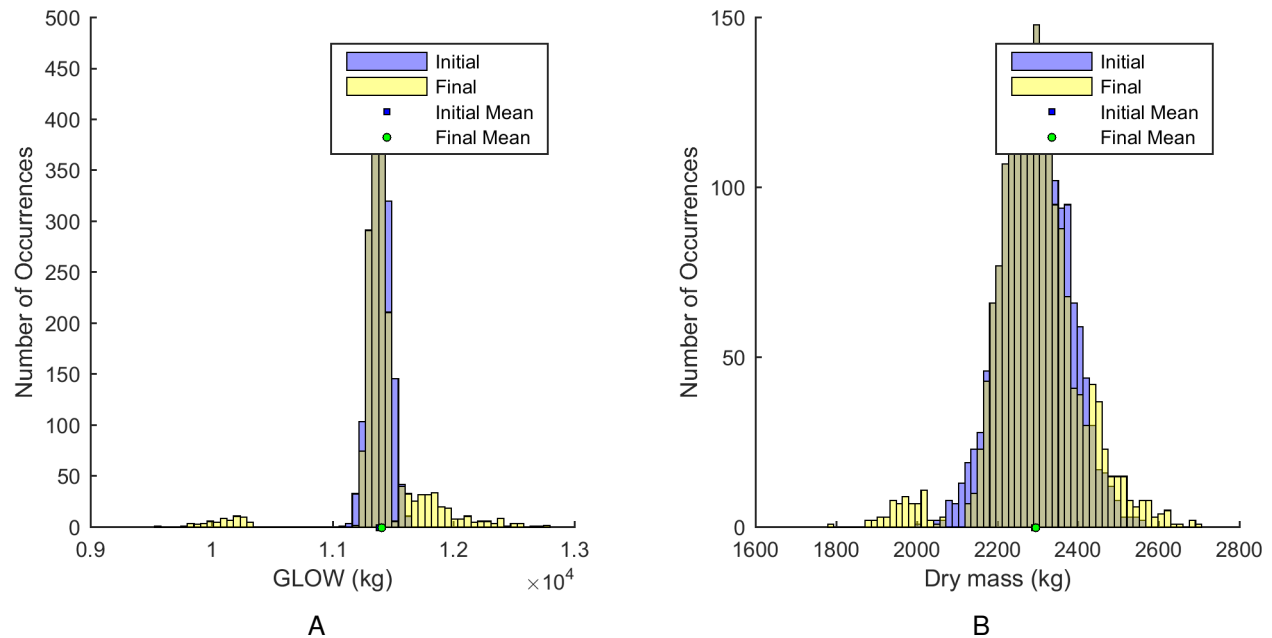


Figure 5-15. Distributions of GLOW and dry mass for 20% probability of redesign. Plots show overlapping transparent histograms.

improved design performance of the initial design by being less conservative. On the other hand, redesign for performance allows a designer to improve the performance of the initial design if it is later revealed to be too conservative. It is found that the optimum design strategy includes some probability of both redesign for safety and redesign for performance.

The method is demonstrated on a cantilever beam bending example and then on a multidisciplinary sounding rocket design example. In both examples it is shown that there is a strong correlation between the safety margin and the probability of failure. Therefore, the simple safety margin based redesign criteria is useful for identifying an unsafe or overly conservative design. This type of quality control measure is already incorporated into many engineering design applications. The proposed method allows for more detailed study of the effects of redesign and allows the designer to plan for future design changes and explore the interactions between the probability of redesign, safety margins, design performance, and probability of failure.

## CHAPTER 6

### CONCLUSIONS

Early in the design process, engineers must often rely on computationally cheap, low-fidelity models to select an initial design. Later in the design process, high-fidelity models may be used to evaluate the performance and safety of the initial design. If high-fidelity models reveal unsatisfactory design performance or safety concerns then this usually triggers a redesign process to find an improved final design. Redesign typically results in undesirable delays and increased costs, however, it is also an opportunity for design improvement. Due to the knowledge gained from the high-fidelity evaluation it is possible to calibrate low-fidelity models, reduce uncertainty, and arrive at a safer and/or better performing final design. Traditionally, engineers have used safety margins to provide insurance against design failure and reduce the probability of redesign for safety. However, if the margins are too high then design performance suffers and if the margins are too low then the design may be unsafe. In this research, we propose a method for optimizing the safety margins governing a design/redesign process. The research seeks to improve understanding of the complex relationship between safety margins, design performance, probability of failure, and probability of redesign.

The key contributions of this research are as follows:

- The development of a generalized method for simulating the effects of a future test and possible redesign when model bias is constant. The generalized formulation facilitates the understanding of the method and allows it to be more readily applied to new design examples. The method also introduced global optimization for finding the optimal safety margins. The use of global optimization replaced point cloud based methods [21] in order to reduce the noise in the pareto front of optimal expected performance and probability of redesign.
- A detailed investigation was conducted to determine when it was better to redesign for safety and when it is better to redesign for performance. It was found that the decision depends in part on the ratio of the variance of epistemic uncertainty in the high-fidelity model to the ratio of the variance in the low-fidelity model. In general terms, it depends on the *amount* of epistemic uncertainty in the high-fidelity model relative to the *amount* of uncertainty in the low-fidelity model. It was found that

when the ratio is low it is better to redesign for safety and when the ratio is high it is better to redesign for performance. If there is a large amount of error in the high-fidelity model (i.e. ratio is high) then a dangerous initial design may pass the test unnoticed and therefore redesign for safety is less effective.

- The development of a method for simulating the effects of a future test and possible redesign when model bias may be non-linear and high-fidelity evaluation (i.e. future test) provides incomplete information.
  - *Non-linear model discrepancy*: In general, the discrepancy between a low and high-fidelity model may be non-linear. For example, the models may agree for some designs under some conditions but exhibit large discrepancies for other designs or other conditions. Therefore, a Kriging model was proposed as a robust method for representing the unknown model discrepancy. The Kriging model allows for the convenient simulation of non-linear discrepancy functions through conditional simulations.
  - *Calibration and uncertainty reduction*: If the discrepancy function is non-linear then the methods used for model calibration and uncertainty reduction with constant model bias are no longer applicable. Our intuition tells us that the high-fidelity evaluation of one design under fixed conditions only reduces the uncertainty for *similar* designs under *similar* conditions. For example, if we compare a structural FE model (low-fidelity) of a wing design to a physical test of a wing prototype (high-fidelity) under the same loading conditions then we can quantify the error in our FE model for that wing design under the specified loads. However, we may wish to use the FE model to design other wings or to predict the behavior of the same wing but under many different random load realizations. Therefore, we must account for the *spatial correlations* in the model discrepancy when we calibrate our model and reduce epistemic model uncertainty. Spatial correlations are easily handled through the use of the Kriging model.
- The development of a method for reducing the computational cost of the safety margin optimization by exploiting the correlation between the safety margin and the probability of failure. If the safety margin is calculated with respect to the MPP of the aleatory random variables, then observing a negative safety margin is correlated with a violation of the probability of failure constraint. Therefore, it was proposed that it may be possible to approximate a quantile constraint on the probability of failure as the probability of a negative safety margin. To avoid the high computational cost of repeatedly searching for the MPP for each realization of epistemic model uncertainty, it was proposed that the MPP with respect to the mean model be used as a point approximation of the MPP distribution. This method was shown to produce reasonable results for the cantilever beam and sounding rocket demonstration examples.

- The extension of the method to multi-disciplinary sounding rocket design optimization example. The method was extended to consider increased computational cost of models, increased number of design variables, multi-disciplinary design considerations, design variables that were unique to the high-fidelity model, epistemic uncertainty in the objective function, and additional deterministic design constraints.

**Perspectives.** Based on the work presented in this dissertation there are several areas that may be worthy of further investigation. Some of the interesting areas for future work include:

- The development of a method for simulating multiple future tests. Based on the Kriging framework developed in this dissertation it is theoretically possible to simulate multiple future tests such as test replications to reduce measurement uncertainty or tests of different initial design concepts to reduce uncertainty over a larger area of the design space.
- The consideration of measurement error in addition to non-linear model discrepancy. The method based on the assumption of constant model bias included the consideration of measurement error in the high-fidelity model, but this was not included in later work when non-linear model discrepancy was introduced. Based on the Kriging framework it is theoretically possible to include the effect of measurement error in the analysis by using Kriging with nugget.
- Detailed study of the elicitation of epistemic model uncertainty parameters from experts. The method based on the assumption of constant model bias had a rather cursory discussion of how model uncertainty can be represented as uniform random variables based on expert opinion. In the method with non-linear model discrepancy the error model was based on the preliminary test data rather than expert opinion. The foundation of the proposed method would benefit from more detailed literature review regarding the elicitation of expert opinion (e.g. [28, 34]) and how it relates to developing a model for epistemic model uncertainty in the context of the present work. In particular, future research could address incorporating expert opinion into the definition of the Kriging covariance function.
- The development of a method to combine expected performance and probability of redesign into a single cost function. In theory, there is an optimal probability of redesign in terms of economic cost for a given design problem. That is, the expected performance benefits of redesign likely outweigh the expected cost of redesign up until a certain point. After this point, the cost of redesign may be greater than the expected performance benefits. The definition of a single combined cost function would replace the tradeoff curve between expected performance and probability of redesign with a single curve showing the probability of redesign that minimizes the expected cost. Related work such as the economic



change method of Roser et al. [77] and the flexible design methodology of De Neufville [95] may provide insight into modeling the economics of redesign.

- Preliminary work in this dissertation showed promising results for approximating a quantile probability of failure constraint with an MPP based safety margin constraint. This method was shown to significantly reduce the cost of the safety margin optimization without introducing excessive error in the reliability constraint. More research is needed to identify the limitations of the proposed approximation and to explore developing a strictly conservative approximation.

## REFERENCES

- [1] G. E. P. Box and N. R. Draper, *Empirical model-building and response surfaces*. Wiley, Jan. 1987.
- [2] Federal Aviation Regulations, “§25.303 Factor of safety.” Federal Aviation Administration, 2015.
- [3] D. Ullman, “Less fudging on fudge factors: a statistical approach to determining safety factors provides a more realistic estimate of just how big or strong a part must be,” *Machine Design*, vol. 58, p. 107, Oct. 1986. [Online]. Available: <http://go.galegroup.com/ps/i.do?id=GALE%7CA4447436&v=2.1&u=gain40375&it=r&p=ITOF&sw=w&asid=5e10cd854eb24650cd40ff8cc75e05ea>
- [4] M. Mohaghegh, “Evolution of structures design philosophy and criteria,” *Journal of aircraft*, vol. 42, no. 4, pp. 814–831, 2005. [Online]. Available: <http://arc.aiaa.org/doi/pdf/10.2514/1.11717>
- [5] Y. T. Wu and W. Wang, “Efficient probabilistic design by converting reliability constraints to approximately equivalent deterministic constraints,” *J. Integr. Des. Process Sci*, vol. 2, no. 4, pp. 13–21, 1998.
- [6] Y. T. Wu, Y. Shin, R. Sues, and M. Cesare, “Safety-factor based approach for probability-based design optimization,” in *Proc. 42nd AIAA/ASME/ASCE/AHS/ASC Structures, Structural Dynamics, and Materials Conference, number AIAA-2001-1522, Seattle, WA*, vol. 196, 2001, pp. 199–342.
- [7] X. Du and W. Chen, “Sequential optimization and reliability assessment method for efficient probabilistic design,” *Journal of Mechanical Design*, vol. 126, no. 2, pp. 225–233, 2004. [Online]. Available: <http://mechanicaldesign.asmedigitalcollection.asme.org/article.aspx?articleid=1448042>
- [8] P. Zhu, F. Pan, W. Chen, and F. A. C. Viana, “Lightweight design of vehicle parameters under crashworthiness using conservative surrogates,” *Computers in Industry*, vol. 64, no. 3, pp. 280–289, Apr. 2013. [Online]. Available: <http://www.sciencedirect.com/science/article/pii/S0166361512001959>
- [9] S. Mahadevan and R. Rebba, “Inclusion of Model Errors in Reliability-Based Optimization,” *Journal of Mechanical Design*, vol. 128, no. 4, pp. 936–944, Jan. 2006. [Online]. Available: <http://dx.doi.org/10.1115/1.2204973>
- [10] C. Kim and K. K. Choi, “Reliability-Based Design Optimization Using Response Surface Method With Prediction Interval Estimation,” *Journal of Mechanical Design*, vol. 130, no. 12, pp. 121401–121401, Oct. 2008. [Online]. Available: <http://dx.doi.org/10.1115/1.2988476>

- [11] M. C. Kennedy and A. O'Hagan, "Bayesian calibration of computer models," *Journal of the Royal Statistical Society: Series B (Statistical Methodology)*, vol. 63, no. 3, pp. 425–464, Jan. 2001. [Online]. Available: <http://onlinelibrary.wiley.com/doi/10.1111/1467-9868.00294/abstract>
- [12] A. I. Forrester, A. Sóbester, and A. J. Keane, "Multi-fidelity optimization via surrogate modelling," *Proceedings of the royal society A: mathematical, physical and engineering science*, vol. 463, no. 2088, pp. 3251–3269, 2007. [Online]. Available: <http://rspa.royalsocietypublishing.org/content/463/2088/3251.short>
- [13] W. Chen, Y. Xiong, K.-L. Tsui, and S. Wang, "A design-driven validation approach using Bayesian prediction models," *Journal of Mechanical Design*, vol. 130, no. 2, p. 021101, 2008. [Online]. Available: <https://mechanicaldesign.asmedigitalcollection.asme.org/article.aspx?articleid=1449622>
- [14] D. Huang, T. T. Allen, W. I. Notz, and R. A. Miller, "Sequential kriging optimization using multiple-fidelity evaluations," *Structural and Multidisciplinary Optimization*, vol. 32, no. 5, pp. 369–382, 2006. [Online]. Available: <http://link.springer.com/article/10.1007/s00158-005-0587-0>
- [15] Z. Qian, C. C. Seepersad, V. R. Joseph, J. K. Allen, and C. J. Wu, "Building surrogate models based on detailed and approximate simulations," *Journal of Mechanical Design*, vol. 128, no. 4, pp. 668–677, 2006. [Online]. Available: <https://mechanicaldesign.asmedigitalcollection.asme.org/article.aspx?articleid=1448978>
- [16] P. Z. Qian and C. J. Wu, "Bayesian hierarchical modeling for integrating low-accuracy and high-accuracy experiments," *Technometrics*, vol. 50, no. 2, pp. 192–204, 2008. [Online]. Available: <http://www.tandfonline.com/doi/abs/10.1198/004017008000000082>
- [17] Y. Xiong, W. Chen, and K.-L. Tsui, "A New Variable-Fidelity Optimization Framework Based on Model Fusion and Objective-Oriented Sequential Sampling," *Journal of Mechanical Design*, vol. 130, no. 11, pp. 111 401–111 401, Oct. 2008. [Online]. Available: <http://dx.doi.org/10.1115/1.2976449>
- [18] E. Zio and G. E. Apostolakis, "Two methods for the structured assessment of model uncertainty by experts in performance assessments of radioactive waste repositories," *Reliability Engineering & System Safety*, vol. 54, no. 2–3, pp. 225–241, Nov. 1996. [Online]. Available: <http://www.sciencedirect.com/science/article/pii/S0951832096000786>
- [19] D. Villanueva, R. T. Haftka, and B. V. Sankar, "Including the Effect of a Future Test and Redesign in Reliability Calculations," *AIAA Journal*, vol. 49, no. 12, pp. 2760–2769, 2011. [Online]. Available: <http://arc.aiaa.org/doi/pdf/10.2514/1.J051150>

- [20] T. Matsumura and R. T. Haftka, "Reliability Based Design Optimization Modeling Future Redesign With Different Epistemic Uncertainty Treatments," *Journal of Mechanical Design*, vol. 135, no. 9, pp. 091 006–091 006, Jul. 2013. [Online]. Available: <http://dx.doi.org/10.1115/1.4024726>
- [21] D. Villanueva, R. T. Haftka, and B. V. Sankar, "Accounting for future redesign to balance performance and development costs," *Reliability Engineering & System Safety*, vol. 124, pp. 56–67, Apr. 2014. [Online]. Available: <http://www.sciencedirect.com/science/article/pii/S0951832013003104>
- [22] M. Mohaghegh, "Validation and Certification of Aircraft Structures." Austin, Texas: American Institute of Aeronautics and Astronautics, Apr. 2005. [Online]. Available: <http://arc.aiaa.org/doi/abs/10.2514/6.2005-2162>
- [23] N. B. Price, T. Matsumura, R. T. Haftka, and N. H. Kim, "Deciding How Conservative A Designer Should Be: Simulating Future Tests and Redesign," in *16th AIAA Non-Deterministic Approaches Conference*. National Harbor, Maryland: American Institute of Aeronautics and Astronautics, Jan. 2014.
- [24] N. Price, N. H. Kim, R. Haftka, M. Balesdent, S. Defoort, and R. Le Riche, "Deciding Degree of Conservativeness in Initial Design Considering Risk of Future Redesign," *Journal of Mechanical Design*, 2016, accepted with revisions.
- [25] N. B. Price, M. Balesdent, S. Defoort, R. L. Riche, N. H. Kim, and R. T. Haftka, "Simulating Future Test and Redesign Considering Epistemic Model Uncertainty," in *18th AIAA Non-Deterministic Approaches Conference*. San Diego, California: American Institute of Aeronautics and Astronautics, Jan. 2016. [Online]. Available: <http://arc.aiaa.org/doi/abs/10.2514/6.2016-0950>
- [26] M. Balesdent, L. Brevault, N. Price, S. Defoort, R. Le Riche, N. H. Kim, R. Haftka, and N. Bérend, "Space vehicle design taking into account multidisciplinary couplings and mixed epistemic / aleatory uncertainties," in *Space Engineering: Modeling and Optimization with Case Studies*. Springer, 2016, in press.
- [27] M. H. Faber, "On the Treatment of Uncertainties and Probabilities in Engineering Decision Analysis," *Journal of Offshore Mechanics and Arctic Engineering*, vol. 127, no. 3, pp. 243–248, Mar. 2005. [Online]. Available: <http://dx.doi.org/10.1115/1.1951776>
- [28] A. O'Hagan and J. E. Oakley, "Probability is perfect, but we can't elicit it perfectly," *Reliability Engineering & System Safety*, vol. 85, no. 1–3, pp. 239–248, Jul. 2004. [Online]. Available: <http://www.sciencedirect.com/science/article/pii/S0951832004000638>
- [29] A. Der Kiureghian and O. Ditlevsen, "Aleatory or epistemic? Does it matter?" *Structural Safety*, vol. 31, no. 2, pp. 105–112, 2009. [Online]. Available: <http://www.sciencedirect.com/science/article/pii/S0167473008000556>

- [30] S. Ferson, C. A. Joslyn, J. C. Helton, W. L. Oberkampf, and K. Sentz, "Summary from the epistemic uncertainty workshop: consensus amid diversity," *Reliability Engineering & System Safety*, vol. 85, no. 1-3, pp. 355–369, Jul. 2004. [Online]. Available: <http://www.sciencedirect.com/science/article/pii/S0951832004000729>
- [31] S. Ferson and L. R. Ginzburg, "Different methods are needed to propagate ignorance and variability," *Reliability Engineering & System Safety*, vol. 54, no. 2–3, pp. 133–144, Nov. 1996. [Online]. Available: <http://www.sciencedirect.com/science/article/pii/S0951832096000713>
- [32] S. Ferson, V. Kreinovich, L. Ginzburg, D. S. Myers, and K. Sentz, "Constructing probability boxes and Dempster-Shafer structures," Sandia National Laboratories, Tech. Rep., 2002.
- [33] J. C. Helton, J. D. Johnson, and W. L. Oberkampf, "An exploration of alternative approaches to the representation of uncertainty in model predictions," *Reliability Engineering & System Safety*, vol. 85, no. 1, pp. 39–71, 2004. [Online]. Available: <http://www.sciencedirect.com/science/article/pii/S0951832004000511>
- [34] J. Kadane and L. J. Wolfson, "Experiences in elicitation," *Journal of the Royal Statistical Society: Series D (The Statistician)*, vol. 47, no. 1, pp. 3–19, 1998. [Online]. Available: <http://onlinelibrary.wiley.com/doi/10.1111/1467-9884.00113/abstract>
- [35] T. Nilsen and T. Aven, "Models and model uncertainty in the context of risk analysis," *Reliability Engineering & System Safety*, vol. 79, no. 3, pp. 309–317, Mar. 2003. [Online]. Available: <http://www.sciencedirect.com/science/article/pii/S0951832002002399>
- [36] W. L. Oberkampf, S. M. DeLand, B. M. Rutherford, K. V. Diegert, and K. F. Alvin, "Estimation of total uncertainty in modeling and simulation," Sandia National Laboratories, Tech. Rep. SAND2000-0824, 2000. [Online]. Available: [http://infoserve.sandia.gov/sand\\_doc/2000/000824.pdf](http://infoserve.sandia.gov/sand_doc/2000/000824.pdf)
- [37] —, "Error and uncertainty in modeling and simulation," *Reliability Engineering & System Safety*, vol. 75, no. 3, pp. 333–357, Mar. 2002. [Online]. Available: <http://www.sciencedirect.com/science/article/pii/S095183200100120X>
- [38] R. Haftka, "Combining global and local approximations," *AIAA Journal*, vol. 29, no. 9, pp. 1523–1525, 1991. [Online]. Available: <http://dx.doi.org/10.2514/3.10768>
- [39] K. J. Chang, R. T. Haftka, G. L. Gary, and K. Pi-Jen, "Sensitivity-based scaling for approximating structural response," *Journal of Aircraft*, vol. 30, no. 2, pp. 283–288, 1993. [Online]. Available: <http://dx.doi.org/10.2514/3.48278>
- [40] S. E. Gano, J. E. Renaud, and B. Sanders, "Hybrid Variable Fidelity Optimization by Using a Kriging-Based Scaling Function," *AIAA Journal*, vol. 43, no. 11, pp. 2422–2433, 2005. [Online]. Available: <http://arc.aiaa.org/doi/abs/10.2514/1.12466>

- [41] S. E. Gano, J. E. Renaud, H. Agarwal, and A. Tovar, "Reliability-based design using variable-fidelity optimization," *Structures and Infrastructure Engineering*, vol. 2, no. 3-4, pp. 247–260, 2006. [Online]. Available: <http://www.tandfonline.com/doi/abs/10.1080/15732470600590408>
- [42] M. G. Hutchison, E. R. Unger, W. H. Mason, B. Grossman, and R. T. Haftka, "Variable-complexity aerodynamic optimization of a high-speed civil transport wing," *Journal of Aircraft*, vol. 31, no. 1, pp. 110–116, 1994. [Online]. Available: <http://dx.doi.org/10.2514/3.46462>
- [43] N. O. Siu and G. E. Apostolakis, "Probabilistic models for cable tray fires," *Reliability Engineering*, vol. 3, no. 3, pp. 213–227, May 1982. [Online]. Available: <http://www.sciencedirect.com/science/article/pii/0143817482900312>
- [44] E. Acar, R. T. Haftka, and N. H. Kim, "Effects of structural tests on aircraft safety," *AIAA Journal*, vol. 48, no. 10, pp. 2235–2248, 2010. [Online]. Available: <http://arc.aiaa.org/doi/pdf/10.2514/1.J050202>
- [45] A. J. Keane, "Wing optimization using design of experiment, response surface, and data fusion methods," *Journal of Aircraft*, vol. 40, no. 4, pp. 741–750, 2003. [Online]. Available: <http://arc.aiaa.org/doi/abs/10.2514/2.3153>
- [46] M. C. Kennedy and A. O'Hagan, "Predicting the output from a complex computer code when fast approximations are available," *Biometrika*, vol. 87, no. 1, pp. 1–13, 2000. [Online]. Available: <http://biomet.oxfordjournals.org/content/87/1/1.short>
- [47] M. J. Bayarri, J. O. Berger, R. Paulo, J. Sacks, J. A. Cafeo, J. Cavendish, C.-H. Lin, and J. Tu, "A framework for validation of computer models," *Technometrics*, vol. 49, no. 2, 2007. [Online]. Available: <http://amstat.tandfonline.com/doi/abs/10.1198/004017007000000092>
- [48] P. D. Arendt, D. W. Apley, and W. Chen, "Quantification of Model Uncertainty: Calibration, Model Discrepancy, and Identifiability," *Journal of Mechanical Design*, vol. 134, no. 10, pp. 100908–100908, Sep. 2012. [Online]. Available: <http://dx.doi.org/10.1115/1.4007390>
- [49] Federal Aviation Regulations, "§25.301 Loads." Federal Aviation Administration, 2015.
- [50] —, "§25.613 Material strength properties and material design values." Federal Aviation Administration, 2015.
- [51] G. E. Muller and C. J. Schmid, "Factor of Safety-USAF Design Practice," DTIC Document, Tech. Rep., 1978. [Online]. Available: <http://oai.dtic.mil/oai/oai?verb=getRecord&metadataPrefix=html&identifier=ADA070237>



- [52] J. J. Zipay, C. T. Modlin Jr, and C. E. Larsen, "The Ultimate Factor of Safety for Aircraft and Spacecraft Its History, Applications and Misconceptions," in *57th AIAA/ASCE/AHS/ASC Structures, Structural Dynamics, and Materials Conference*, San Diego, California, Jan. 2016. [Online]. Available: <http://ntrs.nasa.gov/search.jsp?R=20150003482>
- [53] D. G. Ullman, *The mechanical design process*. McGraw-Hill New York, 1992, vol. 2. [Online]. Available: [http://maelabs.ucsd.edu/mae3/Assignments/Energy\\_Analysis/factor\\_of\\_safety/FactorOfSafetyGuidelines-Ullman.pdf](http://maelabs.ucsd.edu/mae3/Assignments/Energy_Analysis/factor_of_safety/FactorOfSafetyGuidelines-Ullman.pdf)
- [54] J. Tu, K. K. Choi, and Y. H. Park, "A new study on reliability-based design optimization," *Journal of Mechanical Design*, vol. 121, no. 4, pp. 557–564, 1999. [Online]. Available: <http://mechanicaldesign.asmedigitalcollection.asme.org/article.aspx?articleid=1445722>
- [55] B. J. Bichon, M. S. Eldred, L. P. Swiler, S. Mahadevan, and J. M. McFarland, "Efficient Global Reliability Analysis for Nonlinear Implicit Performance Functions," *AIAA Journal*, vol. 46, no. 10, pp. 2459–2468, 2008. [Online]. Available: <http://arc.aiaa.org/doi/abs/10.2514/1.34321>
- [56] V. Dubourg, "Adaptive surrogate models for reliability analysis and reliability-based design optimization," Ph.D. dissertation, Université Blaise Pascal-Clermont-Ferrand II, 2011. [Online]. Available: <https://tel.archives-ouvertes.fr/tel-00697026/>
- [57] E. Acar, A. Kale, R. T. Haftka, and W. J. Stroud, "Structural safety measures for airplanes," *Journal of Aircraft*, vol. 43, no. 1, pp. 30–38, 2006. [Online]. Available: <http://arc.aiaa.org/doi/pdf/10.2514/1.14381>
- [58] E. Acar, R. T. Haftka, and T. F. Johnson, "Tradeoff of uncertainty reduction mechanisms for reducing weight of composite laminates," *Journal of Mechanical Design*, vol. 129, no. 3, pp. 266–274, 2007. [Online]. Available: <http://computingengineering.asmedigitalcollection.asme.org/article.aspx?articleid=1449287>
- [59] A. G. Watson and R. J. Barnes, "Infill sampling criteria to locate extremes," *Mathematical Geology*, vol. 27, no. 5, pp. 589–608, 1995. [Online]. Available: <http://link.springer.com/article/10.1007/BF02093902>
- [60] D. R. Jones, M. Schonlau, and W. J. Welch, "Efficient global optimization of expensive black-box functions," *Journal of Global optimization*, vol. 13, no. 4, pp. 455–492, 1998. [Online]. Available: <http://link.springer.com/article/10.1023/A:1008306431147>
- [61] M. Schonlau, "Computer experiments and global optimization," Ph.D. dissertation, University of Waterloo, 1998. [Online]. Available: <http://www.collectionscanada.gc.ca/obj/s4/f2/dsk3/ftp04/nq22234.pdf>

- [62] M. J. Sasena, P. Papalambros, and P. Goovaerts, "Exploration of Metamodeling Sampling Criteria for Constrained Global Optimization," *Engineering Optimization*, vol. 34, no. 3, pp. 263–278, Jan. 2002. [Online]. Available: <http://dx.doi.org/10.1080/03052150211751>
- [63] M. J. Sasena, P. Y. Papalambros, and P. Goovaerts, "The use of surrogate modeling algorithms to exploit disparities in function computation time within simulation-based optimization," in *4th World Congress of Structural and Multidisciplinary Optimization*, Dalian, China, 2001. [Online]. Available: <http://citeseerx.ist.psu.edu/viewdoc/download?doi=10.1.1.29.2793&rep=rep1&type=pdf>
- [64] J. Parr, C. M. Holden, A. I. Forrester, and A. J. Keane, "Review of efficient surrogate infill sampling criteria with constraint handling," in *2nd International Conference on Engineering Optimization*, Lisbon, Portugal, 2010, pp. 1–10. [Online]. Available: <http://eprints.soton.ac.uk/336169/>
- [65] J. Villemonteix, E. Vazquez, and E. Walter, "An informational approach to the global optimization of expensive-to-evaluate functions," *Journal of Global Optimization*, vol. 44, no. 4, pp. 509–534, 2009. [Online]. Available: <http://link.springer.com/article/10.1007/s10898-008-9354-2>
- [66] F. O. Hoffman and J. S. Hammonds, "Propagation of Uncertainty in Risk Assessments: The Need to Distinguish Between Uncertainty Due to Lack of Knowledge and Uncertainty Due to Variability," *Risk Analysis*, vol. 14, no. 5, pp. 707–712, Oct. 1994. [Online]. Available: <http://onlinelibrary.wiley.com/doi/10.1111/j.1539-6924.1994.tb00281.x/abstract>
- [67] M. E. Paté-Cornell, "Uncertainties in risk analysis: Six levels of treatment," *Reliability Engineering & System Safety*, vol. 54, no. 2–3, pp. 95–111, Nov. 1996. [Online]. Available: <http://www.sciencedirect.com/science/article/pii/S0951832096000671>
- [68] I. C. Wright, "A review of research into engineering change management: implications for product design," *Design Studies*, vol. 18, no. 1, pp. 33–42, 1997. [Online]. Available: <http://www.sciencedirect.com/science/article/pii/S0142694X96000294>
- [69] T. A. W. Jarratt, C. M. Eckert, N. H. M. Caldwell, and P. J. Clarkson, "Engineering change: an overview and perspective on the literature," *Research in engineering design*, vol. 22, no. 2, pp. 103–124, 2011. [Online]. Available: <http://link.springer.com/article/10.1007/s00163-010-0097-y>
- [70] P. J. Clarkson, C. Simons, and C. Eckert, "Predicting Change Propagation in Complex Design," *Journal of Mechanical Design*, vol. 126, no. 5, pp. 788–797, Oct. 2004. [Online]. Available: <http://dx.doi.org/10.1115/1.1765117>
- [71] G. A. Ollinger and T. F. Stahovich, "RedesignIT—A Model-Based Tool for Managing Design Changes," *Journal of Mechanical Design*, vol. 126, no. 2, pp. 208–216, May 2004. [Online]. Available: <http://dx.doi.org/10.1115/1.1666888>



- [72] L. Chen, A. Macwan, and S. Li, "Model-based Rapid Redesign Using Decomposition Patterns," *Journal of Mechanical Design*, vol. 129, no. 3, pp. 283–294, Mar. 2006. [Online]. Available: <http://dx.doi.org/10.1115/1.2406099>
- [73] B. Hamraz, N. H. M. Caldwell, and P. John Clarkson, "A Multidomain Engineering Change Propagation Model to Support Uncertainty Reduction and Risk Management in Design," *Journal of Mechanical Design*, vol. 134, no. 10, pp. 100 905–100 905, Sep. 2012. [Online]. Available: <http://dx.doi.org/10.1115/1.4007397>
- [74] F. I. Romli and M. y. Harmin, "Use of Monte Carlo method to estimate subsystem redesign risk for complex products: aircraft redesign case study," *Aircraft Engineering and Aerospace Technology*, vol. 87, no. 6, pp. 563–570, Sep. 2015. [Online]. Available: <http://www.emeraldinsight.com/doi/abs/10.1108/AEAT-02-2015-0044>
- [75] C. Roser and D. Kazmer, "Risk effect minimization using flexible product and process design," in *Proceedings of the Design Engineering Technical Conferences*. Las Vegas, Nevada: ASME, 1999, pp. 4:383–94. [Online]. Available: [http://www.allaboutlean.com/wp-content/uploads/2014/05/1999\\_Roser\\_DET-C-Risk-Effect-Minimization\\_Preprint.pdf](http://www.allaboutlean.com/wp-content/uploads/2014/05/1999_Roser_DET-C-Risk-Effect-Minimization_Preprint.pdf)
- [76] C. H. Roser, "A flexible design methodology," Ph.D. dissertation, University of Massachusetts Amherst, 2000. [Online]. Available: [http://www.allaboutlean.com/wp-content/uploads/2014/05/2000\\_Roser\\_DISSERTATION-A-Flexible-Design-Methodology.pdf](http://www.allaboutlean.com/wp-content/uploads/2014/05/2000_Roser_DISSERTATION-A-Flexible-Design-Methodology.pdf)
- [77] C. Roser, D. Kazmer, and J. Rinderle, "An Economic Design Change Method," *Journal of Mechanical Design*, vol. 125, no. 2, pp. 233–239, Jun. 2003. [Online]. Available: <http://dx.doi.org/10.1115/1.1561040>
- [78] B. D. Youn and K. K. Choi, "Selecting probabilistic approaches for reliability-based design optimization," *AIAA Journal*, vol. 42, no. 1, pp. 124–131, 2004. [Online]. Available: <http://arc.aiaa.org/doi/pdf/10.2514/1.9036>
- [79] Z. Jiang, W. Chen, Y. Fu, and R.-J. Yang, "Reliability-based design optimization with model bias and data uncertainty," *SAE International Journal of Materials and Manufacturing*, vol. 6, no. 3, 2013.
- [80] C. Eckert, C. Earl, S. Lebjoui, and O. Isaksson, "Components Margins through the Product Lifecycle," in *Product Lifecycle Management for Society*, ser. IFIP Advances in Information and Communication Technology, A. Bernard, L. Rivest, and D. Dutta, Eds. Springer Berlin Heidelberg, Jul. 2013, pp. 39–47. [Online]. Available: [http://link.springer.com/chapter/10.1007/978-3-642-41501-2\\_5](http://link.springer.com/chapter/10.1007/978-3-642-41501-2_5)
- [81] A. C. Thornton, "Optimism vs. Pessimism: Design Decisions in the Face of Process Capability Uncertainty," *Journal of Mechanical Design*, vol. 123, no. 3, pp. 313–321, Oct. 1998. [Online]. Available: <http://dx.doi.org/10.1115/1.1371774>

- [82] N. Hansen, "The CMA evolution strategy: a comparing review," in *Towards a new evolutionary computation*. Springer, 2006, pp. 75–102. [Online]. Available: [http://link.springer.com/chapter/10.1007/3-540-32494-1\\_4](http://link.springer.com/chapter/10.1007/3-540-32494-1_4)
- [83] J. S. Agte, J. Sobieszczanski-Sobieski, and R. R. Sandusky, "Supersonic business jet design through bi-level integrated system synthesis," SAE Technical Paper, Tech. Rep., 1999. [Online]. Available: <http://papers.sae.org/1999-01-5622/>
- [84] R. T. Rockafellar and S. Uryasev, "Optimization of conditional value-at-risk," *Journal of Risk*, vol. 2, pp. 21–42, 2000.
- [85] J. C. Helton, "Treatment of uncertainty in performance assessments for complex systems," *Risk analysis*, vol. 14, no. 4, pp. 483–511, 1994. [Online]. Available: <http://onlinelibrary.wiley.com/doi/10.1111/j.1539-6924.1994.tb00266.x/abstract>
- [86] J.-P. Chilès and P. Delfiner, "Chapter 7 - Conditional Simulations," in *Geostatistics: Modeling Spatial Uncertainty, Second Edition*. John Wiley & Sons, Inc., 2012, pp. 478–628. [Online]. Available: <http://onlinelibrary.wiley.com/doi/10.1002/9781118136188.ch7/summary>
- [87] J. Bect and E. Vazquez, "STK: a Small (Matlab/Octave) Toolbox for Kriging," 2014. [Online]. Available: <http://kriging.sourceforge.net>
- [88] F. Castellini, "Multidisciplinary design optimization for expendable launch vehicles," Ph.D. dissertation, Politecnico di Milano, 2012. [Online]. Available: <https://www.politesi.polimi.it/handle/10589/56841>
- [89] S. Gordon and B. J. McBride, "Computer Program for Calculation of Complex Chemical Equilibrium Compositions and Applications I: Analysis," NASA Lewis Research Center, Tech. Rep., Oct. 1994. [Online]. Available: <http://ntrs.nasa.gov/search.jsp?R=19950013764>
- [90] B. J. McBride and S. Gordon, "Computer Program for Calculation of Complex Chemical Equilibrium Compositions and Applications II. Users Manual and Program Description," NASA Lewis Research Center, Tech. Rep., Jun. 1996. [Online]. Available: <http://ntrs.nasa.gov/search.jsp?R=19960044559>
- [91] S. Lophaven, H. Nielsen, and J. Søndergaard, "DACE – A MATLAB Kriging Toolbox," Informatics and Mathematical Modelling, Technical University of Denmark, Tech. Rep. IMM-TR-2002-12, 2002.
- [92] R. Rohrschneider, "Development of a mass estimating relationship database for launch vehicle conceptual design," *AE8900 Special Project, School of Aerospace Engineering, Georgia Institute of Technology*, 2002. [Online]. Available: <http://ssdl.gatech.edu/papers/mastersProjects/RohrschneiderR-8900.pdf>

- [93] W. B. Blake, "Missile Datcom: User's Manual-1997 FORTRAN 90 Revision." DTIC Document, Tech. Rep., 1998. [Online]. Available: <http://oai.dtic.mil/oai/oai?verb=getRecord&metadataPrefix=html&identifier=ADA344707>
- [94] D. E. Koelle, *Handbook of Cost Engineering and Design of Space Transportation Systems: With TransCost 8.2 Model Description; Statistical-analytical Model for Cost Estimation and Economic Optimization of Launch Vehicles*. TCS - TransCostSystems, 2013.
- [95] R. De Neufville and S. Scholtes, *Flexibility in engineering design*, ser. Engineering systems. Cambridge, Mass: MIT Press, 2011, 00190. [Online]. Available: <http://site.ebrary.com/lib/univflorida/Doc?id=10524447>

## BIOGRAPHICAL SKETCH

Nathaniel Price was born in St. Augustine, Florida in 1988. He graduated magna cum laude with a Bachelor of Science in mechanical engineering from the University of Florida (UF) in 2012. As an undergraduate he held internships with E&S Consulting, Inc. in St. Augustine, Florida and Space Exploration Technologies (SpaceX) in Cape Canaveral, Florida; he performed undergraduate research in the UF Materials Design & Prototyping Laboratory under the advisement of Dr. Michele Manuel. Under the advisement of Dr. Nam-Ho Kim, he was awarded the 2012 Biomedical Engineering Society (BMES) Design and Research Award and the 2013 Knox T. Millsaps Outstanding Undergraduate Paper Award for his honors thesis research on the effects of cortical thickness, bone strength, and screw length on rigid sternal fixation stability. After graduation, he joined the Structural and Multidisciplinary Optimization Group at the University of Florida as a Ph.D. student where he was awarded the Graduate School Fellowship Award. In 2014, he earned a non-thesis Master of Science in mechanical engineering with a certificate in scientific computing. The same year he began research at ONERA - The French Aerospace Lab in Palaiseau, France and entered a dual PhD program with École des Mines de Saint-Étienne.